Número: 414/2010

UNIVERSIDADE ESTADUAL DE CAMPINAS
INSTITUTO DE GEOCIÊNCIAS
PÓS-GRADUAÇÃO EM GEOCIÊNCIAS
ÁREA DE GEOLOGIA E RECURSOS NATURAIS

DISSERTAÇÃO DE MESTRADO

O DEPÓSITO DE ÓXIDO DE FERRO–COBRE–OURO BACABA, PROVÍNCIA MINERAL DE CARAJÁS, PA: GEOCRONOLOGIA U–Pb DAS ROCHAS HOSPEDEIRAS

CAROLINA PENTEADO NATIVIDADE MORETO

Orientadora: Profa. Dra. Lena Virgínia Soares Monteiro
Co-Orientador: Prof. Dr. Roberto Perez Xavier

Campinas, São Paulo
Fevereiro de 2010

© by Carolina Penteado Natividade Moreto, 2010

Catalogação na Publicação elaborada pela Biblioteca do Instituto de Geociências/UNICAMP

Moreto, Carolina Penteado Natividade.
M817d O depósito de óxido de ferro-cobre-ouro Bacada, Província Mineral de Carajás, PA: Geocronologia U-Pb das rochas hospedeiras / Carolina Penteado Natividade Moreto-- Campinas,SP.: [s.n.], 2010.

Orientador: Lena Virgínia Soares Monteiro, Roberto Perez Xavier
Dissertação (mestrado) Universidade Estadual de Campinas, Instituto de Geociências.

1. Depósitos de óxido de Fe-Cu-Au – Carajás, Serra dos (PA). 2. Geocronologia. 3. Cratons. 4. Minas e recursos minerais – Carajás, Serra dos (PA). I. Monteiro, Lena Virgínia Soares. II. Xavier, Roberto Perez. III. Universidade Estadual de Campinas, Instituto de Geociências. IV. Título.

Título em inglês. Iron oxide-Cu-Au Bacaba deposit, Carajás Mineral Province (PA), Brazil: U-Pb geocronology of the host rocks.
Keywords: - Iron oxide-Cu-Au deposits – Carajás, Serra dos (PA);
- Geochronology;
- Cratons;
- Mines and mineral resources – Carajás, Serra dos (PA)
Área de concentração: Geologia e Recursos Naturais
Titulação: Mestre em Geociências.
Banca examinadora: - Lena Virgínia Soares Monteiro;
- Carlos Eduardo de Mesquita Barros;
- Ticiano José Saraiva dos Santos.
Data da defesa: 08/02/2010
Programa de Pós-graduação em Geociências

UNICAMP

UNIVERSIDADE ESTADUAL DE CAMPINAS
INSTITUTO DE GEOCIÊNCIAS
PÓS-GRADUAÇÃO EM GEOCIÊNCIAS NA
ÀREA DE GEOLOGIA E RECURSOS NATURAIS

AUTORA: Carolina Penteado Natividade Moreto

"Depósito de Óxido de Ferro-Cobre-Ouro Bacaba, Província Mineral de Carajás-PA: geocronologia U-Pb das Rochas Hospedeiras"

ORIENTADORA: Profa. Dra. Lena Virginia Soares Monteiro

Aprovada em: 08 / 02 / 2010

EXAMINADORES:

Profa. Dra. Lena Virginia Soares Monteiro _____ - Presidente

Prof. Dr. Carlos Eduardo de Mesquita Barros _____

Prof. Dr. Ticiano José Saraiva dos Santos _____

Campinas, 08 de fevereiro de 2010.

Dedico este trabalho aos meus pais, José Luiz e Maria Stella, ao meu irmão Bruno e ao meu namorado Wagner (Lobinho), por todo carinho e apoio durante os anos de convívio.

AGRADECIMENTOS

Agradeço primeiramente à Deus, por todas as oportunidades que tive em minha vida.

Devo total gratidão à minha orientadora, profa. Dra. Lena Virgínia Soares Monteiro, pela oportunidade que me foi dada, pela confiança, paciência, por ter acreditado em mim, pelo conhecimento e aprendizado, e por todo o apoio e incentivo para realização deste trabalho.

Ao meu co-orientador prof. Dr. Roberto Perez Xavier por todo o incentivo, apoio e aprendizado, e por ter me apresentado à geologia econômica.

Ao CNPq pela concessão da minha bolsa de mestrado e por ter financiado a etapa de campo e as análises isotópicas e químicas.

À VALE (Companhia Vale do Rio Doce), em particular aos geólogos Márcio Godoy e Benevides Aires, pelo apoio logístico durante a etapa de campo.

Ao prof. Dr. Ticiano José Saraiva dos Santos pelo imensurável apoio durante esses anos.

Aos profs. Drs. Elson Paiva de Oliveira e Ticiano José Saraiva dos Santos, que participaram da banca de qualificação e contribuíram com críticas e sugestões relevantes para o aprimoramento desse trabalho.

Aos professores do IGe/UNICAMP pelos anos de aprendizado, em especial aos profs. Drs. Lena Monteiro, Roberto Xavier, Ticiano Santos, Elson de Oliveira, Wanilson Luiz Silva, Alfonso Schrank, Carlos Roberto de Souza Filho e Alvaro Crósta.

Ao prof. Dr. Caetano Juliani pelo auxílio o e por compartilhar seu vasto conhecimento geológico em campo.

Ao meu namorando, amigo e companheiro Wagner Amaral, que esteve ao meu lado em todos os momentos, me auxiliando em tudo que precisei. Contribuiu de forma direta para a realização deste trabalho.

Ao prof. Dr. Elton Dantas pelo apoio durante minhas estadias em Brasília e pelas discussões acerca dos dados isotópicos. À Bárbara Lima e Sérgio Junges pelo auxílio nas etapas analíticas na UNB.

Aos meus pais José Luiz e Maria Stella e meu irmão Bruno por existirem em minha vida e também aos meus familiares.

Às minhas queridas amigas Fernanda (Ferzinha) Lourenço e Maria Fernanda (Ferzona) Grisolia pela amizade sincera, companheirismo e cumplicidade. Uma amizade para a vida toda.

À todos os colegas da pós-graduação, em especial aos da sala 11 (Paty, Ferzona, Bairral, Ju, Ignacio, Rafael e André).

Ao André, meu aliado (Carajás vs. PAAF, rsrs.), pelas discussões relevantes.

À querida Val, simplesmente por TUDO. A pós-graduação não existiria sem ela!

Aos funcionários do Ige/UNICAMP, em especial ao Seu Aníbal, Guerreiro, Jô, Cristiano, Ednalva e Gorete pela ajuda e consideração durante esses anos. E também ao Dailto pelo apoio e auxilio.

À minhas queridas amigas do colégio, em especial à Bruna, Mirelle, Luana e Bia, por tantos anos de convívio e alegrias.

SÚMARIO

ÍNDICE DE FIGURAS

ÍNDICE DE TABELAS

ANEXO: Moreto, C.P.N., Monteiro, L.V.S., Xavier, R.P., Amaral, W.S., Santos, T.J.S., Juliani, C., Souza Filho, C.R., 2010. Mesoarchean (3.0 and 2.86 Ga) host rocks of the iron oxide–Cu–Au Bacaba deposit, Carajás Mineral Province: U–Pb geochronology and metallogenetic implications (*Mineralium Deposita*, Submetido).

Appendix

UNIVERSIDADE ESTADUAL DE CAMPINAS
INSTITUTO DE GEOCIÊNCIAS
PÓS-GRADUAÇÃO EM GEOCIÊNCIAS
ÁREA DE GEOLOGIA E RECURSOS NATURAIS

O depósito de óxido de ferro–cobre–ouro Bacaba, Província Mineral de Carajás, PA: Geocronologia U-Pb das rochas hospedeiras

RESUMO

Dissertação de Mestrado

Carolina Penteado Natividade Moreto

O depósito de óxido de ferro–cobre–ouro Bacaba, situado no Cinturão de Cisalhamento Itacaiúnas, Província Mineral de Carajás, representa um alvo satélite do depósito de classe mundial Sossego, e possivelmente também representa as porções distais e profundas do mesmo sistema hidrotermal. O depósito Bacaba localiza-se ao longo de uma zona de cisalhamento com direção WNW–ESE que define o contato entre o embasamento, representado pelo Complexo Xingu (ca. 3,0 Ga), e a unidade metavulcano-sedimentar do Supergrupo Itacaiúnas (ca. 2,76 Ga). As principais rochas hospedeiras do minério no depósito Bacaba são representadas pelo Granito Serra Dourada, Tonalito Bacaba e por corpos gabróicos, que foram intensamente afetados por alterações hidrotermais sódica (albita-escapolita), potássica, clorítica e hidrolítica. Os dados de U–Pb LA–ICP–MS em zircão de uma amostra com alteração sódica do Granito Serra Dourada forneceram a idade de 2858 ± 30 Ma (MSWD = 9,7). Três amostras do Tonalito Bacaba, sendo uma com alteração potássica e duas com alteração potássica e mineralização de Cu-Au, forneceram idades em 2997,2 ± 4,7 Ma (MSWD = 1,15), 2993,1 ± 7,1 Ma (MSWD = 1,1) e 3004,7 ± 7,8 Ma (MSWD = 2,1), respectivamente. As idades em 2,86 e ca. 3,0 Ga são interpretadas como idade de cristalização do Granito Serra Dourada e do Tonalito Bacaba, respectivamente. As estruturas internas e morfologia dos cristais de zircão de ambas as rochas, observadas em imagens de catodoluminescência e de elétrons retro-espalhados, confirmam a ocorrência de processos de recristalização, que pode ser relacionado com episódios de hidrotermalismo e/ou deformação/metamorfismo que ocorreram na Província Mineral de Carajás. Contudo, esse (s) evento (s) não pode (puderam) ser datado (s) devido à ausência de abertura total do sistema isotópico U-Pb e ausência de cristais de zircão de origem hidrotermal.O Granito Serra Dourada e o Tonalito Bacaba são as rochas graníticas mais antigas até então reconhecidas no Cinturão de Cisalhamento Itacaiúnas. A presença dessas rochas tão antigas implica na existência de um importante magmatismo anterior à instalação da Bacia de Carajás (Supergrupo Itacaiúnas), e em uma história evolutiva mais complexa para o Cinturão de Cisalhamento Itacaiúnas. As similaridades petrográficas e geocronológicas dessas intrusivas félsicas do depósito Bacaba com suítes de rochas graníticas e tonalíticas reconhecidas no Terreno Granito-*Greenstone* Rio Maria, porção sul da Província Mineral de Carajás, implica na ocorrência de um magmatismo de ca. 3,0 e 2,86 Ga mais amplo e extenso. O Granito Serra Dourada e o Tonalito Bacaba não poderiam ser responsáveis pelo estabelecimento do sistema magmático–hidrotermal associado com a gênese do depósito Bacaba. Isso seria improvável porque outros depósitos com características similares são hospedados por unidades metavulcano-sedimentares mais novas (2,76 Ga). Nesse contexto, os depósitos de óxido de ferro–cobre–ouro do setor sul do Cinturão de Cisalhamento Itacaiúnas devem ser controlados principalmente por importantes descontinuidades crustais, como a zona de cisalhamento regional com direção WNW–ESE, ao invés de serem associados com um litotipo particular. Esses resultados indicam alto potencial de ocorrência de depósitos de óxido de ferro–cobre–ouro nas rochas mesoarqueanas do embasamento sob a Bacia de Carajás, particularmente aquelas cortadas por zonas de cisalhamento neoarqueanas.

UNIVERSIDADE ESTADUAL DE CAMPINAS
INSTITUTO DE GEOCIÊNCIAS
PÓS-GRADUAÇÃO EM GEOCIÊNCIAS
ÁREA DE GEOLOGIA E RECURSOS NATURAIS

Iron oxide–Cu–Au Bacaba deposit, Carajás Mineral Province (PA), Brazil: U-Pb geochronology of the host rocks

ABSTRACT

Master's Thesis

Carolina Penteado Natividade Moreto

The Bacaba iron oxide–copper–gold deposit, situated in the Itacaiúnas Shear Belt, Carajás Mineral Province (Brazil), represents a satellite prospect of the world-class Sossego deposit, and might also represent a distal and deeper portion of the same or related hydrothermal system. The Bacaba deposit is located along a WNW–ESE-striking shear zone that defines the contact of the basement represented by the Xingu Complex (ca. 3.0 Ga) and the metavolcano-sedimentary Itacaiúnas Supergroup (ca. 2.76 Ga). The main host rocks at Bacaba deposit comprise the Serra Dourada Granite, the Bacaba Tonalite and croscutting gabbro, which were intensely affected by sodic (albite-scapolite), potassic, chloritic and hydrolytic hydrothermal alterations.The U–Pb LA–ICP–MS data for zircon from sodic altered sample of the Serra Dourada Granite yielded an 2858 ± 30 Ma (MSWD = 9.7) age. Three samples from the Bacaba Tonalite, including one with potassic alteration and two with potassic alteration and Cu–Au mineralization rendered the 2997.2 ± 4.7 Ma (MSWD = 1.15), 2993.1 ± 7.1 Ma (MSWD = 1.1) and 3004.7 ± 7.8 Ma (MSWD = 2.1) ages, respectively. The 2.86 and ca. 3.0 Ga ages are interpreted as the igneous crystallization of the Serra Dourada Granite and the Bacaba Tonalite, respectively. The internal structures and external morphologies of zircon crystal from both rocks, observed in cathodoluminescence and backscattered electron images, attested the occurrence of zircon recrystallization, which could be related to hydrothermalism and/or deformation/metamorphism episodes that took place in the Carajás Mineral Province. However, the disturbing event (s) could not be dated due to the absence of the total resetting of the U–Pb system and hydrothermal crystallization of zircon. The 2.86 Ga Serra Dourada Granite and the ca. 3.0 Ga Bacaba Tonalite are the oldest granitic rocks so far recognized in the Itacaiúnas Shear Belt. The presence of such old rocks implies in the existence of an important magmatism before the Carajás Basin (Itacaiúnas Supergroup) deposition, and in a more complex evolutionary history for the Itacaiúnas Shear Belt. The petrographical and geochronological similarities of these felsic intrusions with granitic and tonalitic rock suites recognized in the Rio Maria granite-greenstone terrane, southern part of the Carajás Mineral Province, implies in a more widespread ca. 3.0 and 2.86 Ga magmatism in the province. The Serra Dourada Granite and the Bacaba Tonalite are interpreted not to be responsible for the genesis of the Bacaba deposit. This is likely because the Sossego and other deposits interpreted as part of the same hydrothermal system are hosted by younger ca. 2.76 Ga metavolcano-sedimentary units. On this context, the iron oxide-copper-gold deposit in the southern sector of the Itacaiúnas Shear Belt could be mainly controlled by important crustal discontinuities, such as the WNW–ESE-striking regional shear zone, rather than be associated with a particular rock type. These results expand the potentiality of occurrence of iron oxide–copper–gold deposits for the Mesoarchean basement rocks underlying the Carajás Basin, particularly those crosscut by Neoarchean shear zones.

1. INTRODUÇÃO

A Província Mineral de Carajás (PMC), localizada na porção sul do Cráton Amazônico, é considerada uma das maiores províncias metalogenéticas do planeta. Hospeda diferentes classes de depósitos minerais, inclusive os depósitos de óxido de ferro–cobre–ouro (*Iron Oxide–Copper–Gold deposits* ou IOCG), que representam mundialmente um dos grandes alvos da pesquisa mineral. Entre os depósitos dessa classe na PMC, destacam-se Salobo (789 Mt @ 0.96% Cu, 0.52 g/t Au, 55 g/t Ag, Souza & Vieira, 2000), Igarapé Bahia/Alemão (219 Mt @ 1.4% Cu, 0.86 g/t Au, Tallarico *et al*., 2005), Sossego (245 Mt @ 1.1% Cu e 0.28 g/t Au, Lancaster *et al*., 2000), Gameleira (100 Mt @ 0.7% Cu, Rigon, 2000), Alvo 118 (70 Mt @ 1.0% Cu, 0.3 g/t Au, Rigon, 2000) e Cristalino (500 Mt @ 1.0% Cu, 0.3 g/t Au, Huhn *et al*., 1999).

Embora exista controvérsia, a maioria dos modelos genéticos propostos para os depósitos IOCG de Carajás destaca a importância de intrusões graníticas arqueanas (~2,75 ou 2,57 Ga) ou paleoproterozóicas (~1,88 Ga) para o fornecimento de calor e fluidos necessários para a geração de extensos sistemas hidrotermais (Huhn *et al*., 1999; Réquia *et al.*, 2003; Tallarico *et al.*, 2005; Villas *et al.*, 2006; Neves, 2006; Pollard, 2006; Grainger *et al.*, 2008). Contudo, a maioria dos depósitos IOCG de Carajás é hospedado por unidades metavulcano-sedimentares arqueanas do Supergrupo Itacaiúnas (~2,76 Ga; Machado *et al*., 1991) e clara associação espacial e temporal com rochas graníticas foi relatada em poucos casos (e.g. depósito Cristalino de ~2,74 Ga, Huhn *et al*. 1999; depósito Salobo de ~2,57 Ga, Réquia *et al.*, 2003). Em vista disso, até o presente momento não são bem compreendidos os mecanismos relacionados com a gênese dos depósitos IOCG da PMC, incluindo a origem das fontes de calor, metais e fluidos e a importância dos tipos de magmatismo identificados na província.

Os dados geocronológicos existentes para os depósitos IOCG e suas rochas hospedeiras não são suficientemente precisos a fim de comprovar que esses depósitos relacionam-se a um único evento metalogenético. Diferentes métodos aplicados à datação da mineralização forneceram resultados consideravelmente diferentes, inclusive em um mesmo depósito (e.g. depósitos Igarapé Bahia/Alemão, Gameleira, Salobo e Igarapé Cinzento; Pimentel *et al*., 2003; Réquia *et al*., 2003; Marschik *et al*., 2005; Tallarico *et al*., 2005; Galarza *et al*., 2008). Muitos desses dados podem refletir distúrbio dos sistemas isotópicos em resposta ao desenvolvimento e/ou reativação das zonas de cisalhamento arqueanas, e/ou também ao magmatismo arqueano e paleoproterozóico (Xavier *et al*., no prelo).

O depósito Bacaba, localizado a 7 km a leste da Mina de Sossego, representa um alvo satélite deste depósito IOCG de classe mundial. O depósito Bacaba possui uma clara associação espacial com rochas graníticas representadas pelo Tonalito Bacaba e pelo Granito Serra Dourada, o que permite a investigação do papel de tais rochas para a gênese do depósito. Os granitos hospedeiros apresentam intensa alteração hidrotermal de alta temperatura (> 550 ^{o}C, e.g. albitização, escapolitização e alteração potássica), similar às descritas em Sossego (Augusto *et al.*, 2008; Monteiro *et al.*, 2008a,b). Tais características tornam o Alvo Bacaba um depósito de grande interessante para a avaliação de possíveis relações entre magmatismo e geração do sistema hidrotermal de alta tempertura, que na literatura têm sido muitas vezes considerado como magmático-hidrotermal (Pollard 2001, 2006).

Este trabalho apresenta os dados geocronológicos U–Pb obtidos por LA–ICP–MS em zircão do Granito Serra Dourada e do Tonalito Bacaba variavelmente hidrotermalizados. Também propõe novas concepções metalogenéticas relativas aos depósitos IOCG e sobre o magmatismo arqueano na Província Mineral de Carajás, revelando a existência de eventos magmáticos até então desconhecidos na porção norte da província.

2. OBJETIVOS

Este estudo teve como principal objetivo determinar as idades de cristalização das rochas intrusivas félsicas (Granito Serra Dourada e Tonalito Bacaba) que hospedam o depósito IOCG Bacaba, com a finalidade de compreender o significado desses eventos magmáticos no contexto geológico regional, assim como suas implicações para a metalogênese na PMC. Os dados obtidos possibilitaram uma nova compreensão relativa às rochas do embasamento da porção norte da província, e revelaram a extensão do magmatismo arqueano, até então melhor caracterizado na porção sul da província.

3. A PROVÍNCIA MINERAL DE CARAJÁS

A PMC compreende dois domínios tectônicos arqueanos, ao sul, o Terreno Granito-*Greenstone* Rio Maria e, ao norte, o Cinturão de Cisalhamento Itacaiúnas (Fig. 1). O Cinturão de Cisalhamento Itacaiúnas compreende rochas do embasamento e seqüências supracrustais. O embasamento é representado por rochas de alto grau metamórfico dos complexos Xingu (3050 ± 57 Ma, Rodrigues *et al*., 1992) e Pium (3002 ± 14 Ma, Pidgeon *et al*., 2000). As unidades da

Bacia de Carajás foram depositadas sobre essas rochas e constituem unidades metavulcano-metassedimentares de ~2,76 Ga representadas pelo Grupo Rio Novo (Hirata *et al*., 1982) e pelo Supergrupo Itacaiúnas (2,73 a 2,76 Ga; Wirth *et al*., 1986; Docegeo, 1988, Machado *et al*., 1991). Este último hospeda diversos depósitos IOCG (e.g. Salobo, Gameleira, Igarapé Bahia/Alemão, Igarapé Cinzento e Alvo 118). Sobre o Supergrupo Itacaiúnas depositou-se uma seqüência sedimentar fluvial a marinha denominada Grupo Rio Fresco ou Formação Águas Claras (Nogueira *et al*., 1994, 2000) com idade mínima de deposição em 2,68 Ga (Trendall *et al*., 1998).

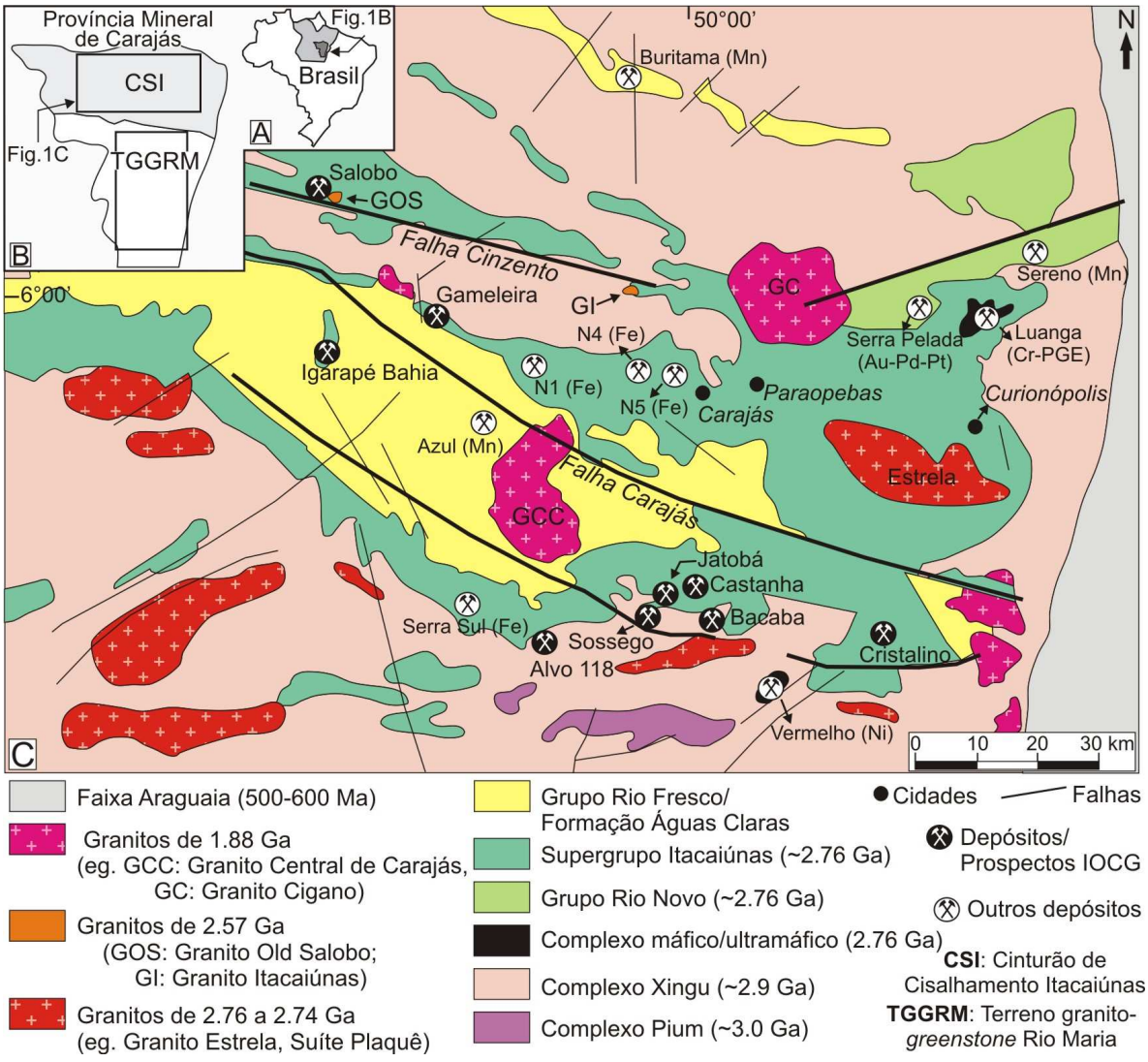

Figura 1. Cinturão de Cisalhamento Itacaiúnas com a localização dos principais depósitos IOCG (modificado de Dardenne & Schobbenhaus, 2001).

No Cinturão de Cisalhamento Itacaiúnas foram individualizados três eventos de granitogênese de distintas idades, sendo representados por granitos alcalinos com idades entre 2,76 e 2,74 Ga (*e.g*. Granito Estrela e Suíte Plaquê; Huhn *et al*., 1999, Avelar *et al*., 1999, Sardinha *et al*., 2006, Barros *et al*., 2004), granitos alcalinos do tipo-A de 2,57 Ga (*e.g*. granitos *Old Salobo* e Itacaiúnas; Machado *et al*., 1991, Souza *et al*., 1996) e granitos do tipo-A, alcalinos a sub-alcalinos com idade de 1,88 Ga (*e.g.* Granito Central de Carajás e Cigano; Machado *et al*., 1991; Dall'Agnoll *et al*. 1994; Lindenmayer and Teixeira, 1999; Tallarico 2003). Outras rochas intrusivas no Cinturão de Cisalhamento Itacaiúnas são representadas por intrusões máfico-ultramáficas arqueanas de 2,75 Ga, denominadas Luanga, Onça, Vermelho e Jacaré-Jacarezinho (Machado *et al*., 1991).

O Terreno Granito-*Greenstone* Rio Maria compreende sequências *greenstone belt* de 2,97 a 2,90 Ga do Supergrupo Andorinhas (Docegeo, 1988; Macambira & Lancelot, 1992, 1996; Pimentel & Machado, 1994; Souza *et al*., 2001). Diversas suítes graníticas arqueanas com diferentes composições e idades intrudiram a sequência *greenstone belt* e consistem em: i) suítes TTGs de ~2,95 Ga (Macambira & Lancelot, 1996; Leite *et al*., 2004) ii) sanukitóides com idades em 2,87 Ga (Dall'Agnol *et al*., 2006; Oliveira *et al*., 2009; Macambira & Lancelot, 1996; Pimentel & Machado, 1994); iii) suítes TGGs de 2,86 Ga (Macambira *et al*., 2000; Leite *et al*., 2004); e iv) leucogranitos potássicos com afinidade cálcio-alcalina e idades ao redor de 2,86 Ga (Leite *et al*., 2004; Lafon *et al*., 1994; Barbosa & Lafon, 1996).

O Terreno Granito-*Greenstone* Rio Maria também foi intrudido por diversos corpos graníticos do tipo-A com idades em 1,88 Ga, semelhantes aos granitos paleoproterozóicos observados no Cinturão de Cisalhamento Itacaiúnas. Outras unidades encontradas correspondem a rochas básicas a ultrabásicas de 2,97 Ga (Pimentel & Machado, 1994) e a sequência sedimentar da Formação Águas Claras/Grupo Rio Fresco (Macambira & Lancelot, 1996; Macambira *et al*., 1998), também presente no Cinturão de Cisalhamento Itacaiúnas.

4. DEPÓSITOS DE ÓXIDO DE FERRO–COBRE–OURO

A classe de depósitos IOCG representa mundialmente um dos grandes alvos da pesquisa mineral, desde a descoberta do depósito de Olympic Dam na Austrália (Roberts & Hudson, 1983), por apresentar reservas e teores significativos de Cu, além de enriquecimento polimetálico que inclui Au, Ag, U, ETR, Co, Ni, Pd, Nb e P. Apesar do grande número de estudos realizados

nesses depósitos, ainda não há um modelo genético consensual, uma vez que a diversidade de características dos depósitos IOCG relativas ao seus ambientes geotectônicos de formação, idades, rochas hospedeiras e tipos de alteração hidrotermal sugerem que distintos processos geológicos poderiam ter sido responsáveis pela gênese dos depósitos (Hitzman, 2000; Williams *et al*., 2005).

No Brasil, a PMC apresenta a maior concentração conhecida de depósitos IOCG de classe mundial, tais como, Salobo, Igarapé Bahia, Alemão, Sossego, Gameleira e Alvo 118. De acordo com Monteiro *et al*. (2008a,b), os depósitos IOCG de Carajás apresentam similaridades, incluindo: (i) rochas hospedeiras variáveis, geralmente incluindo unidades metavulcânicas-sedimentares do Supergrupo Itacaiúnas; (ii) forte controle estrutural; (iii) proximidade com intrusões de diferentes composições (granito, diorito, gabro e pórfiros de composição dacítica ou riolítica); (iv) intensas alterações hidrotermais, incluindo sódica, sódica-cálcica e/ou potássica, além de cloritização, turmalinização e silicificação; (v) formação de magnetita seguida por precipitação de sulfetos; e (vi) um amplo intervalo de temperaturas de homogenização (100 a 570 °C) e salinidades (0 a 69% eq. peso NaCl) em inclusões fluidas em minerais de ganga relacionados aos minerais de minério.

É notável a ocorrência de depósitos IOCG, na PMC, ao longo de extensas zonas de cisalhamento regionais dúcteis ou dúcteis-rúpteis que definem tanto o contato norte entre o Supergrupo Itaciaúnas e o Complexo Xingu (e.g. Salobo, Igarapé Cinzento), como o contato sul (e.g. Alvo 118, Sossego, Alvo Bacaba, Cristalino). Tais zonas de cisalhamento exerceram importante papel no controle do desenvolvimento das associações de alteração hidrotermal regionais de alta temperatura (> 550 ^{o}C). Em todos os depósitos, entretanto, a mineralização relaciona-se a estruturas rúpteis, subsidiárias, e a associações hidrotermais de menor temperatura (< 300 ^{o}C).

4.1 GEOCRONOLOGIA DOS DEPÓSITOS DE ÓXIDO DE FERRO-COBRE-OURO DA PROVÍNCIA MINERAL DE CARAJÁS

A maioria dos modelos genéticos dos depósitos IOCG da PMC enfatiza a importância das intrusões graníticas do Neoarqueano (~2.57 Ga) e/ou Paleoproterozóico (~1.88 Ga) para o estabelecimento de extensivos sistemas magmático-hidrotermais (e.g., Tallarico *et al*., 2005; Tavaza & Oliveira, 2000; Réquia *et al*., 2003; Pimentel *et al*., 2003; Lindenmayer, 2003).

Entretanto, modelos vulcânicos singenéticos (Lindenmayer, 1990; Villas & Santos, 2001; Dreher, 2004; Dreher & Xavier, 2005) também foram propostos para a gênese dos depósitos Salobo e Igarapé Bahia.

Datações Re-Os em molibdenita de veio mineralizado no depósito Salobo forneceram as idades de 2576 ± 8 Ma e 2562 ± 8 Ma, enquanto que a idade 2579 ± 71 Ma foi obtida pelo método Pb-Pb em bornita e calcopirita (Réquia *et al*., 2003). Estas idades são contemporâneas às atribuídas ao granito *Old Salobo* (2573 ± 2 Ma, Machado *et al*., 1991). Idades em 2705 ± 42, 2587 ± 150, 2427 ± 130 e 2112 ± 12 Ma foram apontadas pelo método Pb-Pb por lixiviação de calcocita, turmalina, calcopirita e magnetita de Salobo, respectivamente (Tassinari *et al*., 2003). A idade de ca. 2,7 Ga foi interpretada como a idade da mineralização, enquanto que as idades ao redor de 2,58 e 2,42 Ga estariam associadas à reativação tectônica das zonas de cisalhamento Carajás e Cinzento. A idade de 2,1 Ga seria decorrente da colocação do granito paleoproterozóico *Young Salobo*.

No depósito Igarapé Cinzento (GT 46), localizado ao longo do mesmo *trend* estrutural de Salobo, datações Ar-Ar em biotita hidrotermal indicaram idades paleoproterozóicas de 1809 ± 6 Ma e 1845 ± 5 Ma (Silva *et al*., 2005). Idades Re-Os em molibdenita de 2711 ± 9 Ma e 2554 ± 8 Ma foram obtidas em vênulas com sulfetos em anfibolitos e granitos no mesmo depósito, respectivamente (Silva *et al*., 2005). Estas últimas foram associadas à colocação de corpos monzograníticos datados pelo método Sm-Nd em 2668 ±100 Ma (Silva *et al*., 2005).

Em relação ao depósito Gameleira, os métodos Sm-Nd em veio mineralizado e Ar-Ar em biotita apontaram idades de 1839 ± 15 Ma e 1700 ± 31 Ma, e 1734 ± 8 Ma, respectivamente (Pimentel *et al*., 2003). A primeira idade sugere relação da mineralização com episódio paleoproterozóico de atividade hidrotermal (ca. 1,83 Ga). Neste caso, os fluidos mineralizantes teriam derivado de granitos crustais paleoproterozóicos, a exemplo do granito Pojuca. As idades em 1,7 Ga refletiriam as baixas temperaturas de fechamento da biotita em relação aos sistemas isotópicos Sm-Nd e Ar-Ar. No entanto, Marschik *et al*. (2005) obtiveram a idade de 2614 ± 14 Ma pelo método Re-Os em molibdenita de brechas e veios mineralizados. Esses autores sugerem uma relação genética da mineralização com granitóides arqueanos alcalinos (2,56 a 2,76 Ga) ou com magmatismo cálcio-alcalino a tholeiítico (2,6 a 2,7 Ga). Esta idade também coincide com as reativações tectônicas associadas aos sistemas de falhas Carajás e Cinzento. Idades Pb-Pb em calcopirita de 2419 ± 12 Ma, 2217 ± 19 Ma e 2180 ± 84 Ma também foram obtidas para o

depósito Gameleira (Galarza & Macambira, 2002), sendo interpretadas como rejuvenescimento parcial provocado pelas intrusões graníticas proterozóicas (1,58 e 1,87 Ga) e/ou pelas reativações tectônicas associadas aos sistemas de falhas Carajás e Cinzento.

No depósito Igarapé Bahia, Tallarico *et al*. (2005) utilizaram o método U-Pb SHRIMP II em monazita de brecha mineralizada e obtiveram a idade de 2575 ±12 Ma, que sugere uma relação temporal entre a mineralização e granitos arqueanos, como o *Old Salobo*. Ouro em brecha hidrotermal, em rocha metavulcânica máfica e em *gossan* foi datado pelo método Pb-Pb fornecendo a idade de 2744 ± 12 Ma (Galarza *et al*., 2008). Datação Pb-Pb em calcopirita de brecha hidrotermal, de metavulcânica máfica, de metapiroclástica e de intrusiva máfica indicaram idades em 2772 ± 46 Ma, 2756 ± 24 Ma, 2754 ± 36 Ma e 2777 ± 22 Ma, respectivamente (Galarza *et al*., 2008), enquanto que a idade de 2764 ± 22 Ma foi obtida pelo método Pb-Pb em calcopirita e ouro (Galarza, 2002). As idades ao redor de 2,7 Ga sugeririam, segundo os autores, afinidade genética entre a mineralização e as rochas vulcânicas do Supergrupo Itacaiúnas. Idades em 2385 ±122 Ma e 2417 ±120 Ma foram obtidas pelo método Pb-Pb em calcopirita em brecha hidrotermal (Galarza *et al*. 2008), e sugerem remobilização relacionada às reativações tectônicas regionais associadas aos sistemas de falhas Carajás e Cinzento.

Datação Pb-Pb em calcopirita e pirita do minério do depósito Cristalino forneceu a idade de 2719 ± 36 Ma (Soares *et al*., 2001), que é próxima à idade de 2747 ± 2 Ma (Pb-Pb em zircão) do granito Planalto, e da idade de 2738 ±2 Ma (Pb-Pb em zircão) de corpos dioríticos (Hunh *et al*., 1999) presentes na área do depósito.

No depósito Sossego, datações Pb-Pb em calcopirita indicaram idades de 2530 ± 25 Ma e 2608 ± 25 Ma para o minério do corpo Sequeirinho e 1592 ± 45 Ma para o minério do corpo Sossego (Neves, 2006). Segundo a autora, a mineralização estaria associada à granitogênese de 2,76 a 2,74 Ga e as idades representariam abertura do sistema isotópico causada por eventos termais e/ou deformacionais subseqüentes. Alternativamente, a mineralização poderia ser atribuída a processos metamórficos e essas idades registrariam o desenvolvimento de zonas de cisalhamento. À idade mesoproterozóica não foi atribuído nenhum significado geológico (Neves, 2006). Através do método Sm-Nd em rocha total, foi obtida a idade de 2578 ± 29 Ma para o minério do corpo Sequeirinho, que pode refletir reequilíbrio isotópico em resposta a eventos posteriores (Neves, 2006).

No depósito Alvo 118, foram obtidas as idades U-Pb SHRIMP II 1869 ± 7 e 1868 ± 7 Ma em xenotima de minério maciço e veio de minério, respectivamente (Tallarico, 2003). O autor considera essas idades paleoproterozóicas como uma evidência de um evento metalogenético distinto em relação aos eventos associados aos principais depósitos IOCG de Carajás, o que teria implicações para a classificação do depósito Alvo 118 como pertencente à classe de depósitos IOCG.

5. O DEPÓSITO DE ÓXIDO DE FERRO-COBRE-OURO SOSSEGO

O depósito Sossego, operado pela VALE, representou o primeiro depósito IOCG a entrar em produção no Brasil, em 2004. É constituído por dois grupos de corpos de minério (Sequerinho-Baiano-Pista e Sossego-Curral) com associações de alteração hidrotermal distintas (Fig. 2) que podem refletir a natureza das diferentes rochas hospedeiras (granito, granito granofírico, gabro e metavulcânica félsica com lentes subordinadas de rochas metaultramáficas), intensidade variável de processos de interação fluido-rocha e distintos níveis crustais (Monteiro *et al*., 2008a,b).

Nos corpos Sequerinho-Baiano-Pista podem ser reconhecidas zonas de alteração sódica (albita–hematita) e sódica–cálcica (actinolita-albita-titanita-epidoto-allanita) associadas com a formação de corpos maciços de magnetita–(apatita), envelopados por zonas constituídas predominantemente por actinolita (actinolititos), semelhantes às descritas em partes profundas de sistemas IOCG em outras partes do mundo (Monteiro *et al.,* 2008a). Zonas de alteração potássica são restritas, mas ocorrem espacialmente relacionadas às brechas mineralizadas, cortando as zonas de alteração sódico-cálcica.

Os corpos Sossego-Curral, entretanto, apresentam evidências de alteração potássica mais intensa, caracterizada pela formação de feldspato potássico e biotita rica em cloro, que substituem minerais do granito granofírico hospedeiro das mineralizações. Alteração clorítica predomina em halos externos e alteração hidrolítica com sericita, hematita e quartzo, típicas de partes bastante rasas de sistemas IOCG, foram reconhecidas apenas nesses corpos.

A mineralização cupro-aurífera nesse depósito associa-se a brechas hidrotermais. Em Sequeirinho, tais brechas apresentam predominância de calcopirita na matriz envolvendo fragmentos de actinolititos/magnetititos e de cristais de actinolita, apatita e magnetita, comumente também hidrotermalizados (Monteiro *et al*., 2008a,b). A mineralização de cobre-ouro foi tardia e

desenvolveu-se em condições essencialmente rúpteis, relacionadas a sistemas de falhas de direção NE (Morais & Alkmim, 2005). Em Sossego, as brechas apresentam fragmentos da rocha hospedeira hidrotermalizada envolvidos por magnetita e matriz com calcopirita, carbonatos e quartzo com texturas de preenchimento de espaços abertos (Monteiro *et al*., 2008a,b), que também denotam condições rúpteis.

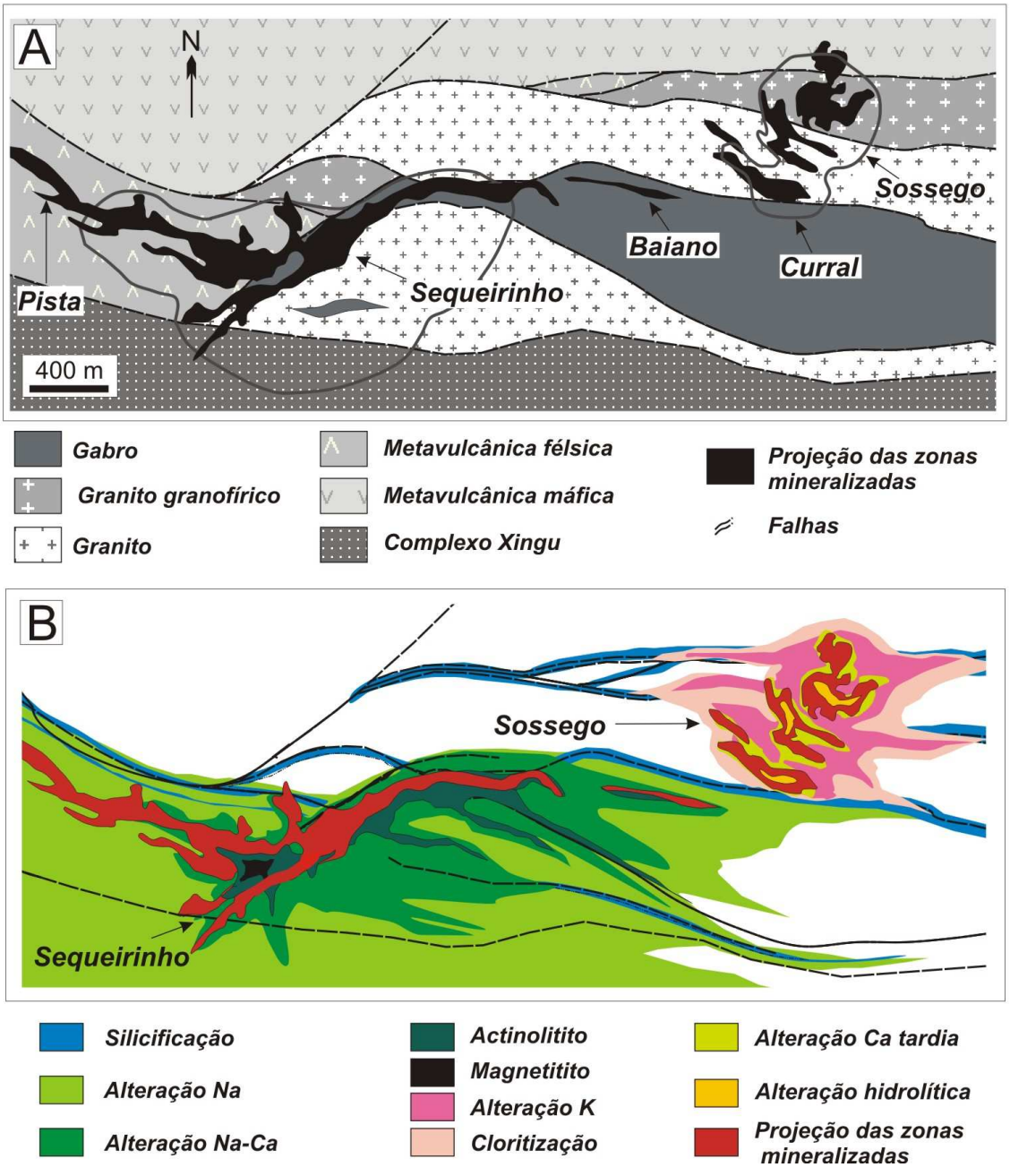

Figura 2. A. Mapa geológico simplificado da área da Mina Sossego (modificado de VALE por Monteiro et al., 2008a); B. Distribuição esquemática das zonas de alteração hidrotermais na Mina Sossego (Monteiro et al., 2008a).

A mineralização de cobre-ouro é representada pela associação de calcopirita com pirita, siegenita, millerita, vaesita, ouro, Pd-melonita e, subordinadamente, hessita, cassiterita, esfalerita, galena e molibdenita. Apatita, monazita, epidoto, allanita, actinolita e clorita comumente associam-se aos sulfetos e indicam que o estágio de mineralização nos diferentes corpos foi associado a menores temperaturas (~300 ^{o}C) em relação àquelas registradas pelas associações de alteração sódica e sódico-cálcica (~550 ^{o}C) ou potássica (> 450 ^{o}C). Assinatura isotópica de oxigênio do fluido hidrotermal ($\delta^{8}O_{fluido}$= −1.8 ± −3.4‰) em equilíbrio com fases minerais presentes nas brechas mineralizadas indica introdução de fluidos meteóricos durante a mineralização (Monteiro *et al*., 2008a,b).

Episódios de descompressão relacionados com sobrepressão de fluidos podem ter originado as brechas mineralizadas, permitindo o influxo de fluidos meteóricos canalizados em falhas, causando a deposição do minério devido à diluição e resfriamento dos fluidos metalíferos quentes (~550 ^{o}C) associados aos estágios iniciais de alteração.

O depósito Sossego distingue-se por apresentar zonas mineralizadas e de alteração hidrotermal semelhantes às reconhecidas mundialmente como formadas em níveis crustais distintos, possibilitando a reconstituição vertical do zoneamento em um sistema hidrotermal IOCG. As porções mais profundas desse sistema, representadas principalmente pelo corpo Sequeirinho, caracterizam-se pela predominância de alteração sódica e sódico-cálcica. Zonas de alteração potássica que cortam as zonas de alteração sódico-cálcicas predominam nos corpos Sossego-Curral, e gradam lateralmente para zonas de cloritização nos níveis crustais mais rasos (Fig. 3).

Embora os dados geocronológicos disponíveis para o depósito Sossego não comprovem a sincronicidade do processo de mineralização nos corpos Sequeirinho-Baiano-Pista e Sossego-Curral, a relação entre alteração hidrotermal e desenvolvimento de estruturas regionais, semelhanças na evolução paragenética, na composição química do minério, nos padrões de zoneamento de minerais hidrotermais presentes nas brechas e na assinatura de isotópos estáveis dos fluidos mineralizantes, indicam que tais corpos foram parte do mesmo sistema hidrotermal.

6. O DEPÓSITO DE ÓXIDO DE FERRO-COBRE-OURO BACABA

O depósito Bacaba (Figs. 4 e 5) localiza-se a 7 km a leste do depósito Sossego, sendo considerado satélite do mesmo. Assim como os depósitos IOCG de Sossego, Alvo 118 e

Cristalino, o depósito Bacaba está inserido em uma zona de cisalhamento regional de direção WNW–ESE, situada na zona de contato entre o embasamento, representado pelo Complexo Xingu e o Supergrupo Itacaiúnas.

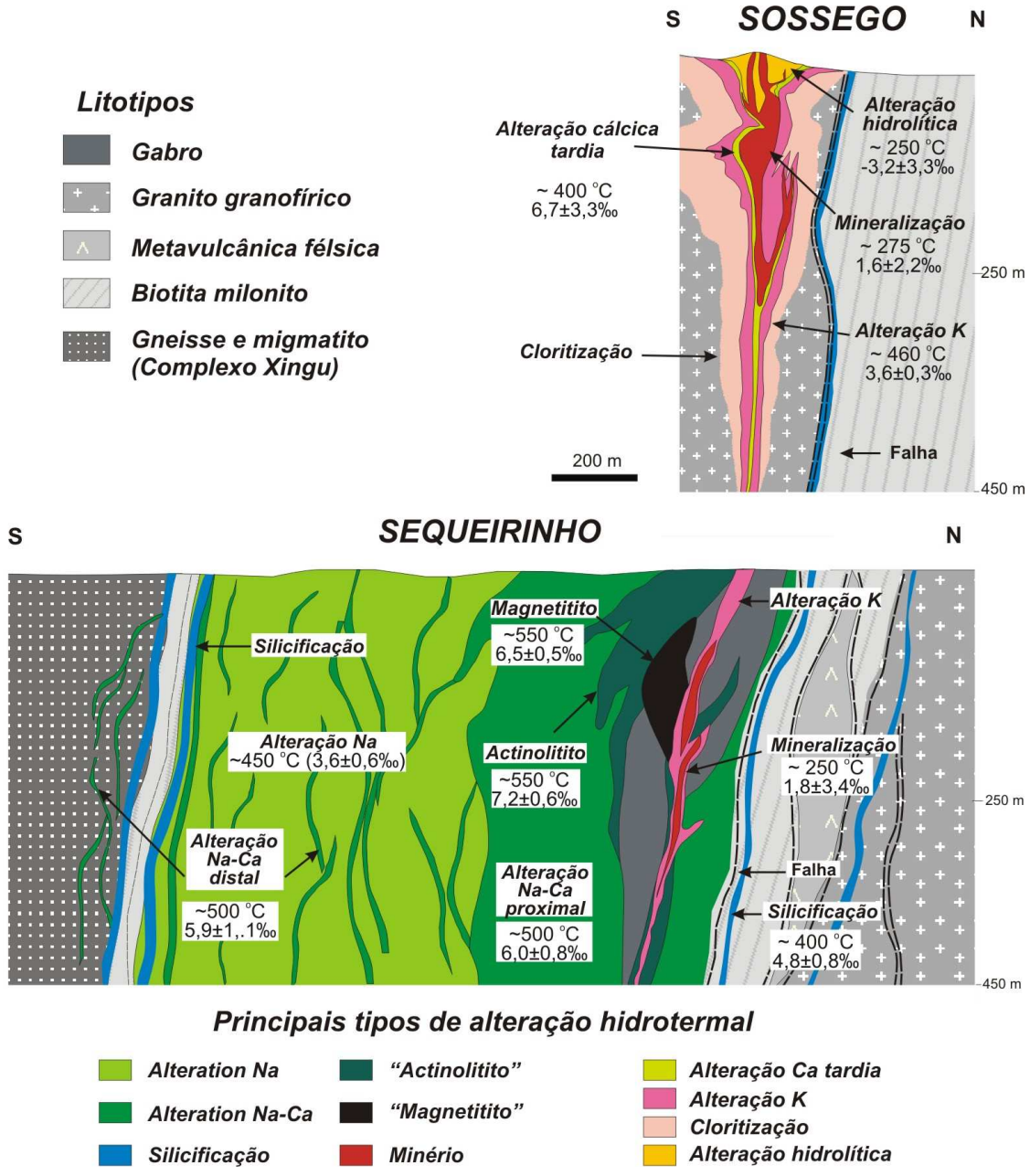

Figura 3. Seção esquemática dos corpos Sequeirinho e Sossego, mostrando a distribuição das zonas de alteração hidrotermais e temperaturas e assinatura isotópica de oxigênio dos fluidos hidrotermais estimadas para cada estágio de alteração (Monteiro et al., 2008a).

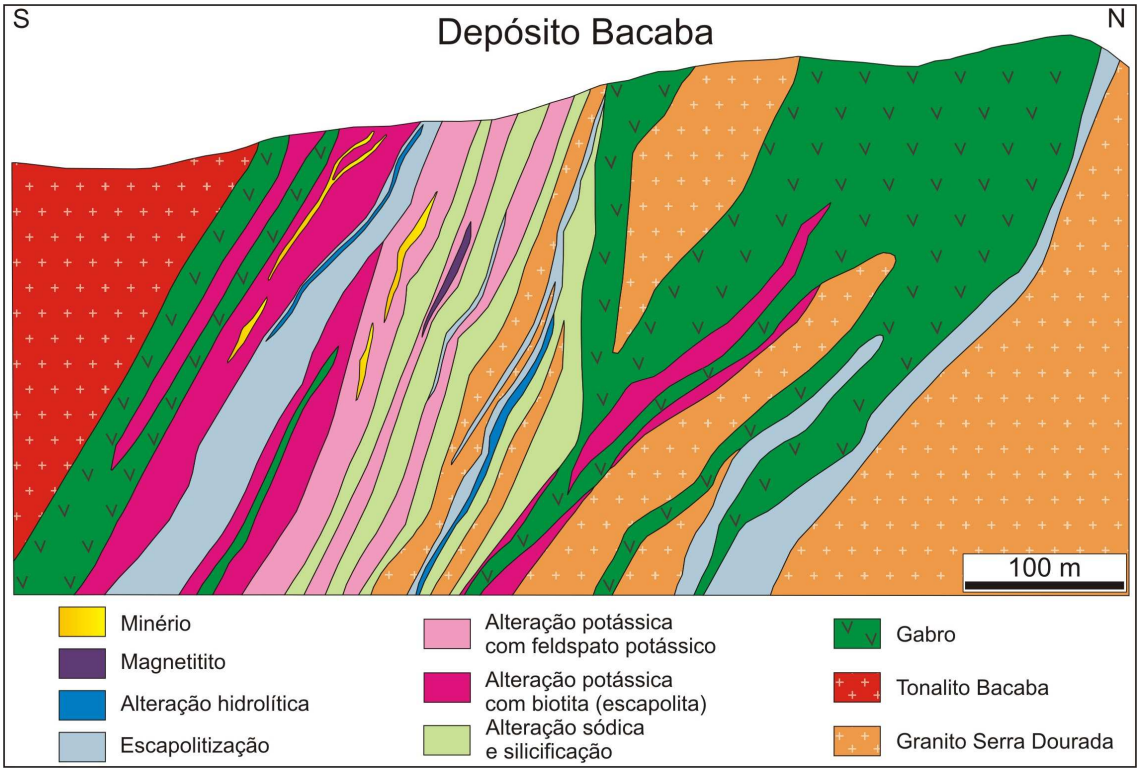

Figura 4. Seção esquemática mostrando as rochas hospedeiras do depósito Bacaba e a distribuição das zonas de alteração hidrotermal (modificado de Augusto et al., 2008).

O minério cuprífero do depósito Bacaba é hospedado por rochas graníticas (Granito Serra Dourada, Figs. 5A, I, K, P, Q e R e Tonalito Bacaba, Figs. 5E e N) e gabróicas (Figs. 5B, C, D, J e L) variavelmente hidrotermalizadas. Diferentemente da maioria dos depósitos IOCG de Carajás, o depósito Bacaba tem uma clara associação espacial com rochas graníticas, permitindo a investigação do papel dos granitos hospedeiros na gênese do depósito.

A seqüência de alterações hidrotermais (Fig. 5) presente tanto nos granitos quanto no gabro inicia-se por alteração sódica, representada por albitização (albita e hematita; Figs. 5D, G, H, J, K, N e Q) e por intensa escapolitização (escapolita marialítica, magnetita, quartzo e fluorita; Figs. 5D e M), seguida por alteração potássica (feldspato potássico, biotita, turmalina, potássio-cloro hastingsita; Figs. 5A, B, D, F, I, K e Q) e formação de magnetita (Figs. 5B e E), cloritização/epidotização (Figs. 5A, H, J, K, L e M), mineralização cuprífera (Figs. 5C, F, O e P) e sericitização tardia (Fig. 5R) (Augusto *et al*., 2008). A evolução paragenética do depósito Bacaba é semelhante à descrita para o depósito de Sossego (Monteiro *et al*., 2008a,b), sendo a principal diferença representada pela predominância de escapolita marialítica no depósito Bacaba, que ocorre em veios e zonas de substituição.

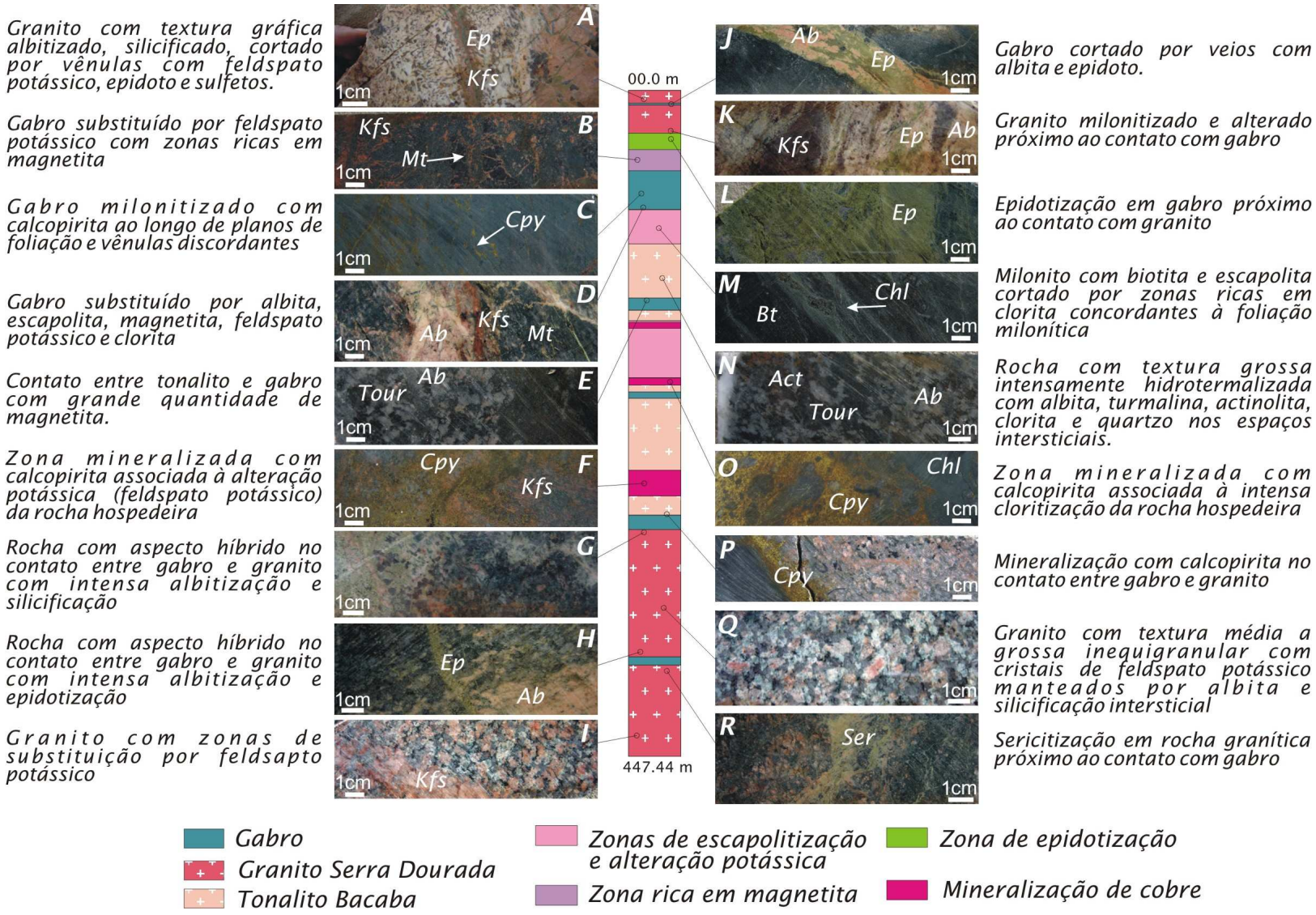

Figura 5. Principais feições das rochas hospedeiras hidrotermalizadas e mineralizadas do depósito Bacaba (Furo de sondagem BACD 15). Abreviações: Ab: albita; Act: actinolita; Bt: biotita; Chl: clorita; Cpy:calcopirita; Ep: epidoto; Kfs: feldspato potássico; Mt: magnetita; Ser: sericita; Tour: turmalina.

O principal mineral de minério é calcopirita que ocorre associada com bornita e calcocita e, subordinadamente, galena, teluretos (melonita, hessita, altaita) e óxidos (magnetita, hematita, uraninita, cassiterita). A assinatura geoquímica é caracterizada por enriquecimento em Cu-Fe-Ni-Co-Te-Ag-Pb-U-Sn, além de significativos conteúdos de ETR, Th e P evidenciados pela ocorrência de minerais de ganga (allanita, apatita, monazita, cheralita; Augusto *et al*., 2008).

Augusto *et al*. (2008) e Monteiro *et al*. (2008a,b) consideram que o depósito Bacaba e o depósito Sossego representem porções diferentes do mesmo sistema hidrotermal. A comparação das características desses depósitos com o modelo teórico proposto por Hitzman *et al.* (1992) sugere que o depósito Bacaba, notadamente pela escapolitização mais intensa, teria sido formado em zonas mais profundas e distais em relação ao depósito de Sossego (Fig. 6). Nessas condições a predominância de fluidos hipersalinos, atribuídos tanto a fontes magmáticas (Pollard, 2001; 2006) como a fontes externas, evaporíticas, (Barton & Johnson, 1996; 2000), seria condizente com a presença e abundância de escapolita marialítica.

No depósito Bacaba, as zonas de escapolitização seriam, portanto, relacionadas com o fluxo de fluidos metalíferos hipersalinos, que podem representar um halo distal ao redor dos corpos maiores de minério, reconhecidos no depósito Sossego. Neste contexto, as zonas de maior concentração de minério estariam associadas a falhas que teriam permitido a entrada de fluidos mais frios e de baixa salinidade (e.g. meteóricos) em maior escala, aumentando a eficiência da deposição do minério.

7. MÉTODOS

A caracterização das rochas hospedeiras, dos estágios de alteração hidrotermal e das paragênese de minério foram feitas através de mapeamento geológico nas proximidades do depósito Bacaba, descrição detalhada de testemunhos de sondagem de aproximadamente 16 furos de sondagem, e estudos petrográficos em luz transmitida e refletida. A etapa de campo teve duração de 15 dias, entre os dias 15 e 29 de julho de 2009, onde foi realizado um mapeamento geológico de uma área de aproximadamente 100 km², entre os municípios de Canaã dos Carajás e Paraopebas, Pará.

As amostras selecionadas para a geocronologia U-Pb correspondem a intervalos de testemunhos de sondagem com 1/4 do diâmetro total do testemunho. Os concentrados de zircão

foram extraídos de aproximadamente 300 a 500 g de rocha utilizando os métodos gravimétricos e magnéticos convencionais:

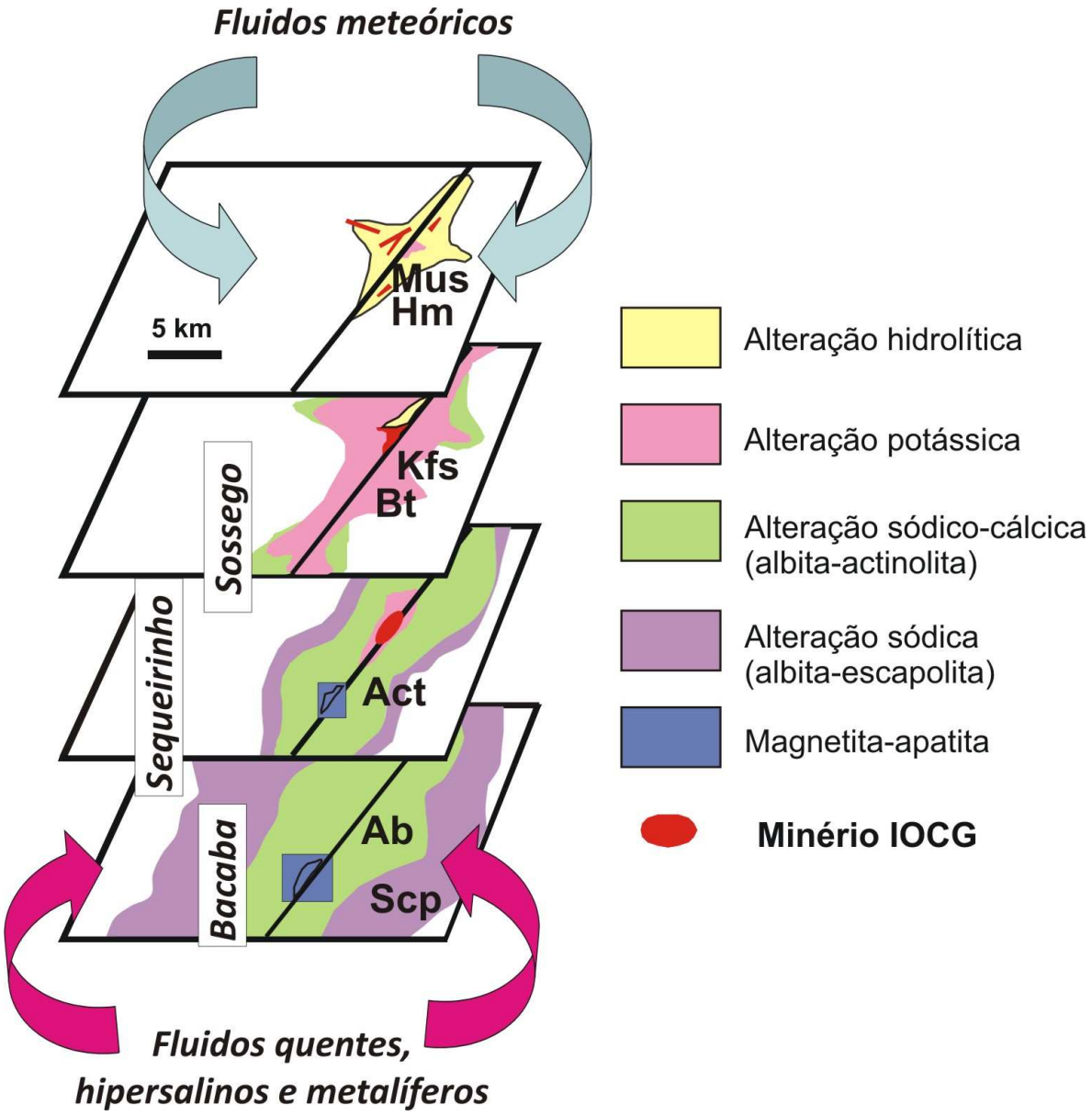

Figura 6. Modelo teórico de distribuição das zonas de alteração hidrotermais em sistemas hidrotermais IOCG em relação aos níveis crustais (adpatado de Hitzman et al., 1992). Abreviações: Ab: albita; Act: actinolita; Bt: biotita; Hm: hematita; Kfs: feldspato potássico; Mus: muscovita; Scp: escapolita.

1) Britagem em um britador de mandíbulas;
2) Moagem em um moinho vibratório por tempo inferior a 15 segundos;
3) Peneiragem em peneiras de nylon de 250 µm de abertura;

4) Bateamento manual;
5) Separação magnética através do separador isodinâmico Frantz;
6) Separação manual dos grãos de zircão em lupa binocular

Os grãos de zircão foram montados em *mounts* e fixados com resina epoxy e posteriormente polidos para obter uma superfície regular e lisa.

As análises U-Pb LA–ICP–MS em zircão foram feitas no Laboratório de Geocronologia da Universidade de Brasília. A descrição detalhada da técnica utilizada encontra-se no item "*4. Analytical Procedures"*, do artigo em anexo.

As imagens de elétrons retro-espalhados e de catodoluminescência foram obtidas em microscópio eletrônico de varredura no Instituto de Geociências da Universidade Estadual de Campinas, e na Escola Politécnica da Universidade de São Paulo, respectivamente.

8. RESULTADOS E APRESENTAÇÃO DO ARTIGO

Análises isotópicas U-Pb foram realizadas no Laboratório de Geocronologia da Universidade de Brasília. Foram selecionadas quatro amostras de testemunhos de sondagem do depósito Bacaba. As amostras são representativas das hospedeiras félsicas (Granito Serra Dourada e Tonalito Bacaba) variavelmente hidrotermalizadas, e consistem em: (i) uma amostra com alteração sódica do Granito Serra Dourada; (ii) uma amostra com alteração potássica do Tonalito Bacaba; (iii) duas amostras com alteração potássica e mineralização de Cu-Au do Tonalito Bacaba. As idades obtidas correspondem a 2858 ± 30 Ma (MSWD = 9.7) para o Granito Serra Dourada, e 2997,2 ± 4,7 Ma (MSWD = 1.15), 2993,1 ± 7,1 Ma (MSWD = 1.1) e 3004,7 ± 7,8 Ma (MSWD = 2.1) para o Tonalito Bacaba. As idades em 2,86 e ca. 3,0 Ga são interpretadas como idades de cristalização do Granito Serra Dourada e do Tonalito Bacaba, respectivamente.

Os resultados, discussões e contribuições das análises U-Pb do depósito Bacaba encontram-se sintetizados na forma de artigo submetido ao periódico *"Mineralium Deposita*. Este trabalho de mestrado também resultou na publicação de um resumo expandido, apresentado no "*Simpósio 45 anos de Geocronologia no Brasil"*, na Universidade de São Paulo em dezembro de 2009.

Anexo:

Mesoarchean (3.0 and 2.86 Ga) host rocks of the iron oxide–Cu–Au Bacaba deposit, Carajás Mineral Province: U–Pb geochronology and metallogenetic implications

Carolina P. N. Moreto [1]; Lena V. S. Monteiro [1]; Roberto P. Xavier [1]; Wagner S. Amaral [1]; Ticiano J. S. dos Santos [1]; Caetano Juliani [2]; Carlos Roberto de Souza Filho [1]

[1] *Geoscience Institute, University of Campinas – UNICAMP, Rua João Pandiá Calógeras, 51, CEP 13083–970, Campinas, SP, Brazil*

[2] *Geoscience Institute, University of São Paulo – USP, Rua do Lago, 562, CEP 05508-080, São Paulo, SP, Brazil*

E-mail address of Author: carolina.moreto@ige.unicamp.br
Telephone number of Author: +55 19 35214575
Fax number of Author: +55 19 32891097

Abstract

The Bacaba iron oxide–copper–gold deposit, situated in the Itacaiúnas Shear Belt, Carajás Mineral Province (Brazil), represents a satellite prospect of the world-class Sossego deposit, and might also represent a distal and deeper portion of the same or related hydrothermal system. The Bacaba deposit is located along a WNW–ESE-striking shear zone that defines the contact of the basement represented by the Xingu Complex (ca. 3.0 Ga) and the metavolcano-sedimentary Itacaiúnas Supergroup (ca. 2.76 Ga). The main host rocks at Bacaba deposit comprise the Serra Dourada Granite, the Bacaba Tonalite and croscutting gabbro, which were intensely affected by sodic (albite-scapolite), potassic, chloritic and hydrolytic hydrothermal alterations.

The U–Pb LA–ICP–MS data for zircon from sodic altered sample of the Serra Dourada Granite yielded an 2858 ± 30 Ma (MSWD = 9.7) age. Three samples from the Bacaba Tonalite, including one with potassic alteration and two with potassic alteration and Cu–Au mineralization rendered the 2997.2 ± 4.7 Ma (MSWD = 1.15), 2993.1 ± 7.1 Ma (MSWD = 1.1) and 3004.7 ± 7.8 Ma (MSWD = 2.1) ages, respectively. The 2.86 and ca. 3.0 Ga ages are interpreted as the igneous crystallization of the Serra Dourada Granite and the Bacaba Tonalite, respectively. The internal structures and external morphologies of zircon crystal from both rocks, observed in cathodoluminescence and backscattered electron images, attested the occurrence of zircon recrystallization, which could be related to hydrothermalism and/or deformation/metamorphism episodes that took place in the Carajás Mineral Province. However, the disturbing event (s) could not be dated due to the absence of the total resetting of the U–Pb system and hydrothermal crystallization of zircon.

The 2.86 Ga Serra Dourada Granite and the ca. 3.0 Ga Bacaba Tonalite are the oldest granitic rocks so far recognized in the Itacaiúnas Shear Belt. The presence of such old rocks implies in the existence of an important magmatism before the Carajás Basin (Itacaiúnas Supergroup) deposition, and in a more complex evolutionary history for the Itacaiúnas Shear Belt. The petrographical and geochronological similarities of these felsic intrusions with granitic and tonalitic rock suites recognized in the Rio Maria granite-greenstone terrane, southern part of the Carajás Mineral Province, implies in a more widespread ca. 3.0 and 2.86 Ga magmatism in the province.

The Serra Dourada Granite and the Bacaba Tonalite are interpreted not to be responsible for the genesis of the Bacaba deposit. This is likely because the Sossego and other deposits interpreted as part of the same hydrothermal system are hosted by younger ca. 2.76 Ga metavolcano-sedimentary units. On this context, the iron oxide-copper-gold deposit in the southern sector of the Itacaiúnas Shear Belt could be mainly controlled by important crustal discontinuities, such as the WNW–ESE-striking regional shear zone, rather than be associated with a particular rock type. These results expand the potentiality of occurrence of iron oxide–copper–gold deposits for the Mesoarchean basement rocks underlying the Carajás Basin, particularly those crosscut by Neoarchean shear zones.

Keywords: Bacaba deposit, iron oxide–Cu–Au deposits, U–Pb geochronology, Amazonian Craton, Carajás Mineral Province

1. Introduction

The Carajás Mineral Province (CMP), located in the southern part of the Amazon Craton (Brazil), represents one of the best-endowed mineral provinces in the world. This province hosts different mineral deposits (e.g. iron, manganese, gold, chrome–PGE) and includes the iron oxide–copper–gold (IOCG) deposits, which represents one of the major targets of the mineral research worldwide. The main IOCG deposits of the CMP correspond to Salobo (789 Mt @ 0.96% Cu, 0.52 g/t Au, 55 g/t Ag, Souza and Vieira, 2000), Igarapé Bahia/Alemão (219 Mt @ 1.4% Cu, 0.86 g/t Au, Tallarico *et al*., 2005), Sossego (245 Mt @ 1.1% Cu e 0.28 g/t Au, Lancaster *et al*., 2000), Gameleira (100 Mt @ 0.7% Cu, Rigon, 2000), Alvo 118 (70 Mt @ 1.0% Cu, 0.3 g/t Au, Rigon, 2000) and Cristalino (500 Mt @ 1.0% Cu, 0.3 g/t Au, Huhn *et al*., 1999).

Although controversy about the genetic models of the Carajás IOCG deposits remains, most of the proposed models have reinforced the importance of Archean (~2.75 or 2.57 Ga) or Paleoproterozoic (~1.88 Ga) granite intrusions as source of heat and fluids for the development of extensive hydrothermal systems (Huhn *et al*., 1999; Réquia *et al*., 2003; Tallarico *et al.*, 2005; Villas *et al.*, 2006; Neves, 2006; Pollard, 2006; Grainger *et al.*, 2008). Nonetheless, most of IOCG deposits are hosted by metavolcano-metassedimentary units of the ~ 2.76 Ga Itacaiúnas Supergroup and clear spatial and temporal association with coeval granitic rocks has been reported in few cases (e.g. ~2.74 Ga Cristalino deposit, Huhn *et al*., 1999a,b; ~2.57 Ga Salobo deposit, Réquia *et al.*, 2003). Until now, the source(s) of fluids and metals and genetic relationship with magmatism is an outstanding problem of current metallogenic models.

Available geochronological data for IOCG deposits of the CMP, including for their host rocks, are not sufficiently precise to support that all these deposits are genetically linked. Dating of ore-related minerals has given different ages even in a single deposit (e.g. Igarapé Bahia/Alemão, Gameleira, Salobo and Igarapé Cinzento deposits; Pimentel *et al*., 2003; Réquia *et al*., 2003; Marschik *et al*., 2005; Tallarico *et al*., 2005, Galarza *et al*., 2008). This could reflect a long-term history of isotopic resetting due to the development and/or reactivation of Archean ductile or ductile-brittle shear zones and/or Archean and Paleoproterozoic magmatism (Xavier *et al*., in press).

The Bacaba deposit, located 7 km to east from the Sossego mine, represents a satellite target of this world-class IOCG deposit, which was the first to go into production in 2004 under the responsibility of VALE, former Companhia Vale do Rio Doce (CVRD). Unlikely most of the

IOCG deposits of Carajás, the Bacaba deposit has clear spatial relationship with granitic rocks, represented by the Bacaba Tonalite and the Serra Dourada Granite, allowing the investigation of the host granites role on the genesis of this deposit. These host rocks underwent intense high-temperature (> 550 ^{o}C) hydrothermal alteration (e.g. albitization, scapolitization, potassic alteration), similar to those described at Sossego (Augusto *et al.*, 2008; Monteiro *et al.*, 2008a,b).

This paper presents results of in situ LA–ICP–MS U–Pb zircon geochronological analyses of the hydrothermally altered and mineralized samples of the Serra Dourada Granite and the Bacaba Tonalite. The results provide new insights into the metallogenesis of IOCG deposits and the Archean magmatism of the CMP, revealing the existence of magmatic events so far unconsidered for the northern sector of the CMP.

2. Geological Setting of the Carajás Mineral Province

The CMP is one of the most well-preserved cratonic areas in the world and comprises two Archean tectonic domains: i) the Itacaiúnas Shear Belt in the northern part (Fig. 1); and ii) the Rio Maria granite-greenstone terrane in the southern portion (Fig. 2). The two domains are limited by a regional E–W shear zone located to the north of Sapucaia city, where a Transition Domain was characterized (Dall'Agnol *et al*., 2006). These authors defined the Transition Domain as a terrane originally similar to the Rio Maria granite-greenstone terrane that was intensively affected by the magmatic and tectonic events recorded in the Itacaiúnas Shear Belt (Gomes, 2003; Gomes *et al*., 2004; Sardinha *et al*., 2004).

2.1 Itacaiúnas Shear Belt

The Itacaiúnas Shear Belt (Fig. 1) comprises the basement and supracrustal sequences. A summary of the available geochronological data of the Itacaiúnas Shear Belt is shown in Table 1. The basement is composed of tonalitic to trondhjemitic gneisses and migmatites of the Xingu Complex and mafic to felsic (enderbites and charnockites) orthogranulites of the Pium Complex. Crystallization ages of igneous protolith of the Pium granulites yielded 3002 ± 14 Ma (U–Pb SHRIMP zircon; Pidgeon *et al*., 2000) and 3050 ± 57 Ma (Pb–Pb whole-rock; Rodrigues *et al*., 1992) ages. The migmatization event that affected the Xingu Complex and the high-grade metamorphism of the Pium Complex were coeval and took place at 2859 ± 2 Ma (U–Pb zircon;

Machado *et al*., 1991) and 2859 ± 9 Ma (U–Pb SHRIMP zircon; Pidgeon *et al*., 2000), respectively.

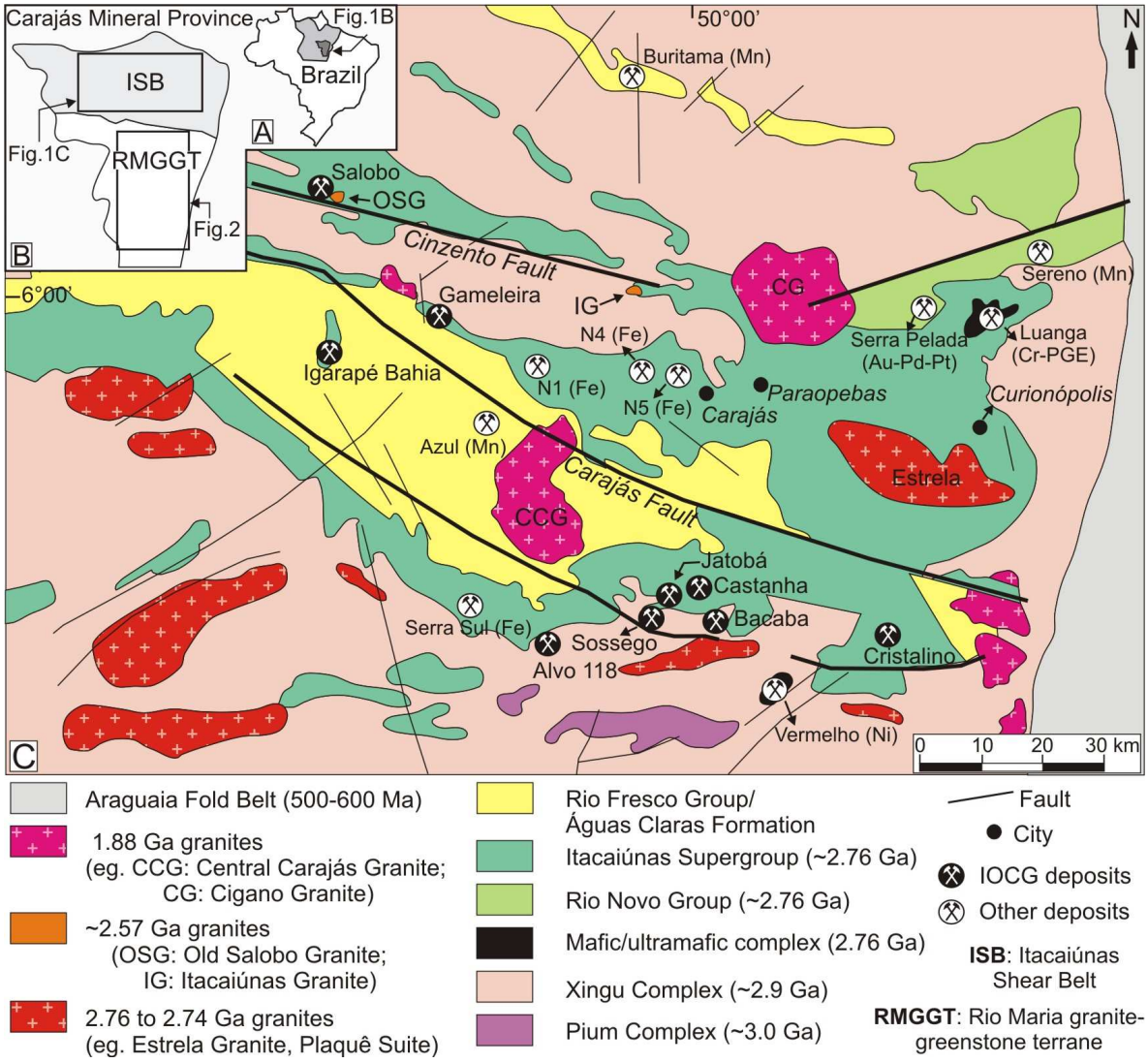

Figure 1. Geological map of the Itacaiúnas Shear Belt (modified from Dardenne and Schobbenhaus, 2001).

The Carajás Basin overlies the basement rocks and comprises the ca. 2.76 Ga metavolcanic-sedimentary Rio Novo Group (Hirata *et al*., 1982) and the 2.73 to 2.76 Ga Itacaiúnas Supergroup, divided into the Igarapé Bahia, Grão Pará, Igarapé Pojuca and Salobo groups (Wirth *et al*., 1986; DOCEGEO, 1988; Machado *et al*., 1991).

Table 1. Available geochronological data of the Itacaiúnas Shear Belt

Unit	Age (Ma)	Method	Reference
Granitic rocks			
Formiga Granite	ca. 600	U–Pb, Zr (*)	Grainger et al. 2008
Gameleira Granite	1583 ± 9	U–Pb, Zr (*)	Pimentel et al. 2003
Central Carajás Granite	1880 ± 2	U–Pb, Zr	Machado et al. 1991
	1820 ± 49	U–Pb, Zr	Wirth et al. 1986
Pojuca Granite	1874 ± 2	U–Pb, Zr	Machado et al. 1991
	2560 ± 37	Pb–Pb, Zr	Souza et al. 1996
Breves Granite	1879 ± 6	U–Pb, Zr (*)	Tallarico et al. 2004
Young Salobo Granite	1880 ± 80	Rb–Sr, WR	Cordani 1981
Cigano Granite	1883 ± 2	U–Pb, Zr	Machado et al. 1991
Old Salobo Granite	2573 ± 2	U–Pb, Zr	Machado et al. 1991
Itacaiúnas Granite	2525 ± 38	Pb–Pb, Zr	Souza et al. 1996
dacitic to rhyolitic porphyry	2645 ± 9, 2654 ± 9	U–Pb, Zr (*)	Tallarico 2003
Estrela Granite	2527 ± 34	Rb–Sr, WR	Barros et al. 1992
	2763 ± 7	Pb–Pb, Zr	Barros et al. 2004
biotite-hornblende granite	2734 ± 4	Pb–Pb, Zr	Sardinha et al. 2004
trondhjemite	2765 ± 39	U–Pb, Zr	Sardinha et al. 2004
Serra do Rabo Granite	2743 ± 1.6	U–Pb, Zr	Sardinha et al. 2006
Plaquê Suite	2736 ± 24	Pb–Pb, Zr	Avelar et al. 1999
Planalto Granite	2747 ± 2	Pb–Pb, Zr	Hunh et al. 1999
leucomonzogranite	2928 ± 1	Pb–Pb, Zr	Sardinha et al. 2004
Águas Claras Formation/ Rio Fresco Group			
sandstone (with zircon derived from syndepositional volcanic rock)	2681 ± 5	U–Pb, Zr (*)	Trendall et al. 1998
crosscutting gabbro dikes	2645 ± 12	U–Pb, Zr	Dias et al. 1996
Mafic dikes and sills, metagabbros			
metagabbro	2708 ± 37	U–Pb, Zr	Mougeot et al. 1996
mafic intrusive rock	2705 ± 2	Pb–Pb, Zr	Galarza and Macambira 2002b
metagabbro and cogenetic metavolcanic rocks	2757 ± 81	Sm–Nd, WR	Pimentel et al. 2003
Itacaiúnas Supergroup			
Igarapé Bahia Group			
mafic metavolcanic rock	2748 ± 34	U–Pb, Zr (*)	Tallarico et al. 2005
mafic metavolcanic rock	2745 ± 1	Pb–Pb, Zr	Galarza and Macambira 2002a
metapyroclastic rock	2747 ± 1	Pb–Pb, Zr	Galarza and Macambira 2002a
Grão Pará Group			
rhyolite	2759 ± 2	U–Pb, Zr	Machado et al. 1991
felsic volcanic rock	2758 ± 39	U–Pb, Zr	Wirth et al. 1986
porphyritic metarhyolite	2760 ± 11	U–Pb, Zr (*)	Trendall et al. 1998
rhyodacite	2759 ± 2	Pb–Pb, Zr	Machado et al. 1991
basalt and basaltic andesite	2687 ± 54	Rb–Sr, WR	Gibbs et al. 1986
Igarapé Pojuca Group			
amphibolite	2732 ± 2	U–Pb, Zr	Machado et al. 1991
meta-andesite	2719 ± 80	Sm–Nd, WR	Pimentel et al. 2003

Table 1. (continued)

Unit	Age (Ma)	Method	Reference
Salobo Group			
foliated amphibolite	2761 ± 3	U–Pb, Zr	Machado et al. 1991
	2497 ± 5	U–Pb, Ti	Machado et al. 1991
granitic vein	2732	Pb–Pb, Zr	Machado et al. 1991
	2581 ± 5, 2584 ± 5	U–Pb, Ti	Machado et al. 1991
amphibolite	2555 +4/-3	U–Pb, Zr	Machado et al. 1991
banded iron formation	2551 ± 2	U–Pb, Mz	Machado et al. 1991
Basic-ultrabasic layred complex (Luanga Complex)			
anorthositic gabbro	2763 ± 6	U–Pb, Zr	Machado et al. 1991
Xingu Complex			
amphibolite	2856 ± 3	Pb–Pb, Zr	Machado et al. 1991
	2519 ± 5	U–Pb, Ti	Machado et al. 1991
granitic leucosome	2859 ± 2, 2860 ± 2	U–Pb, Zr	Machado et al. 1991
felsic gneiss	2851 ± 2	U–Pb, Zr	Machado et al. 1991
granodioritic orthogneiss	2974 ± 15	Pb–Pb, Zr	Avelar et al. 1999
Pium Complex			
granulite	3050 ± 57	Pb–Pb, Zr	Rodrigues et al. 1992
protoliths of the enderbite	3002 ± 14	U–Pb, Zr (*)	Pidgeon et al. 2000
granulitization event	2859 ± 9	U–Pb, Zr (*)	Pidgeon et al. 2000

Abbreviations : (*): SHRIMP; Zr: zircon; Ti: titanite; Mz: monazite; WR: whole rock.

The Itacaiúnas Supergroup hosts several IOCG deposits (e.g. Salobo, Sossego, Gameleira, Igarapé Bahia/Alemão and Alvo 118 deposits) and consists of basic and felsic metavolcanic rocks, metapyroclastic and metavolcaniclastic rocks, banded iron formations, amphibolite and schist.

The complex structural evolution of the CMP and dynamic metamorphism of the Archean units have been attributed to the development of regional E–W trending, steeply dipping fault zones that show evidence of several episodes of movement (Holdsworth and Pinheiro, 2000). According to these authors, the Itacaiúnas sinistral transpressive strike-slip ductile shear zone was developed between 2.85 to 2.76 Ga. Dextral transtension led to the development of the Carajás and Cinzento strike-slip fault systems between 2.7 and 2.6 Ga. A late sinistral transpressional regime developed about 2.6 Ga resulted in moderate to strong deformation of the rocks immediately adjacent to the Carajás and Cinzento fault systems. At ca. 1.9 Ga, extension or

transtension events were accompanied by the emplacement of anorogenic granites and mafic dike swarms.

The Itacaiúnas Supergroup is overlain by low-grade metasedimentary rocks deposited in fluvial to shallow marine environment, known as the Rio Fresco Group (DOCEGEO, 1988) or Águas Claras Formation (Nogueira *et al*., 1994, 2000). Dating of detrital zircon in sandstones (2681 ± 5 Ma; Trendall *et al*., 1998) and meta-gabbro sills (2645 ± 12 Ma and 2708 ± 37 Ma; Dias *et al*., 1996; Mougeot *et al*., 1996) constrains the age of the Águas Claras Formation to the Archean. This sequence hosts the Breves Cu–Au, Águas Claras and Serra Pelada Au–Pd–Pt deposits.

In the Itacaiúnas Shear Belt, three events of granitic magmatism were identified: i) 2.76 to 2.74 Ga alkaline granites, comprising the Plaquê, Planalto, Estrela and Serra do Rabo suites (Huhn *et al*., 1999; Avelar *et al*., 1999; Sardinha *et al*., 2006; Barros *et al*., 2004); ii) 2.57 Ga peralkaline to meta-aluminous granites, characterized by the Old Salobo and Itacaiúnas granites (Machado *et al*., 1991; Souza *et al*., 1996); and iii) 1.88 Ga A-type alkaline to sub-alkaline granites, including the Central de Carajás, Young Salobo, Cigano, Pojuca, Breves, Musa, Jamon, Seringa and Velho Guilherme granites (Machado *et al*., 1991; Dall'Agnoll *et al*., 1994; Lindenmayer and Teixeira, 1999; Tallarico, 2003).

Other intrusive rocks correspond to ca. 2.75 Ga mafic-ultramafic intrusions of Luanga, Onça, Vermelho and Jacaré-Jacarezinho (Machado *et al*., 1991). Additionally, dacitic to rhyolitic porphyry dated at 2645 ± 9 Ma and 2654 ± 9 Ma (Pb–Pb SHRIMP zircon; Tallarico, 2003) were recognized at Carajás. Alkali-rich leucogranite dyke with a U–Pb SHRIMP age of 1583 + 9/ − 7 Ma (Pimentel *et al*., 2003) was also described in the Gameleira deposit area. Neoproterozoic (~600–550 Ma) age was estimated for the Formiga Granite, which can represent the younger granite magmatism in the province (Grainger *et al*., 2008). The province was also affected by other magmatic events represented by late underformed diabase, diorite, and gabbro dykes, whose ages are uncertain.

Within the Transition Domain, Feio *et al*. (2009) distinguished five magmatic associations based on geochemistry evidence: i) calc-alkaline leucogranites; ii) tonalitic calc-alkaline associations; iii) TTG-like trondhjemites; iv) Ti, Y and Zr-rich tonalitic/trondhjemitic associations; and v) sub-alkaline A-type granites. Geochronology data for these magmatic associations are not available and correlation among these rocks and those of the Itacaiúnas Shear

Belt or the Rio Maria granite-greenstone terrane is still poorly understood. However, Sardinha *et al*. (2004) reported Pb–Pb zircon ages for leucogranite (2928 ± 1 Ma), biotite-hornblende granite (2734 ± 4 Ma), and trondhjemite (2765 ± 39 Ma) from the Transition Domain. The Neoarchean ages are comparable to those related to the extensive ca. 2.74 to 2.76 Ga alkaline magmatism recorded in the Itacaiúnas Shear Belt, whereas the leucogranite could be correlated, according the authors, to the Guaratã Granite or the Caracol Tonalite from the Rio Maria granite-greenstone terrane.

2.2 The Rio Maria granite-greenstone terrane

The Rio Maria granite-greenstone terrane (Fig. 2) comprises greenstone belt sequences of the 2.97 to 2.90 Ga Andorinhas Supergroup (DOCEGEO, 1988; Macambira and Lancelot, 1992, 1996; Pimentel and Machado, 1994; Souza *et al*., 2001). These sequences are composed of komatiites and tholeiitic basalts at the bottom and felsic volcanic and sedimentary rocks at the top. All of these rocks were affected by a tectono-thermal event that caused metamorphism in greenschist to lower amphibolite facies and result in a penetrative W-E to WNW-ESE-trending subvertical shear foliation (Souza *et al*., 1990). A summary of the available geochronological data of the Rio Maria granite-greenstone terrane is given in Table 2.

Several Archean granitic suites with different composition and ages intruded the greenstone belt sequences, and consist of:

1) ~2.95 Ga TTG suite including the Arco Verde (2957 +25/-21 Ma, Macambira and Lancelot, 1996) and Caracol tonalites (2948 ± 5 Ma, Leite *et al*., 2004);

2) ~2.87 Ga sanukitoid rocks (Dall'Agnol *et al*., 2006; Oliveira *et al*., 2009) exemplified by the Rio Maria Granodiorite (2874 +9/-10 Ma, Macambira and Lancelot, 1996; 2872 ± 5 Ma, Pimentel and Machado, 1994);

3) ~2.86 Ga TGG suite, corresponding to Mogno (2857 ± 13 Ma, Macambira *et al*., 2000) and Água Fria trondhjemites (2864 ± 21 Ma, Leite *et al*., 2004);

4) ~2.86–2.89 Ga potassic leucogranites of calc-alkaline affinity (Xinguara, 2865 ± 1 Ma, Leite *et al*., 2004; Mata Surrão, 2872 ± 10 Ma, Lafon *et al*., 1994, 2894 ± 38 Ma, Barbosa and Lafon, 1996; and Rancho de Deus granites).

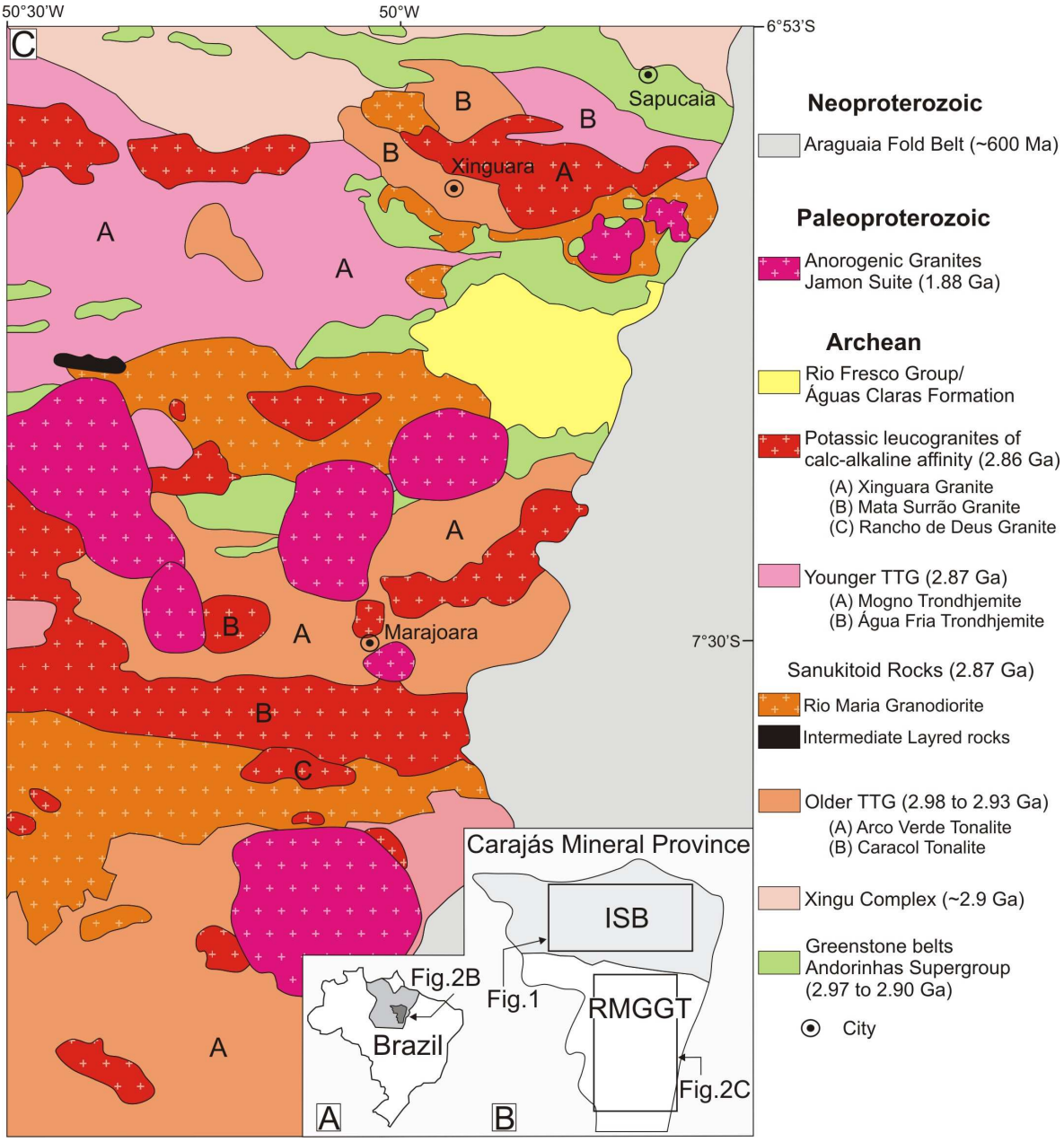

Figure 2. Geological map of the Rio Maria granite-greenstone terrane (Oliveira et al., 2009).

The tonalite and trondhjemite of both TTG suites have been considered as originated from partial melting of eclogite or garnet amphibolite in a subduction zone setting, whereas the granodiorite of the same suites should be the result of partial melting of an oceanic crust (Althoff, 1996; Dall'Agnol *et al*., 1997). The leucogranites are interpreted as partial melting of continental sources (Dall'Agnol *et al*., 1997).

Table 2. Available geochronological data of the Rio Maria granite-greenstone terrane

Unit	Age (Ma)	Method	Reference
Granitic rocks			
Musa Granite	1883 +5/-2	U–Pb, Zr	Machado et al. 1991
	1884 ± 5	U–Pb, Ti	Machado et al. 1991
Jamon Granite	1885 ± 32	Pb–Pb, Zr	Dall' Agnol et al. 1999
Potassic leucogranites of calc-alkaline affinity			
Xinguara Granite	2865 ± 1, 2866 ± 2	Pb–Pb, Zr	Leite et al. 2001
	2800 ± 18	U–Pb, Zr	Macambira 1992
Mata Surrão Granite	2872 ± 10	Pb–Pb, Zr	Rodrigues et al. 1992
	2872 ± 10	Pb–Pb, WR	Lafon et al. 1994
	2894 ± 19	Pb–Pb, WR	Barbosa and Lafon 1996
	2871 ± 7	Pb–Pb, Zr	Althoff et al. 1998
Younger TTG Suites			
Mogno Trondhjemite	2871 ± ?	U–Pb, Ti	Pimentel and Machado 1994
	2900 ± 74	Pb–Pb, Zr	Macambira et al. 2000
	2857 ± 74	Pb–Pb, Zr	Macambira et al. 2000
Água Fria Trondhjemite	2864 ± 21	Pb–Pb, Zr	Leite et al. 2001
Sanukitoids			
Rio Maria Granodiorite	2874 +9/-10	U–Pb, Zr	Macambira and Lancelot 1996
	2872 ± 5	U–Pb, Zr, Ti	Pimentel and Machado 1994
	2852 ± 16	Pb–Pb, Zr	Avelar et al. 1999
	2878 ± 4	Pb–Pb, Zr	Dall' Agnol et al. 1999
Older TTG			
Arco Verde Tonalite	2957 +25/-21	U–Pb, Zr	Macambira and Lancelot 1996
Caracol Tonalite	2948 ± 5, 2936 ± 3, 2924 ± 2	Pb–Pb, Zr	Leite et al. 2001
Xingu Complex			
tonalitic gneiss	2798	Pb–Pb, Ti	Pimentel and Machado 1994
Basic-ultrabasic layred complex (Serra Azul Complex)	2970 ± 7	U–Pb, Zr	Pimentel and Machado 1994
Andorinhas Supergroup (Greenstone belt sequence)			
metagraywackes	2971 ± 18	U–Pb, Zr	Macambira and Lancelot 1991
metarhyodacite	2904 +29/-22	U–Pb, Zr	Macambira and Lancelot 1996
	2979 ± 5	U–Pb, Zr	Pimentel and Machado 1994
metadacite	2944 ± 88	Pb–Pb, WR	Souza 1994

Abbreviations: Zr: zircon; Ti: titanite; WR: whole rock.

The Archean crust was also intruded by several ca. 1.88 Ga A-type granites of the Musa and Jamon suites (Machado *et al*., 1991; Dall'Agnol *et al*., 1999, 2005; Dall'Agnol and Oliveira, 2007) that are similar to the Paleoproterozoic granites observed in the Itacaiúnas Shear Belt.

Other units found in the Rio Maria granite-greenstone terrane are basic to ultrabasic layered rocks, as the ca. 2.97 Ga Serra Azul Complex (Pimentel and Machado, 1994), and the platform sedimentary sequence of the Águas Claras Formation/Rio Fresco Group (Macambira and Lancelot, 1996; Macambira *et al*., 1998) that also occurs in the Itacaiúnas Shear Belt.

3. Iron oxide-copper-gold deposits in the Carajás Mineral Province

Most of the known IOCG deposits of the CMP are located along or in the vicinities of regional shear zones that define the contact of the metavolcano-sedimentary units of the Itacaiúnas Supergroup (~2,76 Ga) and the basement (Xingu Complex, ~3,0 Ga). The Cinzento shear zone, which marks the northern contact zone, hosts the Salobo and Igarapé Cinzento/Alvo GT46 deposits. The southern contact is defined by a WNW–ESE-striking, 60 km-long shear zone, along which the Alvo 118, Sossego, Cristalino and several other satellite deposits (e.g. Bacaba, Castanha, Jatobá, Visconde and Bacuri) occur.

The IOCG deposits in the CMP are hosted mainly by the metavolcano-sedimentary rocks of the Itacaiúnas Supergroup and crosscutting intrusive rocks (e.g. gabbro, diorite, granite, granophyric granite, feldspar-quartz porphyry and tonalite).

Distinct hydrothermal alteration assemblages have been identified along these shear zones, with almandine-, sillimanite-, and fayalite-bearing alteration assemblages recognized only along the Cinzento shear zone. Despite this, high temperature (> 550 ^{o}C) sodic to iron-potassic hydrothermal alteration synchronous to ductile deformation followed by lower temperature (< 300 ^{o}C) chloritic, carbonatic and hydrolytic alterations and copper-gold mineralization associated with hydrostatic brittle conditions have been recognized in the IOCG deposits at Carajás (e.g. Salobo, Lindenmayer, 2003; Sossego, Monteiro *et al.*, 2008a,b; Cristalino, Huhn *et al.* 1999a,b; Alvo 118, Torresi *et al*., Submitted).

A similar ore geochemical signature for the Carajás IOCG deposits (Fe-Cu-Au ± REE, U, P, Co, Ni) is indicated by the mineral association represented by chalcopyrite with subordinated pyrite, bornite, hematite, magnetite, chalcocite, siegenite, vaesite, millerite, melonite, galena, sphalerite, hessite, cassiterite, molybdenite, native gold, monazite, allanite, apatite, xenotime and uraninite.

The distribution of hydrothermal alteration zones in a single deposit reveals spatial zoning as an important feature of the Carajás IOCG deposits. The Sossego deposit is distinctive in this aspect because it appears to contain mineralized zones similar to those recognized worldwide as formed at a range of depths, providing a vertical view of a major IOCG hydrothermal system. The deeper portion of the deposit, represented mainly by the Sequeirinho orebody, has undergone regional sodic (albite-hematite) and actinolite-rich sodic-calcic alterations. The latter was associated with the formation of massive magnetite bodies enveloped by apatite-rich actinolitite (Monteiro *et al*., 2008a,b). Vertically focused potassic alteration zones cut the sodic-calcic alteration zones and grade laterally to chloritic zones, which predominate in the structurally higher Sossego and Curral orebodies. Similar potassic alteration overprinted by chloritic alteration was also identified in the Alvo 118 deposit, which may represent a shallow-emplaced deposit (Torresi, 2009; Torresi *et al*., Submitted).

The Sossego deposit has a wide (> 20 km) external halo of scapolitic and biotite-rich hydrothermal alteration, which is typical of the satellite orebodies located around this deposit, including the Bacaba deposit (Augusto *et al*., 2008).

Relationships between paragenetic and microstructural evolution in several IOCG deposits along the southern contact (e.g. Alvo 118, Cristalino, Sossego and its satellite deposits) suggest synchronicity in the evolution of the hydrothermal paleo-systems responsible for their genesis (Huhn *et al*., 1999; Monteiro *et al*., 2008a,b; Torresi *et al*., Submitted). This could imply that the Bacaba deposit represent a portion of a wide hydrothermal system.

3.1 Geochronology of iron oxide-copper-gold deposits in the Carajás Mineral Province

Available geochronological data for the IOCG deposits of the CMP are still scarce (Fig. 3; Table 3). In general, geochronological data yielded by Pb–Pb systematics reflect older ages (~2.7 Ga) and collectively have suggested metal sources from the Itacaiúnas Supergroup units and genetic relationships with the emplacement of syntectonic alkaline granites (e.g. 2.74 Ga Planalto Granite) and/or ~2.75 to 2.65 Ga gabbro-diorite bodies. Younger Pb–Pb ages have been interpreted as result of partial resseting of the isotopic system due to tectonic reactivation of the Carajás and Cinzento strike-slip fault systems (Gameleira deposit, Galarza and Macambira, 2002;

Table 3. Summary of geochronological data for the IOCG deposits of the Carajás Mineral Province

Deposit	Age (Ma)	Method	Age Interpretation	Reference
Salobo	2576 ± 8	Re–Os Mb	Timing of mineralization is synchronous with the ~ 2.57 Ga Old Salobo granite emplacement	Réquia et al. 2003
	2562 ± 8	Re–Os Mb		
	2579 ± 71	Pb–Pb Bn/ Cpy		
	2705 ± 42	Pb–Pb Cc	Timing of Cu–Au mineralization	Tassinari et al. 2003
	2587 ± 150	Pb–Pb Tour	Tectonic reativation associated with the Carajás and Cinzento strike-slip fault systems	
	2427 ± 130	Pb–Pb Cpy		
	2112 ± 12	Pb–Pb Mt	Resseting related to the ~1.88 Ga Young Salobo granite emplacement	
Igarapé Cinzento	2711 ± 9	Re–Os Mb	Molybdenite formation genetically linked to monzogranite emplacement	Silva et al. 2005
	2554 ± 8	Re–Os Mb		
	1809 ± 6	Ar–Ar Bt	Timing of Cu–Au mineralization	
	1845 ± 5	Ar–Ar Bt		
Gameleira	2614 ± 14	Re–Os Mb	Genetic relationship of mineralization with the 2.56–2.76 Ga Archean alkaline granitoids or with the 2.6–2.7 calc-alkaline to tholeiitic magmatism. This age also coincides with tectonic reactivations associated with the formation of Carajás and Cinzento strike-slip fault systems	Marschik et al. 2005
	2419 ± 12	Pb–Pb Cpy	Parcial Pb–Pb system resseting due to Proterozoic granite emplacement (1.58 and 1.87 Ga) or/and tectonic reativation of Carajás and Cinzento strike-slip fault systems	Galarza and Macambira 2002
	2217 ± 19	Pb–Pb Cpy		
	2180 ± 84	Pb–Pb Cpy		
	1839 ± 15	Sm–Nd WR	Timing of mineralization related to a Paleoproterozoic (~1.83 Ga) episode of hydrothermal activity. The mineralizing fluids were derived from a Paleoproterozoic crustal granite, similar to the Pojuca Granite	Pimentel et al. 2003
	1700 ± 31	Sm–Nd WR	Lower blocking temperatures of biotite in relation to the Ar–Ar and Sm–Nd isotopic systems	
	1734 ± 8	Ar–Ar Bt		
Igarapé Bahia	2744 ± 12	Pb–Pb Au	Timing of syngenetic Cu–Au mineralization genetically linked with volcanic processes	Galarza et al. 2008
	2772 ± 46	Pb–Pb Cpy		
	2756 ± 24	Pb–Pb Cpy		
	2754 ± 36	Pb–Pb Cpy		
	2777 ± 22	Pb–Pb Cpy		
	2385 ± 122	Pb–Pb Cpy	Remobilization due to regional tectonic reactivation (Carajás and Cinzento strike-slip fault systems)	
	2417 ± 120	Pb–Pb Cpy		
	2764 ± 22	Pb–Pb Cpy/Au	Timing of Cu–Au mineralization coeval with the formation of the Itacaiúnas Supergroup	Galarza 2002
	2575 ± 12	U-Pb Mnz SRHIMP II	Timing of Cu–Au mineralization temporally related to A-type Archean granites of Carajás	Tallarico et al. 2005

Table 3. (continued)

Deposit	Age (Ma)	Method	Age Interpretation	Reference
Cristalino	2719 ± 36	Pb–Pb Cpy/Py	Timing of Cu–Au mineralization and of the Planalto granite and diorite that occur in the deposit area	Soares et al. 2001
Sossego	2530 ± 25	Pb–Pb Cpy	Mineralization would be associated with 2.76-2.74 Ga granite event and these ages would reflect parcial Pb-Pb system openning due to later deformacional/thermal events; or would be related to metamorphic process and these ages would register the shearing event	Neves 2006
	2608 ± 25	Pb–Pb Cpy		
	1592 ± 45	Pb–Pb Cpy	There is no geological meaning	
	2578 ± 29	Sm–Nd WR	Parcial Pb-Pb system resseting due to later events	
Alvo 118	1869 ± 7	U–Pb Xn SRHIMP II	Evidence of a distinct metallogenic event in relation to that associated with the main IOCG deposits at Carajás	Tallarico 2003
	1868 ± 7	U–Pb Xn SRHIMP II		

Abbreviations: Bt: biotite; Bn: bornite; Cc: chalcocite; Cpy: chalcopyrite; Mt: magnetite; Mb: molybdenite; Mnz: monazite; Py: pyrite; Tour: tourmaline; WR: Whole rock; Xn: xenotime.

Salobo deposit, Tassinari *et al*., 2003; Sossego deposit, Neves, 2006; Igarapé Bahia deposit, Galarza *et al*., 2008).

More robust and precise geochronological data, including U–Pb SHRIMP II dating on xenotime and monazite and Re–Os on molybdenite, have pointed to an important metallogenetic event at 2.57 Ga (Réquia *et al*., 2003; Tallarico *et al*., 2005), which has been related to Late Archean magmatism. Nevertheless, Old Salobo and Itacaiúnas are the only two examples of 2.57 to 2.56 Ga granites (Machado *et al*., 1991; Souza *et al*., 1996) in the entire CMP, and occur narrowly close to the Cinzento fault system. Except for the former that was recognized in drill cores from the Salobo deposit, no clear spatial association between IOCG deposits and granitic magmatism of this age has been demonstrated in the province.

Additionally, dating of ore-related minerals has given different ages even in a single deposit (Fig. 3; Table 3). At Gameleira deposit, Marschik *et al*. (2005) consider that the mineralizing event occurred at 2.61 Ga (Re–Os molybdenite) while Pimentel *et al*. (2003) proposed that it took place at 1.84 Ga (Sm–Nd whole rock). At Igarapé Bahia deposit, the mineralization ages would correspond to ca. 2.7 Ga (Pb–Pb chalcopyrite, Galarza *et al*., 2008; Galarza, 2002) or 2.57 Ga (U–Pb SHRIMP II monazite, Tallarico *et al*. 2005). A summary of the

available geochronological data of the IOCG deposits in the Carajás Mineral Province is shown in Table 3 and Fig. 3.

4. Analytical procedures

Characterization of host rocks, hydrothermal alteration stages and ore paragenesis was carried out using mapping in the vicinities of the Bacaba deposit, detailed descriptions of drill cores from 16 drill holes and petrographic studies under transmitted and reflected light. The backscattered electron and the cathodoluminescence images were obtained using a scanning electron microscope at the Institute of Geoscience, University of Campinas and at the University of São Paulo, respectively.

For geochronology, zircon grains were selected using conventional optical microscopy, backscattered electron and cathodoluminescence images. Zircon concentrates were extracted from ca. 400 g rock using conventional gravimetric and magnetic techniques. Mineral fractions were handpicked under binocular microscope, mounted in epoxy blocks and polished in order to obtain a regular smooth surface.

The U–Pb LA–ICP–MS zircon isotopic analyses were carried out at the Geochronology Laboratory of the University of Brasília according to the method described by Bühn *et al*. (2009).

The mounts were cleaned with HNO_3 and loaded into a New Wave UP213 Nd:YAG laser (λ = 213nm), linked to a Thermo Finnigan Neptune Multi-collector ICP–MS. Helium was used as the carrier gas and mixed with argon before entering the ICP. The laser was run at a frequency of 60 Hz and 70% of energy with the spot size of 30 μm.

The standard analyzed was the international zircon standard Gj-1 (Jackson *et al.* 2004), used in a standard-sample bracketing method, accounting for mass bias and drift correction. The resulting correction factor for each sample analysis considers the relative position of each analysis within the sequence of four samples bracketed by one standard and one blank analysis each.

The masses ^{204}Pb, ^{206}Pb and ^{207}Pb were measured with ion counters, while ^{238}U was analyzed on a faraday cup. The signal of ^{202}Hg was monitored on an ion counter for the correction of the isobaric interference between ^{204}Hg and ^{204}Pb. The signals during ablation were taken in 40 cycles of 1 s each. The ^{204}Pb signal intensity was calculated and corrected using a natural $^{202}Hg/^{204}Hg$ ratio of 4.346.

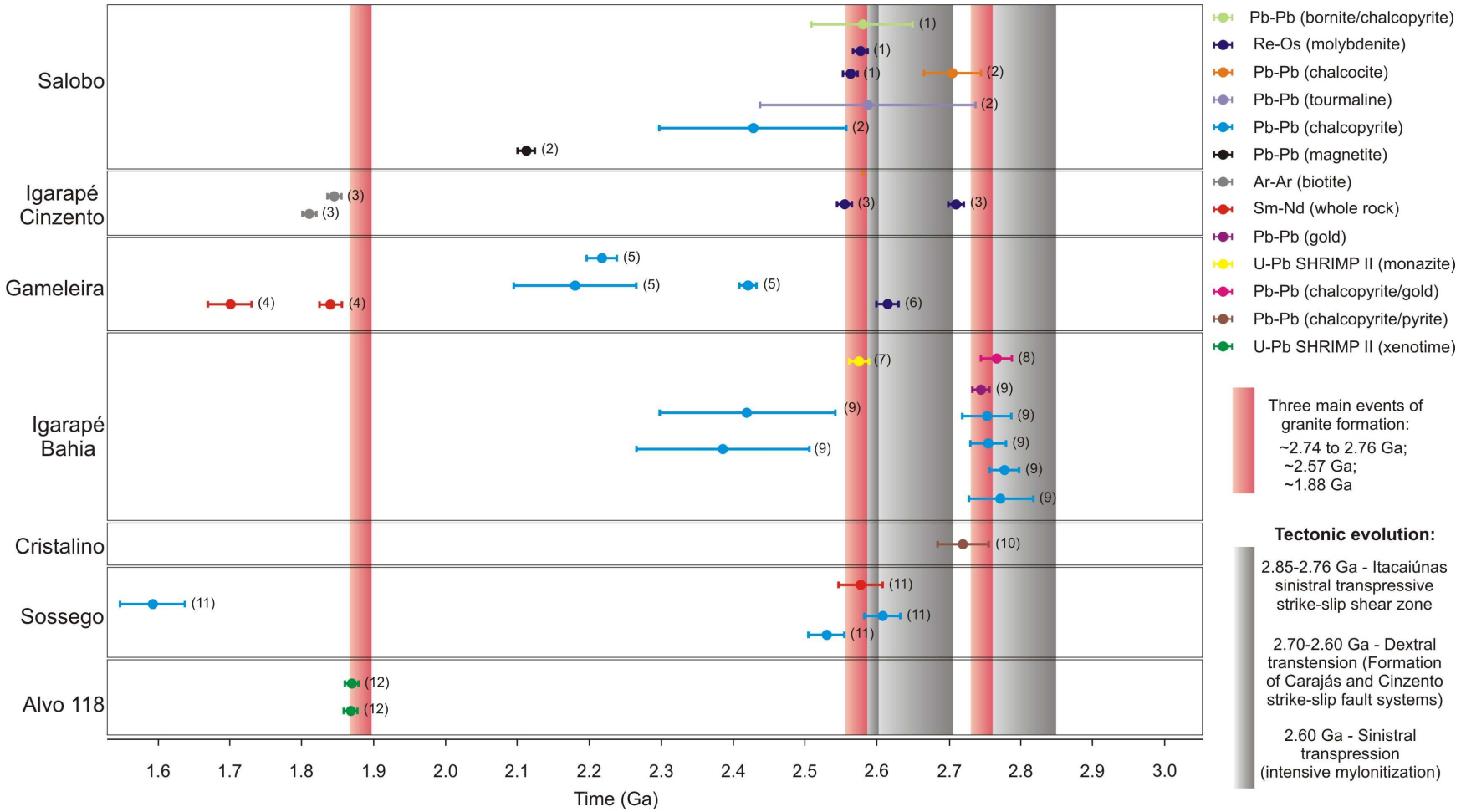

Figure 3. Summary of geochronological data for IOCG deposits of the Carajás Mineral Province and main tectonic and magmatic events recorded in the province. Data source: (1) Réquia et al., 2003; (2) Tassinari et al., 2003; (3) Silva et al., 2005; (4) Pimentel et al., 2003; (5) Galarza and Macambira, 2002; (6) Marschik et al., 2005; (7) Tallarico et al., 2005; (8) Galarza, 2002; (9) Galarza et al., 2008; (10) Soares et al., 2001; (11) Neves, 2006; (12) Tallarico, 2003.

Common Pb correction was applied for zircon with $^{206}Pb/^{204}Pb$ lower than 1000, applying a common lead composition after Stacey and Kramers (1975) model. U–Pb data were plotted on ISOPLOT v.3 (Ludwig, 2003) and the errors for isotopic ratio are presented at the 1σ level.

5. The Bacaba iron oxide-copper-gold deposit

The Bacaba deposit (Figs. 4, 5, 6 and 7) is located in the southern portion of the Itacaiúnas Shear Belt along a WNW–ESE-striking shear zone that defines the contact of the metavolcano-sedimentary Itacaiúnas Supergroup (~2.76 Ga) and the basement represented by migmatites and gneisses of the Xingu Complex (~3.0 Ga). Within this regional shear zone, other economically important IOCG deposits are located, such as Alvo 118, Sossego, Cristalino and several minor copper prospects (e.g. Castanha, Jatobá, Visconde and Bacuri).

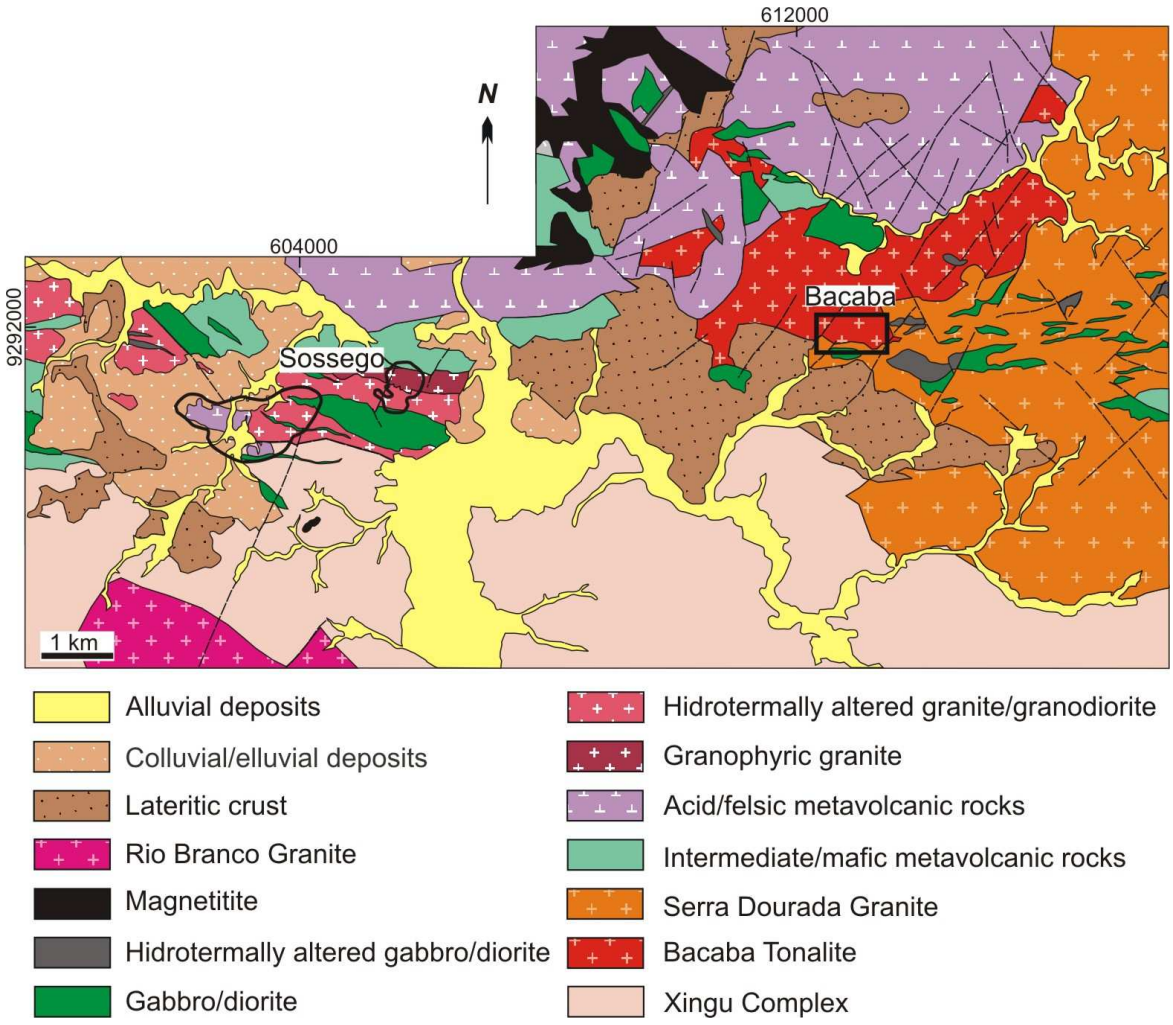

Figure 4. Geological map of the Sossego deposit area, showing the location of the Bacaba deposit (VALE).

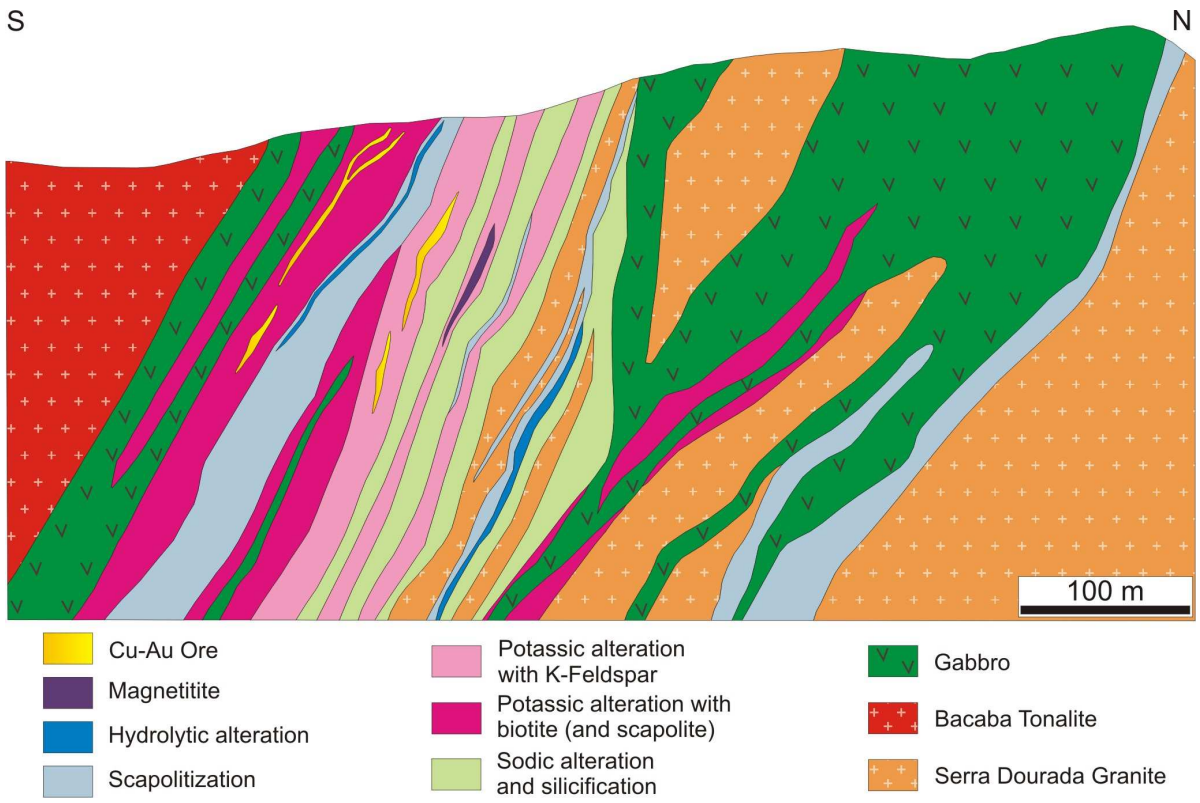

Figure 5. Schematic section showing the host rocks at the Bacaba deposit and the hydrothermal alteration zones (modified from Augusto et al., 2008).

Unlike other IOCG deposits, hosted mainly by metavolcanic units of the Itacaiúnas Supergroup, the Bacaba deposit is hosted by a granite correlated to the Serra Dourada Granite (Feio et al. 2009), a tonalitic rock, denominated as the Bacaba Tonalite, and croscutting gabbro. However, in the vicinities of the deposit acid volcanic and volcaniclastic rocks, lenses of tremolite-talc schist, and porphyritic gabbro were also identified.

The host rocks at Bacaba were intensely affected by hydrothermal alteration (Fig. 5) that causes partial to total obliteration of textural and mineralogical features of the igneous host rocks (Fig. 6 and 7). Hydrothermal alteration and mineralization are controlled by a penetrative sub-vertical to vertical mylonitic foliation related to a transcurrent shear zone. A synthesis of paragenetic evolution of the Bacaba deposit with the temporal evolution of the main hydrothermal alteration stages is presented in the Fig. 8.

The Serra Dourada Granite (Figs. 7C, G, J, K, N and 9A) is isotropic to foliated, coarse-grained, gray to pink in color, has faneritic texture and contains quartz, potassium feldspar, plagioclase and minor biotite. It has pegmatitic facies with macroscale graphic texture with

potassium feldspar and quartz intergrown. The Bacaba Tonalite (Figs. 7H, I and 9C) is foliated, fine-grained, gray in color and has faneritic texture. This rock is composed of quartz, plagioclase, hornblende, biotite and minor potassium feldspar. The gabbro (Figs. 7A, B, C and H) has murky-green color and medium faneritic texture and have relicts of ofitic to subofitic textures defined by intensely saussuritized plagioclase and remnants of pyroxene partially replaced by amphibole and biotite. The gabbro is intrusive in the Bacaba Tonalite and the contact zones between these rocks are, in some cases, characterized by intense hydrothermal alteration in both rocks.

A sequence of hydrothermal events that took place on the host rocks of the Bacaba deposit includes an early sodic alteration stage (Figs. 7C, G and I) related to formation of albite veins and partial replacement of igneous feldspar by pinkish chessboard albite (Fig. 6A). Silicification overlaps initial albitic alteration (Fig. 7G) and it is usually observed in the Serra Dourada Granite. The Bacaba Tonalite was also pervasively replaced by tourmaline (Fig. 7I) and hastingsite during early alteration stages.

These alteration stages are followed by fissure-controlled to pervasive marialitic scapolite alteration (Figs. 7A, J and N), which is extremely intense towards the mineralized zones. Scapolitic alteration represents a pervasive rock alteration in haloes around metric (> 10 m) marialitic scapolite (+ quartz, magnetite and fluorite) veins (Fig. 6B). In those halos, scapolite replaces preexisting igneous feldspar and hydrothermal albite (Fig. 6C). In veins, coarse-grained fibrous marilitic scapolite crystals (Scp I; Fig 6H) usually have undulose extinction and subgrain boundaries. Commonly, scapolite crystals are brecciated and replaced by fine-grained scapolite (Scp II) and U- or Th-bearing minerals, such as haiweeite [$Ca[(UO_2)_2Si_5O_{12}(OH)_2]\cdot 3(H_2O)$] and calciothorite [$(Th,Ca_2)SiO_4 3.5H_2O$].

Magnetite formation (Figs. 7A, C and E) was synchronous with the scapolitic alteration stage and is observed infilling the open-space fractures. Magnetite also occurs disseminated and oriented along the mylonitic foliation, constituting massive magnetite bodies (Augusto et al. 2008).

Potassic alteration (Figs. 7B, E, G, H, K and N) either with biotite or potassium feldspar as the prevailing phase, overprints early alteration stages (Figs. 6D and E). The biotite-rich altered rocks are fine-grained, foliated, have murky-brown color and are composed mostly of biotite (> 50 a < 80 %) with subordinate quartz, magnetite, feldspar, scapolite, hastingsite, and tourmaline (Fig. 6L). Biotite (Bt I) is oriented along the mylonitic foliation (Figs. 6I and J) and

scapolite (Scp III; Figs 6J and K) occurs as zoned and rotated porphyroblasts sometimes with pressure shadow.

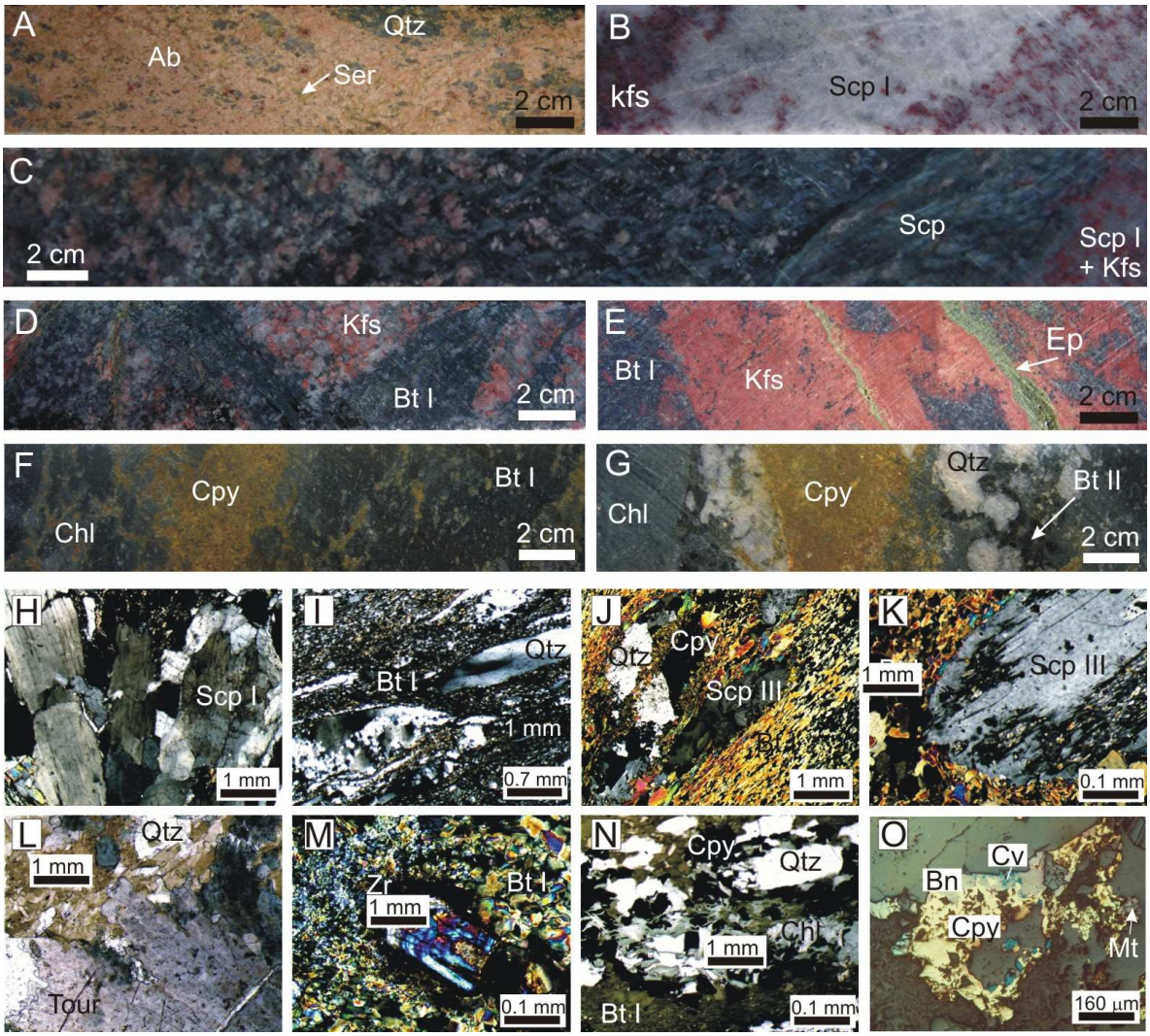

Figure 6. Main hydrothermal alteration stages f the Bacaba deposit. (A) Intense pervasive sodic alteration in the Serra Dourada Granite represented by replacement of igneous minerals by pinkish chessboard albite; (B) Vein with coarse-grained marialitic scapolite (Scp I) partially replaced by red orthoclase along vein walls; (C) Serra Dourada Granite affected by pervasive hydrothermal alteration close to scapolite vein. Preexisting igneous feldspar and hydrothermal albite are mainly replaced by scapolite; (D) Serra Dourada Granite affected by potassic alteration with K feldspar overprinted by potassic alteration with fine-grained biotite (Bt I); (E) Fissural to pervasive potassic alteration with K feldspar and late epidote veinlets; (F) Biotite-rich rock partilaly replaced by chlorite and chalcopyrite; (G) Chlorite-rich rock cut by veinlets with coarse-grained biotite (Bt II), quartz and chalcopyrite; (H) Fibrous marialitic scapolite (Scp I) from veins; (I) Biotite-rich rock with mylonitic foliation; (J) Sample from potassic alteration zones with biotite, scapolite, quartz and minor chalcopyrite oriented along mylonitic foliation; (K) Scapolite porfiroblast partilaly replaced by chlorite, kaolinite and illite; (L) Fibrous-radiated tourmaline crystals in biotite-rich rocks from potassic alteration zones; (M) Fractured and broken zircon crystal with oscillatory zoning in biotite-rich rock; (N) Mineralized rock with biotite partially replaced by chlorite, quartz and chalcopyrite; (O) Ore composed of chalcopyrite, bornite, covelite and magnetite. Abbreviations: Ab: albite; Bt: biotite; Bo: bornite; Chl: chlorite; Cpy: chalcopyrite; Cv: covelite; Ep: epidote; Kfs: potassium feldspar; Mt: magnetite; Qtz: quartz; Scp: scapolite; Ser: sericite; Tour: tourmaline.

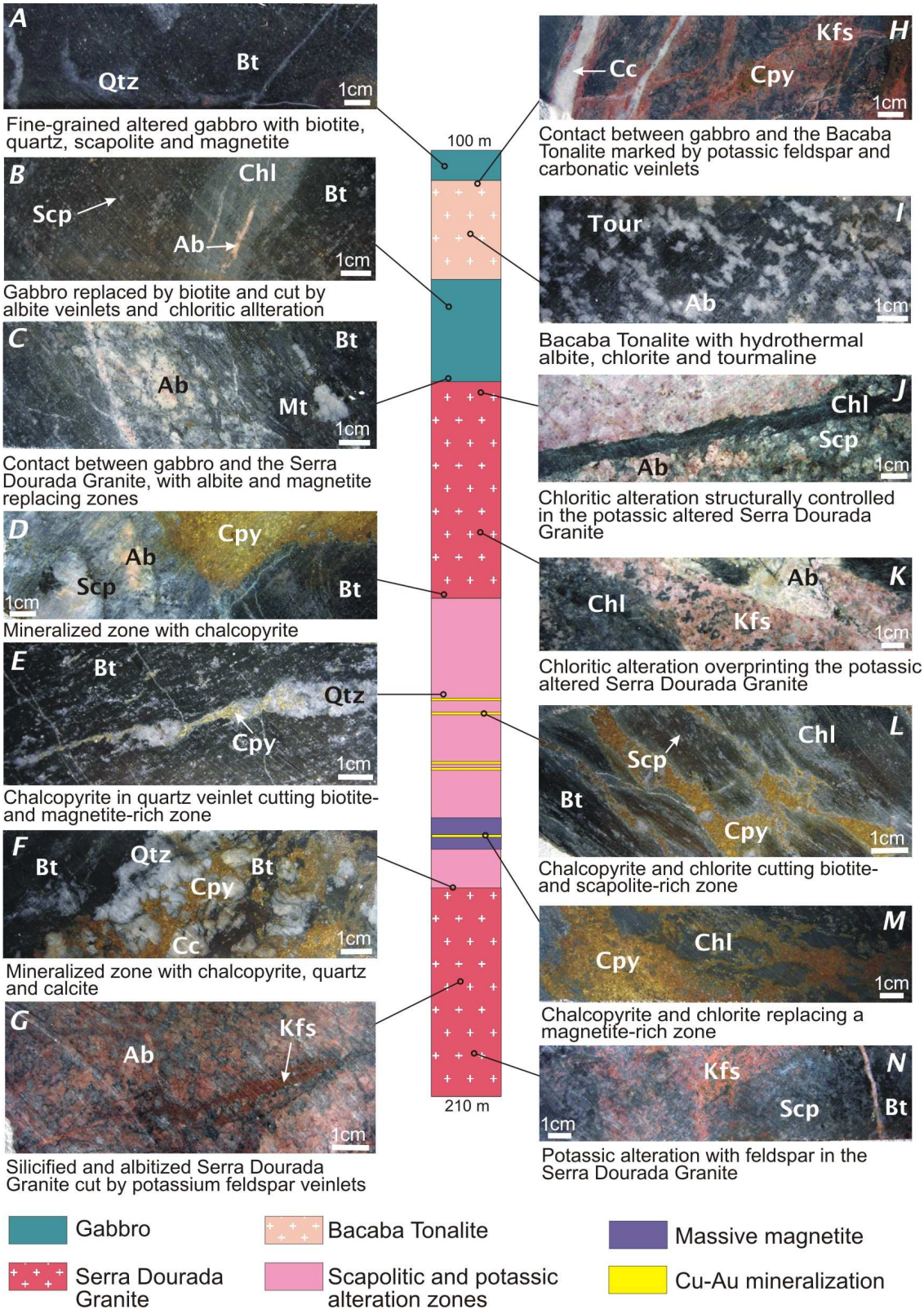

Figure 7. Main features of the hydrothermally altered and mineralized host rocks of the Bacaba deposit (drill core BACD 4). Abbreviations: Ab: albite; Bt: biotite; Cc: calcite; Chl: chlorite; Cpy: chalcopyrite; Kfs: potassium feldspar; Mt: magnetite; Qtz: quartz; Scp: scapolite; Tour: tourmaline.

The potassium feldspar-bearing alteration zones are structure-controlled and defined by replacement of hydrothermal chessboard albite and scapolite (Scp I and II) by red cloudy orthoclase with tiny hematite inclusions. Late veins with potassium feldspar are also observed frequently in mineralized zones crosscuting biotite-rich rocks, which are also cut by veinlets with coarse-grained biotite (Bt II), quartz, calcite, and subordinate chalcopyrite. Coarse-grained zoned zircon crystals, commonly fractured and broken, associated with rutile are abundant in the potassic alteration zones (Fig. 6M).

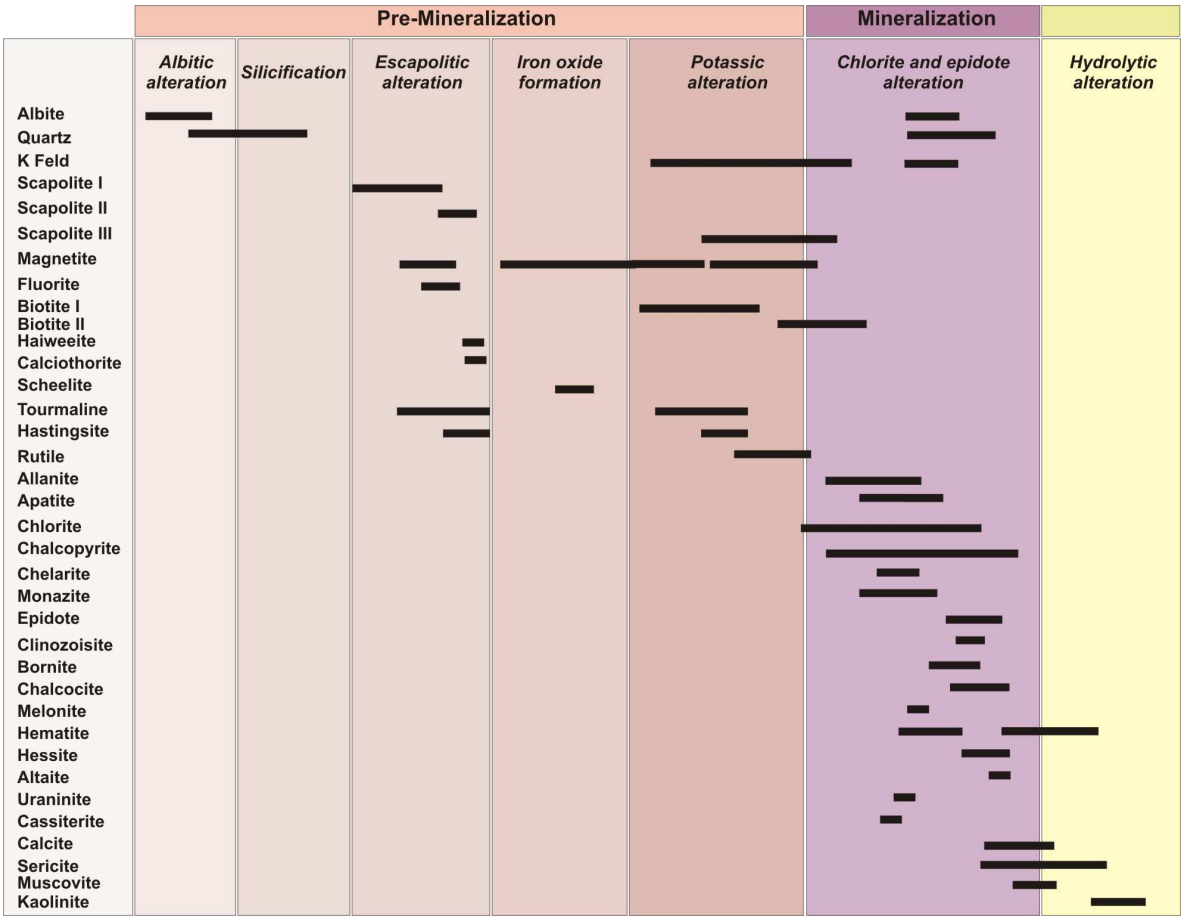

Figure 8. Paragenetic evolution of the Bacaba deposit.

Chlorite and epidote alteration (Figs. 7B, I, J and K) are strongly correlated to the mineralizing stage (Figs. 6F and G). They are both structure-controlled and concordant with the mylonitic foliation (Fig. 6N). These alteration zones replace potassic alteration zones, especially those with biotite and magnetite.

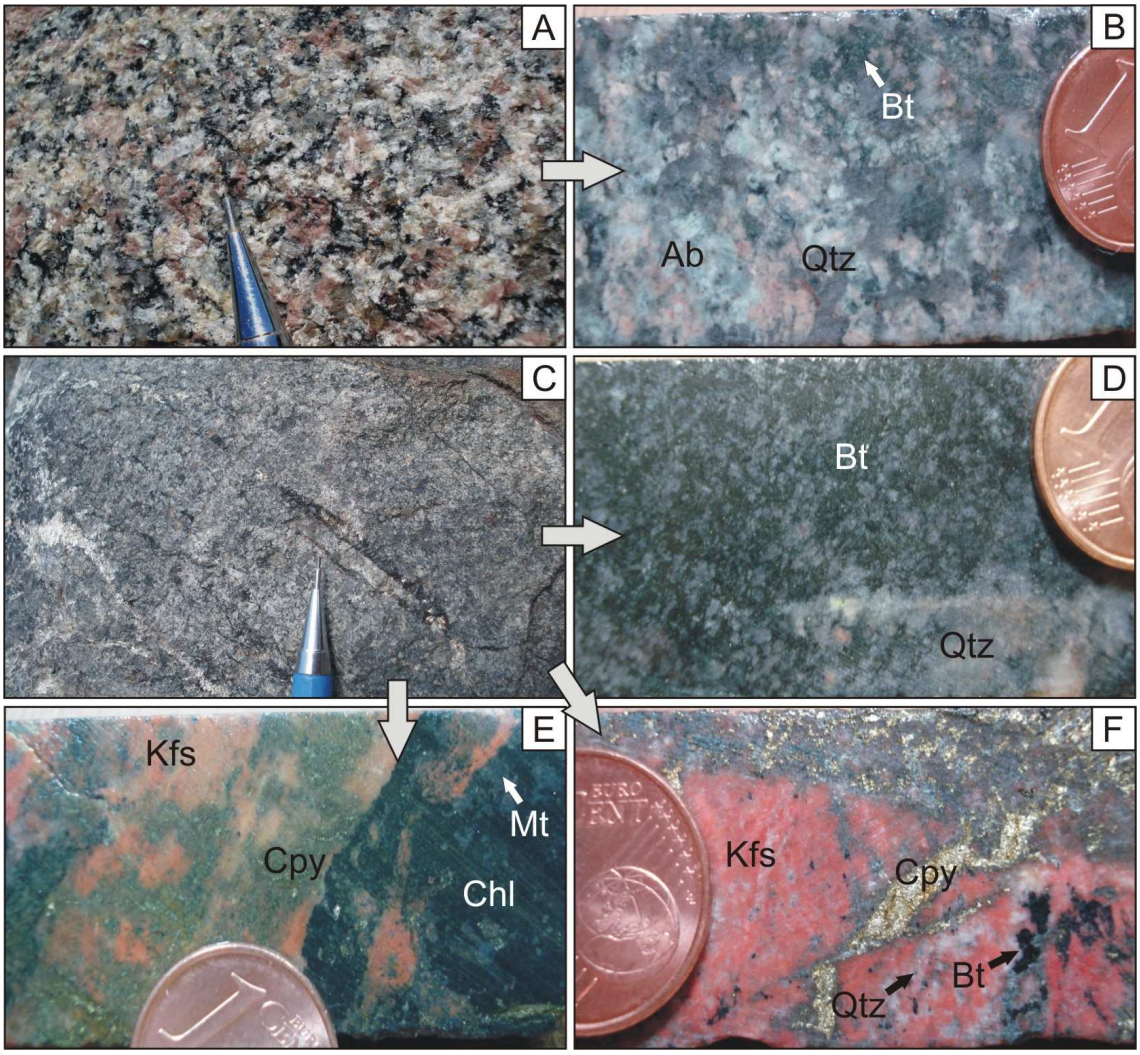

Figure 9. Characteristic features of least to intensely hydrothermally altered and mineralized Serra Dourada Granite and Bacaba Tonalite. A. Least-altered Serra Dourada Granite; B. The Serra Dourada Granite affected by Na-alteration represented by albite (BACD15/237,40); C. The Bacaba Tonalite with incipient fissural potassic alteration (biotite) and scapolitization; D. Potassically altered (biotite) and silicified Bacaba Tonalite (BACD17/73,30); E. Mineralized zone with chalcopyrite and potassium feldspar cutting the previously Bacaba Tonalite (BACD9/257,45); F. Mineralized zone in the Bacaba Tonalite containing potassium feldspar, quartz and biotite cut by chalcopyrite veinlets (BACD25/229,25). Abbreviations: Ab: albite; Bt: biotite; Chl: chlorite; Cpy: chalcopyrite; Kfs: potassium feldspar; Mt: magnetite; Qtz: quartz.

The iron oxide–copper–gold mineralization stage (Figs. 7D, E, F, L and M) was late and spatially related to potassic alteration with predominance of potassic feldspar. Ore occurs as veins and replacement zones of the host rock along mylonitic foliation and comprises chalcopyrite, bornite, covellite (Fig. 6O), chalcosite, magnetite and hematite with subordinated melonite, hessite, altaite, uraninite, cassiterite and ferberite often associated with gangue minerals, such as chlorite, calcite, epidote, clinozoisite, allanite, apatite, monazite and rutile. The late stage of

hydrothermal alteration is characterized by sericitization and hydrolytic alteration with hematite, muscovite, kaolinite and illite.

The sequence of hydrothermal alteration stages in the Bacaba deposit is similar to that described for the Sossego deposit, despite the greater scapolite abundance at Bacaba. This suggests that the two deposits may represent different portions of a single hydrothermal system (Augusto et al. 2008; Monteiro et al. 2008a,b).

6. U–Pb geochronology

The U–Pb isotopic analyses (Tables 4 to 7) were carried out on four samples of drill cores from the Bacaba deposit. The samples are representative of variably hydrothermalized felsic igneous host rocks, consisting of: (i) one sodic altered sample of the Serra Dourada Granite; (ii) one potassic altered sample of the Bacaba Tonalite; and (iii) two Bacaba Tonalite samples with potassic alteration and Cu–Au mineralization.

The hydrothermal alteration is conspicuous and pervasive, and the correlation between the most altered samples and the corresponding igneous protolith is not obvious. However, this information can be extracted from detailed observation of drill cores, as the host rocks display a sequence of hydrothermal alteration, and the least altered portions can reveal the igneous protolith. The sodic altered sample (BACD15/237,40) still preserves igneous texture and corresponds to the coarse-grained Serra Dourada Granite (Fig. 9B). The igneous minerals from the potassic altered sample (BACD 17/73,30) were entirely replaced, but the texture of the Bacaba Tonalite is still preserved (Fig. 9D). Exclusively based on drill cores examination, the two ore samples (BACD9/257,40 and BACD25/229,25) were also correlated to the Bacaba Tonalite (Fig. 9E and 9F). This observation was confirmed by U–Pb data.

In all samples, zircon crystal lengths range from ca. 35 to 220 μm, and aspect ratios (length:width) from 1:1 to 4:1. Zircon occurs as inclusions in major silicate phases, mainly in biotite, but also in quartz and feldspar. Similar external morphology and internal textures were observed in zircon occluded in different mineral phases in each sample.

6.1 Serra Dourada Granite

The sample BACD15/237,45 (Fig. 9B) has predominance of chessboard albite, which represents the initial hydrothermal alteration processes. Zircon crystals from this sample are light-pink and have elongated pyramid forms with well-formed faces (Figs. 10A-F). Most grains display prominent oscillatory zoning patterns (Figs. 10A and B), although structureless areas are noteworthy (Fig. 10C). Radiation damage process leading to partial to total metamictization of zircon grains might have occurred, evidenced by the great amount of inclusions and internal fractures (Figs. 10D and E). Some zircon grains display a 5 to 20µm textureless mantles, with bright response to backscattered electron images (Fig. 10F). The Th/U ratios range from 0.15 to 0.59 with a mean value of 0.46. Fifty-nine raster analyses yielded a discordant result with projected upper intercept age of 2858 ± 30 Ma (MSWD = 9.7; Fig. 11A, Table 4).

6.2 Bacaba Tonalite

The sample BACD17/73,30 (Fig. 9D) has a prevailing pervasive biotite-rich potassic alteration. Zircon crystals are murky-pink and have prismatic forms with well-formed faces (e.g. Fig. 10H), as well as ovoid forms with rounded terminations (e.g. Fig. 10J). The Th/U ratios vary from 0.11 to 0.33 with a mean value of 0.25. The zircon grains produced fifty-eight concordant to slightly discordant analyses resulting in an upper intercept age of 2997.2 ± 4.7 Ma (MSWD = 1.15; Fig. 11B, Table 5).

Samples BACD25/229,25 (Fig. 9E) and BACD9/257,45 (Fig. 9F) are mineralized samples, in which igneous and previous hydrothermal minerals were intensely replaced by ore minerals. Zircon crystals from BACD25/229,25 sample are pink, exhibit poorly-defined prismatic habits to ovoid external forms with rounded to weakly-formed pyramid terminations (Figs. 10K and L). The Th/U ratios range from 0.15 to 0.47 with a mean value of 0.25. Fifty-two concordant to slightly discordant analyses rendered an upper intercept age of 2993.1 ± 7.1 Ma (MSWD = 1.1; Fig. 11C, Table 6), close to the age obtained for the Bacaba Tonalite, sample BACD17/73,30.

Zircon grains of the BACD9/257,45 ore sample are colorless to light-pink and display dominant ovoid morphology, although poorly-defined prismatic forms with rounded terminations were also seen. The Th/U ratios range from 0.07 to 1.10 with a mean value of 0.25. Despite the

radiogenic Pb loss of several zircon grains, the forty-eight raster analyses yielded a discordant result with upper intercept age of 3004.7 ±7.8 Ma (MSWD = 2.1; Fig. 11D, Table 7).

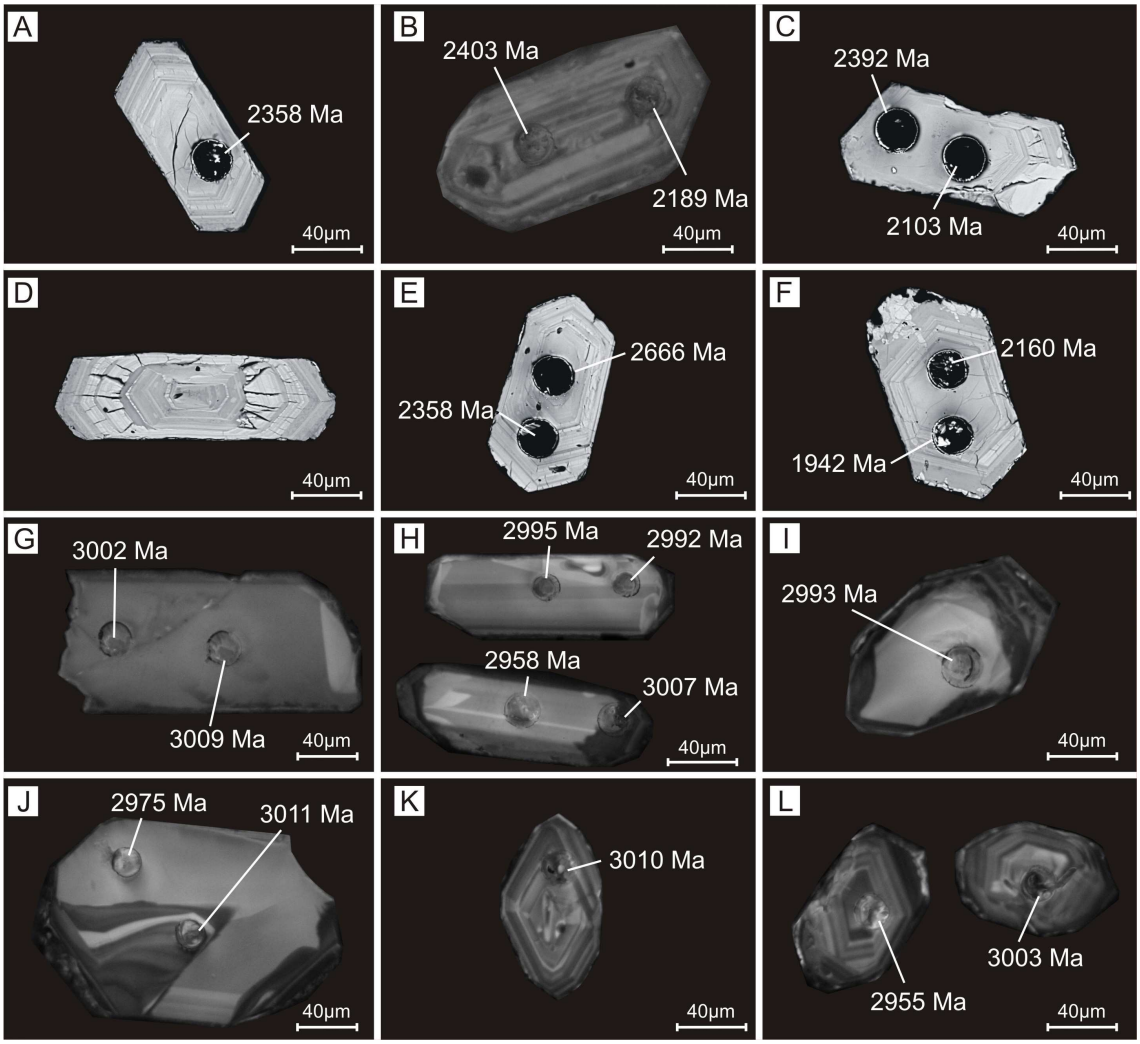

Figure 10. Backscattered electron and cathodoluminescence images of zircon of the Serra Dourada Granite and the Bacaba Tonalite. A,C-F. Backscattered electron images and B. Cathodoluminescence images of metamict zircon with prismatic forms and pyramid terminations of the Serra Dourada Granite showing meaningless $^{207}Pb/^{235}U$ ages. A and B. Typical oscillatory zonation of igneous zircon; C. Weakly oscillatory zoned areas overprinted by textureless domains; D. U-rich core from extremely metamict grain; E. Inclusion-rich metamict zircon; F. Zircon with oscillatory zoning and a 5 to 20 µm (hydrothermal?) mantle; G-L. Cathodoluminescence images of zircon crystals of the Bacaba Tonalite showing more rounded terminations, and $^{207}Pb/^{235}U$ Archean ages; G and H. Zircon showing great structureless areas; I. Structureless cores overlapping oscillatory zoning rims; J. Oscillatory zonation overlapped by textureless areas; K and L. Preserved igneous oscillatory zoning in zircon.

Zircon of the Bacaba Tonalite display high luminescence response and no internal structures in backscattered images. However, the cathodoluminescence images (Fig. 10G-L) show igneous oscillatory zonation in few grains (Figs. 10K and L), whereas most zircon display

either textureless thick cores with surrounding rim with oscillatory zonation (Figs. 10H and I), or almost entirely structureless areas (Figs. 10G). Fig. 10J shows an irregular preserved oscillatory zoning area in a dominant textureless zircon. All these features provide a potential evidence of physical and chemical disturbance.

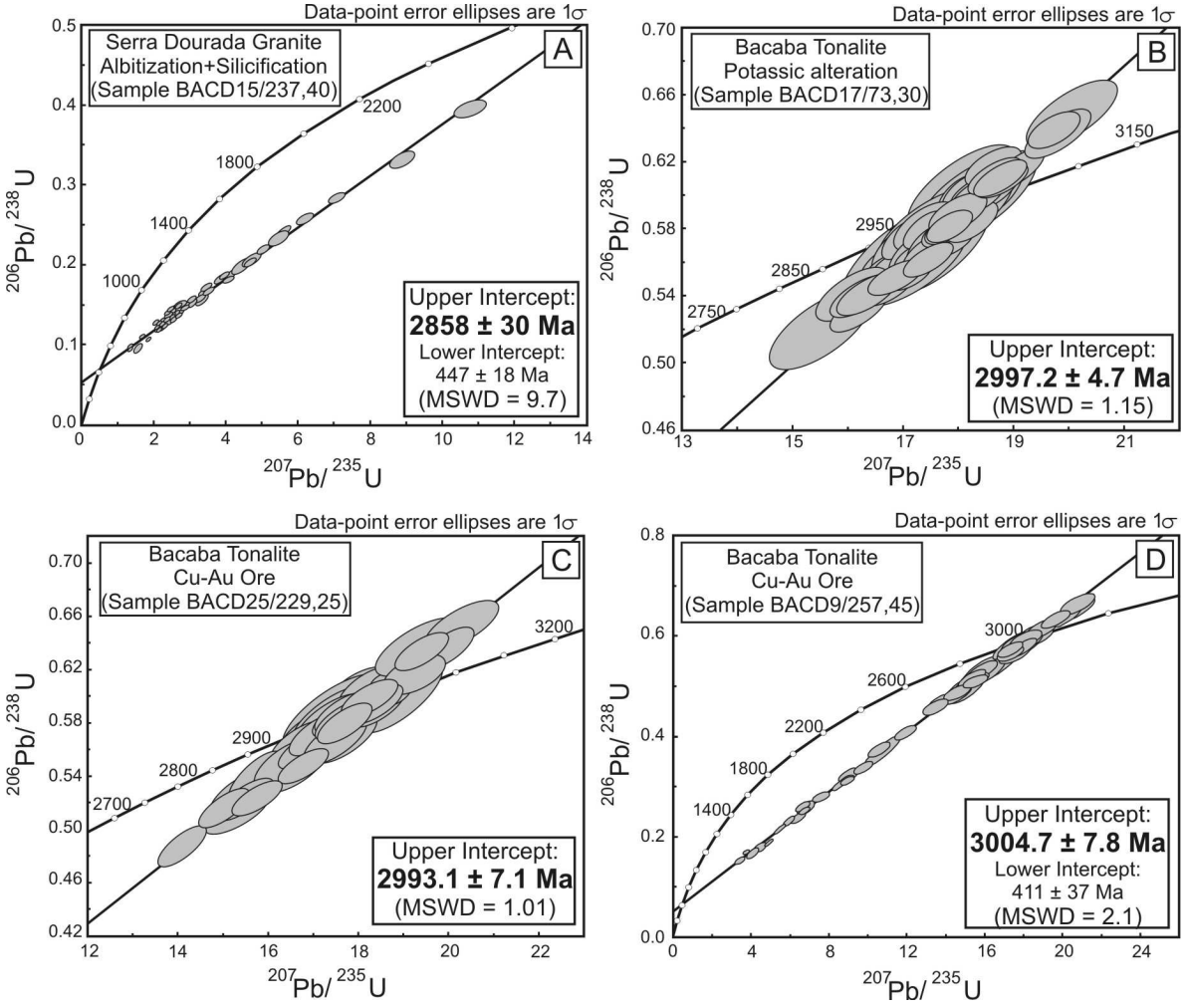

Figure 11. $^{206}Pb/^{238}U$ vs. $^{207}Pb/^{235}U$ diagrams for A. Serra Dourada Granite with sodic alteration and silicification (BACD15/237,40); B. Bacaba Tonalite with potassic alteration (BACD17/73,30); C. and D. Cu-Au ore (Bacaba Tonalite; samples BACD25/229,25 and BACD9/257,45).

7. Discussion

7.1 Zircon features and related process

Zircon grains from the Bacaba Tonalite display conspicuous textureless areas (Figs. 10G-

J), while zircon from the Serra Dourada Granite almost preserve the original oscillatory zoning patterns (e.g. Figs. 10A and B), usually assigned to magmatic crystallization (Vavra *et al*., 1990). Besides, the external morphologies of zircon crystals of both intrusions are dissimilar. Zircon with ovoid morphology and rounded termination are often observed in the Bacaba Tonalite, whereas grains with prismatic forms and pyramid terminations are typical of the Serra Dourada Granite. In addition, zircon crystals of the Serra Dourada Granite have a mean Th/U ratio of 0.46, whereas those from the Bacaba Tonalite have lower mean value of Th/U ratio (0.25).

However, all these values fall within the suggested range for zircon in felsic igneous rocks (e.g. Williams and Claesson, 1987). These discrepancies in zircon features (shape, texture and Th/U ratio) support more than one felsic intrusive rock in the Bacaba deposit.

The analyzed rocks have experienced episodes of intense high-temperature hydrothermal activity. Moreover, the several deformational events known in the Itacaiúnas Shear Belt could have affected the Bacaba deposit host rocks, as they are located within a WNW–ESE regional shear zone. Considering the morphological and textural features of zircon from samples of the Bacaba deposit, it is reasonable to attest the occurrence of a disturbing event, which might be associated with hydrothermal activity or deformational episodes, or both.

The partial to total absence of internal oscillatory zoning in several zircon grains of the Bacaba Tonalite (Figs. 10G-J) could be the result of modifications in zircon structure leading to crystal homogenization caused by recrystallization of the protolith zircon. Recrystallization is one of the several metamorphic zircon-forming processes (Black *et al*., 1986; Friend and Kinny, 1995; Pidgeon, 1992; Fu *et al*., 2009) and causes obliteration of internal oscillatory zoning, generating internally textureless zircon, except for possible blurred oscillatory zonation areas (Hoskin and Black, 2000; Pidgeon, 1992; Pidgeon *et al*., 1998, Vavra *et al*., 1996; Conelly, 2001; Hoskin and Schaltegger, 2003). Partial to total recrystallization of protolith zircon during metamorphic events have been documented worldwide (e.g. enderbites from the Pium Complex, CMP, Brazil, Pidgeon *et al*., 2000; metagranitoids from Queensland, Australia, Hoskin and Black, 2000; granites from Yilgran Craton, Western Australia, Pidgeon, 1992, Pidgeon *et al*., 1998; meta-igneous rocks from Syros, Greece, Tomaschek *et al*., 2003; meta-igneous and metasedimentary rocks, Central Variscan Belt, France, Schaltegger *et al*., 1999).

Recrystallization could have affected, but with least intensity, the zircon crystals of the Serra Dourada Granite, as showed in Fig. 10C, where weakly oscillatory zoned areas are

overprinted by textureless domains. Another evidence for this process was described by Pidgeon *et al.* (1998) in granites from Darling Range Batholith (Australia) and was related to unzoned cores surrounded by rims showing oscillatory zoning that has been modified by recrystallization. Similar feature was also observed in zircon from the studied samples (Figs. 10A, E, F, H and I). Although recrystallization might affected the zircon crystals of the Serra Dourada Granite, the current preservation of primary crystallization texture is possibly due to extremely low intra-crystalline elemental diffusivities in zircon (Cherniak *et al*., 1997a,b).

The ovoid and rounded morphologies found in zircon from the Bacaba Tonalite (Figs. 10I, J and L) could be an additional evidence for zircon modification due to recrystallization. Ovoid morphologies in metamorphic altered zircon were also documented by Schaltegger *et al.* (1999), Degeling *et al.* (2001) and Hoskin and Black (2000). Kröner *et al.* (1994) interpreted sub-rounded zircon to be formed by resorption (dissolution by a melt) by a zircon-undersatured intergranular fluid. On the other hand, zircon from the Serra Dourada Granite preserves euhedral prismatic forms most likely acquired during magmatic crystallization (Figs. 10A-F). The partial recrystallization could not have been efficient enough to cause obliteration in morphology; or this process did not influenced the crystal external forms, even if was of great intensity. Kalsbeek *et al.* (1988) and Pidgeon *et al.* (1990) reported recrystallized zircon crystals with euhedral forms, indicating that recrystallization was not accompanied by significant changes in grain shape. Thus, all of these examples suggest that zircon recrystallization might occur with or without modifications in external morphologies.

Samples from the Bacaba Tonalite exhibit different response to radiogenic Pb loss. Samples BACD 17/73,30 (potassic alteration) and BACD 25/229,25 (ore) show minor radiogenic Pb loss, as seen in the $^{206}Pb/^{238}U$ vs. $^{207}Pb/^{235}U$ diagrams (Figs. 11B and C). In sample BACD 9/257,45 (ore) radiogenic Pb loss was noticeable (Fig. 11D). This Pb loss had a heterogeneous behavior and did not affect all zircon grains. The sample from the Serra Dourada Granite (Sample BACD 15/237,40) display the most conspicuous Pb loss, which has affected all zircon crystals, as shown by highly discordant spot analyse in Fig. 11A.

The radiogenic Pb loss could be or not associated with recrystallization. If not, Pb loss might be due to radiation damage caused by α-decay events. Radiation damage is a common phenomenon in natural zircon and it is caused by self-irradiation due to the radioactive decay of U and Th (Murakami *et al*., 1991; Meldrum *et al*., 1998, 1999). Radiation damage process leads

to partial/total metamictization of zircon grain. The evidence of metamictization in zircon of Serra Dourada Granite are demonstrated by the large amount of inclusions and fractures inside the crystals (Figs. 10D and E). If the core is richer in U than the rim, core expansion during metamictzation will cause fracturing of the more rigid rim (Fig. 11D; Corfu *et al*., 2003). Nevertheless, recrystallization mechanisms can also purge Pb and others non-essential structural constituent cations from the recrystallized structure (Pidegon, 1992; Geisler *et al*., 2003a,b). Pidgeon *et al.* (1966, 1998) and Geisler *et al.* (2003a,b) reported reaction between zircon and an external hydrothermal fluid causing recrystallization of the zircon together with loss of Pb and other trace elements to the environment.

The determination of recrystallization event ages related to metamorphic and/or hydrothermal event was reported in previous works (e.g. Pidgeon, 1992; Pigdeon *et al*., 2000; Hoskin, 2005). However, in the studied samples, the disturbing event recorded by textural zircon patterns from the Bacaba Tonalite and conspicuous Pb loss in zircon from the Serra Dourada Granite was not accompanied by total resetting of the U–Pb system. Thus, the upper intercept ages yielded by concordant to slightly discordant analyses from the Bacaba Tonalite and discordant analyses of Serra Dourada Granite are interpreted as crystallization ages of the igneous rocks. This observation leads to the conclusion that dating the interfering event it is not always assured.

7.2 Mesoarchean magmatism in the Carajás Mineral Province

Despite hydrothermal alteration and mineralization, the upper intercept ages of about 3.0 Ga (3004.7 ± 7.8 Ma, 2997.2 ± 4.7 Ma and 2993.1 ± 7.1 Ma) provide the best estimative of the igneous crystallization of the Bacaba Tonalite. These ages represent the oldest magmatism recorded in the CMP. Similar Archean ages in the Itacaiúnas Shear Belt were attributed only to the crystallization of the igneous protolith of enderbites and charnockite of the Pium Complex (Rodrigues *et al*., 1992; Pidgeon *et al*., 2000), which are part of the Carajás Basin basement. Coeval magmatism to that associated with the Bacaba Tonalite could correspond to the ca. 2.97 Ga TGG suites identified in the Rio Maria granite-greenstone terrane, such as the Arco Verde (Althoff *et al*., 1993; Macambira and Lancelot, 1996) and Caracol tonalites (Leite *et al*., 2004). As far as geochronology is concerned, the Bacaba Tonalite could be correlated to these older TTG suites and would indicate a widespread 3.0–2.97 Ga magmatism in the CMP.

The U–Pb zircon age of 2858 ± 30 Ma for the Serra Dourada Granite is also older than other granitic rocks already recognized in the Itacaiúnas Shear Belt, such as the widespread 2.76 to 2.74 Ga syntectonic alkaline granites (Plaquê, Planalto, Estrela and Serra do Rabo suites; Huhn *et al*., 1999; Avelar *et al*., 1999; Sardinha *et al*., 2006; Barros *et al*., 2004). However, the 2.86 Ga Serra Dourada Granite could correspond to the calc-alkaline leucogranites characterized in the Transition Domain (Feio *et al*., 2009) and in the Rio Maria granite-greenstone terrane (2.86 Ga Xinguara, Mata Surrão and Riacho de Deus granites; Lafon *et al.,* 1994; Barbosa and Lafon, 1996; Leite *et al*., 2004). The Serra Dourada Granite might represent an evidence that the 2.86 Ga magmatism, coeval with the migmatization/granulitization event that affected the Xingu and Pium basement complexes, was much more extensive than previously considered in the CMP.

The existence of such old rocks in the Itacaiúnas Shear Belt, with similar ages to those from the Rio Maria granite-greenstone terrane might be evidence that the two domains shared analogous evolutive history before 2.76 Ga, when the Carajás Basin was installed. Dall'Agnol *et al*. (2006) already considered the Transition Domain as an extension of the Rio Maria granite-greenstone terrane, which have been affected by the younger events registered in the Itacaiúnas Shear Belt.

The new 2.86 Ga and ca. 3.0 Ga ages obtained for the Serra Dourada Granite and the Bacaba Tonalite, respectively, raise evolutive considerations for the southern part of the Itacaiúnas Shear Belt. These Mesoarchean ages can represent the oldest known events of granitic magmatism in the southern portion of the Itacaiúnas Shear Belt, and suggest a more complex geological evolutionary history with at least five important episodes of granite formation for this domain. The first event is represented by the ca. 3.0 Ga Bacaba Tonalite and possibly by the parent rocks of granulites and gneisses to migmatites from Pium and Xingu basement complexes, respectively. The second event is recorded by the 2.86 Ga Serra Dourada Granite and probably by other related intrusions. The other three events are well-known in the literature, corresponding to 2.76 to 2.74 Ga extensive alkaline granites, ca. 2.57 Ga A-type alkaline granites and 1.88 Ga A-type alkaline to sub-alkaline granites. The Serra Dourada Granite and the Bacaba Tonalite are older than the metavolcanic-sedimentary sequence of the Itacaiúnas Supergroup, therefore these rocks also are part of the basement in the southern portion of the Itacaiúnas Shear Belt.

The major mantle-crust differentiation events in the CMP took place at 3.1 to 2.8 Ga and 2.8 to 2.5 Ga (Sato and Tassinari, 1997; Tassinari and Macambira, 1999). The former age interval

is within the T_{DM} (Nd) model age range of the presumable sources for Archean (2.97 to 3.2 Ga; Estrela Granite, Barros et al. 2004) and Paleoproterozoic (e.g. 3.0 to 3.2 Ga; Velho Guilherme Granite, Teixeira et al. 2002) granites, volcanic rocks of the Itacaiúnas Supergroup (e.g. 2.99 to 3.06 Ga; meta-andesites from the Gameleira deposit; Pimentel *et al*., 2003) and gneisses of the Xingu Complex (ca. 3.0 Ga; Sato and Tassinari, 1997). The Sm–Nd model ages and the Pb–Pb zircon ages for the oldest rocks in the Rio Maria granite-greenstone terrane, such as the Arco Verde Tonalite, also suggest that the magma was extracted from the mantle at 3.0 Ga, close to its emplacement into the crust (2.94 to 2.99 Ga; Rolando and Macambira, 2003). The Bacaba Tonalite might share a similar or a little older evolution to the Arco Verde Tonalite, reflecting an important period of crust formation in the Amazonian Craton at ~ 3.0 Ga.

7.3 Implications for IOCG Metallogeny

Relationship of paragenetic evolution in the Carajás IOCG deposits, notably those located along the southern WNW–ESE-striking shear zone (e.g. Cristalino, Alvo 118, Sossego and its satellite deposits), and the development of regional structures could suggest a common and synchronous evolutionary history for the hydrothermal paleo-system associated with the genesis of the IOCG deposits (Xavier *et al.*, in press). However, the available geochronological data for those deposits is not sufficiently precise to define a single metallogenetic IOCG event in the province. Additionally, despite the importance of magmatism to provide heat and fluids for the development of extensive hydrothermal systems, spatial and temporal relationship between intrusions and IOCG orebodies is not well documented in the CMP.

The Bacaba deposit has a clear spatial association with granitic rocks. It is hosted by intrusive igneous rocks, represented by the ca. 3.0 Ga Bacaba Tonalite, the 2.86 Ga Serra Dourada Granite, and crosscutting gabbro. This deposit shares with the Sossego deposit a similar sequence of hydrothermal alteration types characterized by sodic (albite and scapolite formation), potassic (microcline and/or biotite), chloritic and hydrolytic (muscovite and hematite formation) assemblages. Extensive scapolitic alteration zones, however, were recognized only at the Bacaba deposit (Monteiro *et al.*, 2007; Augusto *et al*., 2008).

Chlorine-bearing marialitic scapolite represents a particularly sensitive indicator of fluid hipersalinity. Thus, its abundance could reveal the predominance of hot (> 500 ^{o}C; Vanko and Bishop, 1982) hypersaline fluids during early system evolution. Additionally, marialite formation

requires buffered activity gradients in chlorine in the hydrothermal fluids (Mora and Valley, 1989), implying in limited influx of diluted meteoric fluids. This point to a fluid regime dominated by deeply-sourced brines without significant contribution of surface-derived fluids during the pre-mineralization sodic alteration stage.

Comparison of these characteristics with those predicted in the conceptual model proposed by Hitzman *et al.* (1992) might suggest that the Bacaba deposit represents a distal and deeper portion of a single hydrothermal system (Fig. 12) responsible for the genesis of the world-class Sossego deposit (Augusto *et al*., 2008; Monteiro *et al*., 2008a,b).

The source of hypersaline brines from unmixing of magmatic fluids has been considered of fundamental importance for the genesis of IOCG deposits worldwide (Perring *et al*., 2000; Pollard, 2001, 2006; Beardsmore, 1992; Adshead, 1995; Mark *et al*., 2004; Mustard *et al*., 2004). However, in the CMP, chlorine and boron isotopes combined with Cl/Br – Na/Cl systematics, strongly suggest that fluid regimes responsible for the formation of the IOCG deposits had a significant participation of residual evaporative fluids (e.g., bittern fluids generated by seawater evaporation) that may have mixed with magma-derived brines (Chiaradia *et al.*, 2006; Xavier *et al.*, 2008).

Nevertheless, the relationship between crystallization of the host granitic intrusions and generation of hypersaline fluids should be evaluated. If the Bacaba deposit mineralizing system was associated with the granitic host rocks, this deposit would be considered as related to the oldest IOCG system in the Carajás Mineral Province. However, the record of the oldest Mesoarchean host rocks (ca. 3.0 Ga and 2.86 Ga) for an IOCG deposit in the CMP could imply that the Bacaba Tonalite and the Serra Dourada Granite were not responsible for the establishment of the wide magmatic-hydrothermal system associated with this deposit. This is likely because other deposits with similar characteristics located along the same regional shear zone are also hosted by hydrothermally-altered ca. 2.76 Ga metavolcano-sedimentary units of the Itacaiúnas Supergroup (e.g. Sossego, Cristalino, Alvo 118; Monteiro *et al.* 2008a; Huhn *et al*., 1999; Tallarico, 2003).

Older ages than 2.76 Ga could imply in several similar episodes of IOCG mineralization in the CMP within the same structural framework. Even if the mineralization process was episodic, a long-term duration (> 100 Ma) of the hydrothermal system would be improbable. Dynamic geologic events associated with hydrothermal episodes may, in fact, encompass up to

few millions of years, but the actual duration of ore-forming pulses is on the scale of thousands of years (Stein and Cathles, 1997; Cathles *et al*., 1997). Although a causative not outcropping granite intrusion can not be ruled out, these data may reflect that IOCG deposits in the southern sector of the Itacaiúnas Shear Belt are essentially structural-controlled and not associated with a particular rock type. This suggests that regional scale fluid circulation along an important crustal discontinuity represented by a WNW–ESE-striking regional shear zone was the essential factor that allowed the metal leaching from consolidated igneous rocks and ore deposition (Monteiro *et al*., 2008a).

The genesis of IOCG mineralization in the Carajás Mineral Province could have been intrinsically related to the development of shear zones developed in the crustal brittle-ductile transition zone (Nelson *et al*., 2007). Within the shear zone, the brittle-ductile transition would have been elevated, possibly due to shear heating and microscopic advective fluid flow. Pre-mineralization sodic, sodic-calcic, and potassic hydrothermal alteration would have occurred during inter-seismic phases with fluid-pressure build-up, whereas sulfide ore-mineral precipitation likely occurred during high-strain rate seismic phases with fluid pressure release brecciation (Nelson *et al*., 2007).

Because the Bacaba deposit is satellite of the Sossego IOCG deposit, the 2530 ± 25 Ma and 2608 ± 25 Ma ages obtained for chalcopyrite from the Sossego deposit (Pb–Pb evaporation, Neves, 2006) would represent either resetting of the Pb–Pb isotopic system or the timing of mineralization related with hydrothermal fluid circulation along the main shear zones coeval with the development of the 2.6 Ga sinistral transpression of the Carajás and Cinzento stike-slip fault systems. However, T_{DM} (Nd) model ages (3.16 to 2.96 Ga; Neves, 2006) estimated for Sossego ore samples, would reflect extensive hydrothermal fluid interaction with consolidated Mesoarchean rocks, similar to the Bacaba Tonalite, or with rocks derived from Mesoarchean sources, including the Itacaiúnas Supergroup units and basement gneiss.

Monteiro *et al.* (2008a,b) suggested, based on stable isotope and geothermometric estimation, temperatures exceeding 500 °C for the early sodic–calcic alteration stage in the Sossego deposit. If analogous temperature is estimated for the early alteration stages in the Bacaba deposit, this temperature would be considered not high enough to cause total resetting of the U–Pb system in protolith zircon in order to register the hydrothermal event. However, Geisler

et al. (2003a,b) and Rasmussen *et al.* (2005) reported zircon growth and/or zircon alteration by relative low-temperature hydrothermal fluids, at ca. 250 °C and 120 to 200 °C, respectively.

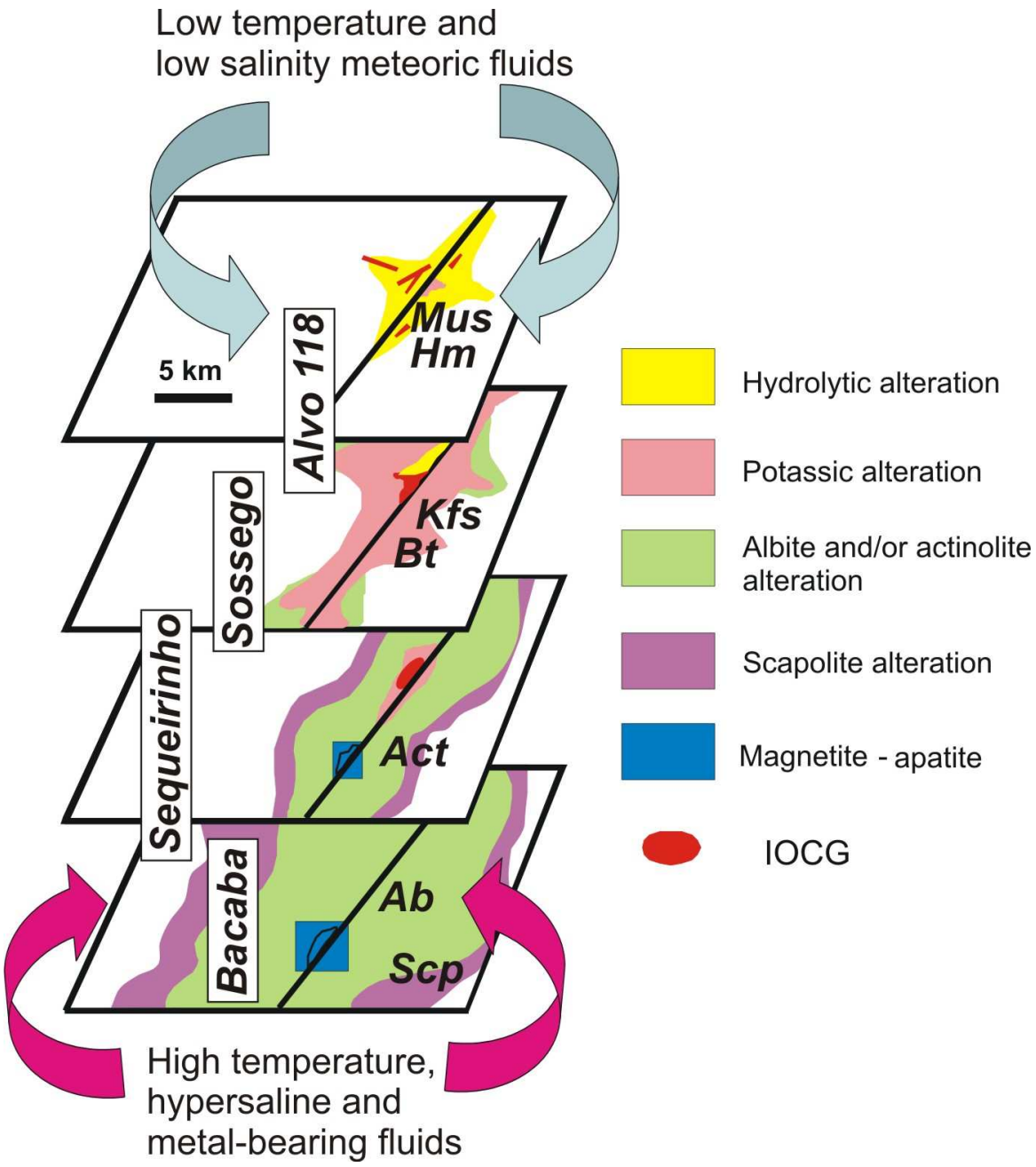

Figure 12. Schematic model of distribution of hydrothermal alteration zones in the iron oxide-copper-gold deposits of the Carajás Mineral Province based on Hiztman et al. (1992) and Hitzman (2000). Abbreviations: Ab: albite; Act: actinolite; Bt: biotite; Kfs: potassium feldspar; Hm: hematite; Mus: muscovite; Scp: scapolite.

On the other hand, several studies have attempted to constrain the timing of IOCG-type mineralization by dating zircon in the altered host rocks in the vicinities of these deposits (e.g., Mortimer *et al*., 1988). Direct dating of Fe oxide–(Cu-Au) mineralization by U–Pb geochronology on hydrothermal zircon from ore samples of IOCG deposits in the Lyon Mountain Granite, Adirondack Mountains, United States, was reported by Valley *et al*. (2009).

Zircon crystals from hydrothermally altered and ore samples from the Bacaba deposit have been compared with hydrothermal zircon from different localities worldwide. Regarding internal structures and external morphologies, hydrothermal zircon reported worldwide display dissimilar features: i) they can be internally textureless and blocky (Hoskin, 2005; Valley *et al*., 2009; Bao *et al*., 2009) or show magmatic zonation (Pelleter *et al*., 2007); ii) they can occur as subhedral to anhedral small grains (Rubin *et al*., 1989; Rasmussen *et al*., 2005) or as mantles on magmatic cores (Hoskin, 2005) and iii) they may be inclusion-free (Rubin *et al*., 1989) or inclusion-rich (Pelleter *et al*., 2007; Bao *et al*., 2009; Valley *et al*., 2009).

However, all analysed zircon crystals, even those from Bacaba ore samples, have typical magmatic features (i.e. internal oscillatory zoning, mean Th/U ratios between 0.25 and 0.46). Only the 5 to 20 µm textureless mantles observed in zircon from the Serra Dourada Granite (Fig. 10E) may represent hydrothermal overgrowth. They might have U–Pb isotopic ages different from the igneous crystallized parts. A response to this question was not possible because the LA–ICP–MS spot size (30 µm) is considerably larger than mantles width, thus not allowing punctual analyses and age determination of the hydrothermal event.

8. Conclusions

The ca. 3.0 Ga and 2.86 Ga ages obtained for the felsic intrusive host rocks of the Bacaba deposit provide new insights about the CMP, as they are listed below:

• At least one disturbing process affected zircon grains from the Bacaba Tonalite and the Serra Dourada Granite, as demonstrated by recrystallization of zircon protolith, which has blurred magmatic oscillatory zonation areas, textureless domains and ovoid and rounded crystal morphologies.

• Radiogenic Pb loss was either associated with recrystallization process (probably in ore BACD9/257,45 sample, Bacaba Tonalite), or with radiation damage leading to partial to total

metamictization of zircon grains (possibly in albitized BACD15/237,40 sample, Serra Dourada Granite).

• The 2.86 and ca. 3.0 Ga Serra Dourada Granite and Bacaba Tonalite, respectively, are the oldest granitic rocks recognized in the Itacaiúnas Shear Belt Domain. These ages not only imply the existence of an important magmatism, yet poorly understood, before the Carajás Basin installation, but also indicate a more complex evolutionary history for the considered area.

• The basement rocks underlying the Carajás Basin also include the Serra Dourada Granite and Bacaba Tonalite, in addition to the Xingu and Pium basement complexes, as they are older than the 2.76 Ga Itacaiúnas Supergroup.

• As the Serra Dourada Granite and the Bacaba Tonalite have the same ages of calc-alkaline leucogranites (Xinguara and Mata Surrão granites) and tonalitic rocks (Arco Verde and Caracol tonalites), respectively, from the Rio Maria granite-greenstone terrain they could be genetically related. This fact would imply both in a more widespread ca. 3.0 and 2.86 Ga magmatism in the CMP than thought, and in a similar evolutional history between the Itacaiúnas Shear Belt and the Rio Maria granite-greenstone terrain previous to the Carajás Basin installation.

• The hydrothermal event associated with ore genesis could not be dated, either because of the total resetting of the U–Pb isotope system by hydrothermal fluids was not accomplished; or the hydrothermal mantles in protolith zircon could not be analyzed by LA–ICP–MS technique.

• The Serra Dourada Granite and the Bacaba Tonalite would possibly not be responsible for the establishment of a magmatic-hydrothermal system associated with the genesis of the Bacaba deposit, because other IOCG deposits with similar characteristics, which have been considered as result of a single hydrothermal paleo-system, are also hosted by the younger ~2.76 Ga Itacaiúnas Supergroup.

• The IOCG deposits in the southern part of the Itacaiúnas Shear Belt are genetically-related to the regional scale fluid circulation along important crustal discontinuities represented by WNW–ESE-striking regional shear zone. In this case, the Carajás IOCG deposits would be conditioned to the existence of structural traps.

• Extensive fluid-rock interaction along shear zones promoted metal lecahing from consolidated Mesoarchean rocks or units derived from ca. 3.0 Ga sources. External sources of heat would be required, as well as long-term fluid circulation involving magma- and externally-derived brines with residual evaporative contribution.

• These results indicate that the potential for the occurrence of IOCG deposits is not limited to the Carajás Basin, but that mineral exploration should be extended to the Mesoarchean basement areas crosscut by Neoarchean regional shear zones.

Acknowledgments

We are very grateful to the VALE for the continuous support provided to the researchers of the Institute of Geosciences–UNICAMP during their activities in the Carajás region. We feel particularly indebted to Márcio Godoy and Benevides Aires for their invaluable orientation in the field. We wish to thank Elton Dantas, Sérgio Junges and Bárbara Lima of the Geochronology Laboratory (UNB) and Dailto Silva (IG–UNICAMP) for the assistence with the analytical procedures. This research has been supported by the MCT/CNPq/CTMineral Process No. 555065/2006-5; CNPq Process No 303359/2008-0 and INCT Geociências da Amazônia (MCT/CNPq/ Fapespa 573733/2008-2).

References

Adshead, N.D., 1995. Geology, Alteration and Geochemistry of the Osborne Cu-Au Deposit, Cloncurry District, NW Queensland. Ph.D. thesis, James Cook University, Townsville, Australia, 382 p.

Althoff, F.J., 1996. Étude pétrologique et structurale des granitoïdes de Marajoara (Pará, Brésil): leur rôle dans l'évolution archéenne du craton Amazonien (2.7–3.2 Ga). Doctoral Thesis. Université Henri Poincaré, Nancy I, France, 296p. (in French).

Althoff, F.J., Barbey, P., Boullier, A.M., Champenois, M., 1993. The Archaean evolution of a crustal segment over 100 Ma: the Amazonian craton. EUG VII, Strasbourg Terra Abstr. 5, 32.

Augusto, R.A., Monteiro, L.V.S., Xavier, R. and Souza Filho, C.R., 2008. Zonas de alteração hidrotermal e paragênese do minério de cobre do Alvo Bacaba, Província Mineral de Carajás (PA). *Rev. Brasil. Geoci.* 38(2), 263–277.

Avelar, V.G., Lafon, J.M., Correia, F.C.Jr., Macambira, B.E.M., 1999. O magmatismo arqueano da região de Tucumã, Província Mineral de Carajás, Amazônia Oriental, Brasil: novos dados geocronológicos. *Rev. Brasil. Geoci.* 29, 453–460.

Bao, Z., Wang, Q., Bai, G., Zhao, Z., 2009. Impact of hydrothermal alteration on the U-Pb isotopic system of zircons from the Fangcheng syenites in the Qinling orogen, Henan Province, China. *Chin J. Geochem.* 28, 163–171.

Barbosa, A.A., Lafon, J.-M., 1996. Geocronologia Pb–Pb e Rb–Sr de granitóides arqueanos da região de Redenção, sul do Pará. *Rev. Brasil. Geoci*. 26, 255–264.

Barros, C.E.M., Dall'Agnol, R., Lafon, J.M., Teixeira N.P., Ribeiro J.W., 1992. Geologia e geocronologia Rb-Sr do Gnaisse Estrela, Curionópolis, PA. *Bol. Mus. Par. Em. Goeldi, Ciênc. da Terra* 4, 83–102.

Barros, C.E.M., Macambira, M.J.B., Barbey, P., Scheller, T., 2004. Dados isotópicos Pb–Pb em zircão (evaporação) e Sm–Nd do Complexo Granítico Estrela, Província Mineral de Carajás, Brasil: implicações petrológicas e tectônicas. *Rev. Brasil. Geoci.* 34, 531–538.

Barros, C.E.M., Sardinha, A.S., Barbosa, J.P.O., Krimski, R. and Macambira, M.J.B., 2001. Pb–Pb and U–Pb zircon ages of Archean syntectonic granites of the Carajás metallogenic province, northern Brazil. *South American Symposium on Isotopic Geology* 3, Proceedings, 94–97.

Beardsmore, T.J., 1992., Petrogenesis of Mount Dore-style Breccia-hosted Copper ± Gold Mineralization in the Kuridala- Selwyn Region of Northwestern Queensland. Ph.D. thesis, James Cook University, Townsville, Australia, 292 p.

Black, L.P., Williams, I.S., Compston, W., 1986. Four zircon ages from one rock: the history of a 3930 Ma-old granulite from Mount Sones, Enderby Land, Antarctica. *Contrib. Mineral. Petrol.* 94, 427–437.

Buhn, B., Pimentel, M.M., Matteini, M., Dantas, E.L., 2009. High spatial resolution analysis of Pb and U isotopes for geochronology by laser ablation multi-collector inductively coupled plasma mass spectrometry (LA-MC-ICP-MS). *Anais Acad. Brasil. Ciências* 81(1), 1–16.

Cathles, L.M., Erendi, A.H.J., Barrie, T., 1997. How long can a hydrothermal system be sustained by a single intrusive event? *Econ. Geol*. 92, 766–771

Cherniak, D.J., Hanchar, J.M., Watson, E.B., 1997a. Rare-earth diffusion in zircon. *Chem. Geol.* 134, 289–301.

Cherniak, D.J., Hanchar, J.M., Watson, E.B., 1997b. Diffusion of tetravalent cations in zircon. *Contrib. Mineral. Petrol.* 127, 383–390.

Chiaradia M., Banks D., Cliff R., Marschik, R., de Haller A., 2006. Origin of fluids in iron oxide–copper–gold deposits: constraints from $\delta^{37}Cl$, $^{87}Sr/^{86}Sr$ and Cl/Br. *Miner. Depos.* 41, 565–573.

Connelly, J.N., 2001. Degree of preservation of igneous zonation in zircon as a signpost for concordancy in U/Pb geochronology. *Chem. Geol.* 172, 25–39.

Cordani, U., 1981. Comentários sobre as determinações geocronológicas da região da Serra dos Carajás. Report, Universidade de São Paulo-Docegeo.

Corfu F., Hanchar J. M., Hoskin P. W. O., Kinny P. D., 2003. An atlas of zircon textures. *In Zircon.* (eds. J. M. Hanchar and P. W. O. Hoskin) Rev. In: *Mineralogy and Geochemistry* **53,** Mineralogical Society of America, Washington, D.C. pp. 469–500.

Dall'Agnol, R., Lafon, J.M., Macambira, M.J.B., 1994. Proterozoic Anaorogenic Magmatism In The Central Amazonian Province, Amazonian Craton: Geochronological, Petrological And Geochemical Aspects. *Mineral. Petrol*. 50, 113–118.

Dall'Agnol, R., Oliveira, D.C., 2007. Oxidized, magnetite-series, rapakivi-type granites of Carajás, Brazil: implications for classification and petrogenesis of A-type granites. *Lithos* 93, 215–233.

Dall'Agnol, R., Souza, Z.S., Althoff, F.J., Barros, C.E.M., Leite, A.A.S. and Jorge-João, X.S., 1997. General aspects of the granitogenesis of the Carajás metallogenetic province. *International Symposium on Granites and Associated Mineralizations*, Salvador, Excursion Guide, 135–161.

Dall'Agnol, R., Oliveira, M.A., Almeida, J.A.C., Althoff, F.J., Leite, A.A.S., Oliveira, D.C., Barros, C.E.M., 2006. Archean and paleoproterozoic granitoids of the Carajás Metallogenic Province, eastern Amazonian craton. *In*: Symposium on magmatism, crustal evolution and metallogenesis of the Amazoniam Craton, Belém, *Excursion Guide*, 99–150.

Dall'Agnol, R., Rämö, O.T., Magalhães, M.S., Macambira, M.J.B., 1999. Petrology of the anorogenic, oxidised Jamon and Musa granites, Amazonian craton: implications for the genesis of Proterozoic A-type granites. *Lithos* 46, 431–462.

Dall'Agnol, R., Teixeira, N.P., Rämö, O.T., Moura, C.A.V., Macambira, M.J.B., Oliveira, D.C., 2005. Petrogenesis of the Paleoproterozoic, rapakivi, A-type granites of the Archean Carajás Metallogenic Province, Brazil. *Lithos* 80, 101–129.

Dardenne, M.A., Schobbenhaus, C.S., 2001. Metalogênese do Brasil. Editora Universidade de Brasília/CNPq, Brasília, 392 p.

Degeling, H., Eggins, S., Ellis, D.J., 2001. Zr budgets for metamorphic reactions, and the formation of zircon from garnet breakdown. *Mineral. Mag.* 65, 749–758.

Dias, G.S., Macambira, M.B., Dall'Ágnol, R., Soares, A.D.V., Barros, C.E.M., 1996. Datações de zircões de sill de metagabro: comprovação de idade arqueana da Formação Águas Claras, Carajás, Pará. *V Simpósio de Geologia da Amazônia*, SBG, 376–378.

DOCEGEO, 1988. Revisão litoestratigráfica da Província Mineral de Carajás – Litoestratigrafia e principais depósitos minerais. *35º Congr. Brasil. Geol.*, Belém, SBG, Proceedings, 11–54.

Feio, G.R.L., Dall'Agnol, R., Soares, J.E.B., Gomes, A.C.B., 2009. Geoquímica do magmatismo granitóide arqueano da região de Canaã dos Carajás. *XI Simp. Geol. Amazon.*, Manaus (CD-ROM).

Friend, C.R.L., Kinny, P.D., 1995. New evidence for protolith ages of Lewisian granulites, northwest Scotland. *Geology* 23, 1027–1030.

Fu, B., Mernagh, T.P., Kita, N.T., Kemp, A.I.S., Valley, J.W., 2009. Distinguishing magmatic zircon from hydrothermal zircon: A case study from the Gidginbung high-sulphidation Au–Ag–(Cu) deposit, SE Australia. *Chem. Geol.* 259, 131–142.

Galarza, M.A. and Macambira, M.J.B. 2002a. Petrologia e geocronologia das rochas encaixantes do depósito de Cu-Au Igarapé Bahia, Província Mineral de Carajás, Pará, Brasil. In: Kein, E.L., Vasquez, M.L., Rosa-Costa, L.T. (Eds.). Contribuições à geologia da Amazônia, vol. 3, SBG/ NN, Belém, p. 153–168.

Galarza, M.A., 2002. Geocronologia e Geoquímica Isotópica dos Depósitos de Cu-Au Igarapé Bahia e Gameleira, Província Mineral de Carajás (PA), Brasil. Ph.D. thesis, Universidade Federal do Pará, Brazil.

Galarza, M.A., Macambira, M.J.B., 2002b. Geocronologia e Evolução Crustal da Área do Depósito de Cu–Au Gameleira, Província Mineral de Carajás (Pará), Brasil. *Geol. USP Série Científica* 2, 143–159.

Galarza, M.A., Macambira, M.J.B., Villas, R.N., 2008. Dating and isotopic characteristics (Pb and S) of the Fe oxide–Cu–Au–U–REE Igarapé Bahia ore deposit, Carajás Mineral province, Pará state, Brazil. *J. South Am. Earth Sci.* 25, 377–397.

Geisler, T., Pidgeon, R.T., Kurtz R., Van Bronswijk, W., Schleicher, H., 2003a. Experimental hydrothermal alteration of partially metamict zircon. *Am. Mineral.* 88, 1496–1513.

Geisler, T., Rashwan, A. A., Rahn, M. K.W., Poller, U., Zwingmann, H., Pidgeon, R.T., Schleicher, H., Tomaschek, F., 2003b. Low temperature hydrothermal alteration of natural metamict zircons from the Eastern Desert, Egypt. *Mineral. Mag.* 67, 485–508.

Gibbs, A.K., Wirth, K.R., Hirata, W.K., Olzewski Jr, W.J., 1986. Age and composition of the Grão-Pará Group volcanics, Serra dos Carajás. *Rev. Brasil. Geoci.* 16, 201– 211.

Gomes, A.C.B., 2003. Geologia, petrografia e geoquímica dos granitóides de Canaã dos Carajás, SE do Estado do Pará. Belém. MSc Thesis, Universidade Federal do Pará, Brazil, 160 p.

Gomes, A.C.B., Dall'Agnol, R., Oliveira, M.A., 2004. Granitos arqueanos cálcico-alcalinos e do tipo-A da região a leste de Canaã dos Carajás. In: Anais do Congr. Brasil. Geol., 42, Araxá. (CD-ROM).

Grainger, C.J., Groves, D.I., Tallarico, F.H.B, Fletcher, I.R., 2008. Metallogenesis of the Carajás Mineral Province, Southern Amazon Craton, Brazil: Varying styles of Archean through Paleoproterozoic to Neoproterozoic base- and precious-metal mineralisation. *Ore Geol. Rev.* 33, 451–489.

Hitzman, M.W., Oreskes, N, Einaudi, M.T., 1992. Geological characteristics and tectonic setting of Proterozoic iron oxide (Cu-U-Au-REE) deposits. *Precamb. Res.* 58, 241–287.

Hirata, W.K., Rigon, J.C., Kadekaru, K., Cordeiro, A.A.C., Meireles, E.A., 1982. Geologia Regional da Província Mineral de Carajás. *I Simp. Geol. Amazônia*, Belém, SBG/NO, 1: 100–110.

Holdsworth, R., Pinheiro, R., 2000. The anatomy of shallow-crustal transpressional structures: insights from the Archean Carajás fault zone, Amazon, Brazil. *J. Struc. Geol.* 22, 1105–1123.

Hoskin, P.W.O., 2005. Trace-element composition of hydrothermal zircon and the alteration of Hadean zircon from the Jack Hills, Australia. *Geochim. Cosmochim. Acta* 69, 637–648.

Hoskin, P.W.O., Black, L.P., 2000. Metamorphic zircon formation by solid-state recrystallization of protolith igneous zircon. *J. Metamor. Geol.* 18, 423–439.

Hoskin, P.W.O., Schaltegger, U., 2003. The composition of zircon and igneous and metamorphic petrogenesis. In: J. M. Hanchar and P. W. O. Hoskin (eds). Zircon. *Rev. Mineral. Geochem*. 53, 27–62.

Huhn, S.R.B., Souza, C.I.J., Albuquerque, M.C., Leal, E.D., Brustolin, V., 1999. Descoberta do depósito Cu(Au) Cristalino: Geologia e mineralização associada região da Serra do Rabo, Carajás – PA. *VI Simpósio de Geologia da Amazônia*, SBG/NO, 140–143.

Jackson, S.E., Pearson, N.J., Griffin, W.L., Belousova, E.A., 2004. The application of laser ablation-inductively coupled plasma-mass spectrometry to in situ U–Pb zircon geochronology. *Chem. Geol*. 211, 47–69.

Kalsbeek, F., Taylor, P.N., Pigdeon, R.T., 1988. Unreworked Archean basement and Proterozoic supracrustal rocks from northeastern Disko Bugt, West Greenland: implications for the nature of Proterozoic mobile belts in Greenland. *Can. J. Earth Sci.* 25, 773–782.

Kröner, A., Jaeckel, P., Williams, I. S., 1994. Pb-loss patterns in zircons from a high-grade metamorphic terrain as revealed by different dating methods: U–Pb and Pb–Pb ages for igneous and metamorphic zircons from northern Sri Lanka. *Precamb. Res*. 66, 151–181.

Lafon, J.-M., Rodrigues, E., Duarte, K.D., 1994. Le granite Mata Surrão: un magmatisme monzogranitique contemporain des associations tonalitiques-trondhjé-mitiques-granodioritiques archeénnes de la région de Rio Maria (Amazonie orientale, Brésil). C. R. *Acad. Sci. Paris* 318, 643–649.

Lancaster Oliveira J., Fanton, J., Almeida, A.J., Leveille, R.A., Vieira, S., 2000. Discovery and geology of the Sossego copper–gold deposit, Carajás District, Pará State, Brazil. *31st International Geology Congress*, IUGS, [CD-ROM].

Leite, A.A.S., Dall'Agnol, R., Macambira, M.J.B., Althoff, F.J., 2004. Geologia e geocronologia dos granitóides arqueanos da região de Xinguara (PA) e suas implicações na evolução do Terreno Granito-Greenstone de Rio Maria. *Rev. Brasil. Geoci*. 34, 447–458.

Lindenmayer, Z.G., 1990. Salobo sequence, Carajás, Brasil: Geology, Geochemistry and Metamorphism. PhD Thesis, *University of Ontario, Canada*, 407p.

Lindenmayer, Z.G., 2003. Depósito de Cu–Au do Salobo, Serra dos Carajás: Uma revisão. In: L.H. Ronchi and F.J. Althoff (Eds.), Caracterização e modelamento de depósitos minerais. Editora Unisinos, São Leopoldo, 69–98.

Lindenmayer, Z.G., Teixeira, J.B.G., 1999. Ore genesis at the Salobo Copper deposit, Serra dos Carajás. In: Silva, M.G. and Misi, A. (eds), *Base Metal Deposits of Brazil*. MME/CPRM/DNPM, 33–43.

Ludwig, K.R., 2003. User's Manual for Isoplot/Ex v. 3.00. A Geochronological Toolkit for Microsoft Excel. BGC Special Publication 4, Berkeley, 71 pp.

Macambira, M.J.B., Costa, J.B.S., Althoff, F.J., Lafon, J.-M., Melo, J.C.V., Santos, A., 2000. New geochronological data for the Rio Maria TTG terrane; implications for the time constraints of the Carajás Province, Brazil. In: 31st Intern. Geol. Congr., Rio de Janeiro, CD-ROM.

Macambira, M.J.B., Lafon, J.-M., Pidgeon, R.T., 1998. Crescimento crustal arqueano registrado em zircões de sedimentos da região de Rio Maria, Província Carajás, Pará. In: 40th Congr. Bras. Geol., SBG, Belo Horizonte. Proceedings, p. 55.

Macambira, M.J.B., Lancelot J., 1996. Time constraints of Archean Rio Maria crust, Southeastern Amazonian Craton, Brazil. Intern. *Geol. Rev*. 38 (12), 1134–1142.

Macambira, M.J.B., Lancelot, J., 1992. Idade U–Pb em zircocões de metavulcânica do greenstone do Supergrupo Andorinhas; delimitante da estratigrafia arqueana de Carajás, Estado do Pará. Congr. Bras. Geol., São Paulo 2, 188– 189.

Machado, N., Lindenmayer, D.H., Krough, T.E., Lindenmayer, Z.G. 1991. U-Pb geochronology of Archean magmatism and basement reactivation in the Carajás area, Amazon Shield, Brazil. *Precamb. Res.* 49, 329-354.

Mark, G., Foster, D.W., Pollard, P.J., Williams, P.J., Tolman, J., Darwall, M., Blake, K.L. 2004 Stable isotope evidence for magmatic fluid input during large-scale Na-Ca alteration in the Cloncurry Fe oxide Cu-Au district, NW Queensland, Australia. *Terra Nova* 16, 54–61.

Marschik, R., Mathur, R., Ruiz, J., Leveille, R., Almeida, A.J., 2005. Late Archean Cu-Au-Mo mineralization at Gameleira and Serra Verde, Carajás Mineral Province, Brazil: constraints from Re-Os molybdenite ages. *Miner. Depos.* 39, 983–991.

Meldrum, A., Boatner, L.A., Weber, W.J., Ewing, R.C., 1998. Radiation damage in zircon and monazite. *Geochim. Cosmochim. Acta* 62, 2509–2520.

Meldrum, A., Zinkle, S.J., Boatner, L.A., Ewing, R.C., 1999. Amorphization, recrystallization, and phase decomposition in the ABO_4 orthosilicates. *Phys. Rev. B.* 59, 3981– 3992

Monteiro, L.V.S., Xavier, R. P., Souza Filho, C.R., Augusto, R.A., 2007. Aplicação de isótopos estáveis ao estudo dos padrões de distribuição das zonas de alteração hidrotermal associados ao sistema de óxido de ferro-cobre-ouro Sossego, Província Mineral de Carajás. *XI Congresso Brasileiro de Geoquímica*, 2007, Atibaia, SBGq, [CD-ROM].

Monteiro, L.V.S., Xavier, R.P., Carvalho, E.R., Hitzman, M.W., Johnson, C.A., Souza Filho, C.R., Torresi, I., 2008a. Spatial and temporal zoning of hydrothermal alteration and mineralization in the Sossego iron oxide–copper–gold deposit, Carajás Mineral Province, Brazil: paragenesis and stable isotope constraints. *Miner. Depos.* 43, 129–159.

Monteiro, L.V.S., Xavier, R.P., Hitzman, M.W., Juliani, C., Souza Filho, C.R., Carvalho, E.R., 2008b. Mineral chemistry of ore and hydrothermal alteration at the Sossego iron oxide–copper–gold deposit, Carajás Mineral Province, Brazil. *Ore Geol Rev.* 34, 317-336.

Mora C. I. and Valley J. W. (1989) Halogen-rich scapolite and biotite: Implications for metamorphic fluid-rock interactions. *Am. Mineral*. 74, 721–737.

Mortimer, G.E., Cooper, J.A., Paterson, H.L., Cross, K., Hudson, G.R.T., Uppill, R.K. 1988. Zircon U-Pb dating in the vicinity of the Olympic Dam Cu-U-Au deposit, Roxby Downs, South Australia. *Econ. Geol*. 83, 694– 709

Mougeot, R., Respaut, J.P., Briqueu, L., Ledru, P., Milesi, J.P., Macambira, M.J.B., Huhn, S.B., 1996. Geochronological constrains for the age of the Águas Claras Formation (Carajás Province, Pará, Brazil). In: CONG. BRAS. GEOL., 39, Salvador, 1996. Anais., Salvador, SBG. 6, 579–581.

Murakami, T., Chakoumakos, B.C., Ewing, R.C., Lumpkin, G.R., Weber, W.J., 1991. Alpha-decay event damage in zircon. *Am. Mineral.* 76, 1510–1532.

Mustard, R., Baker, T., Williams, P.J., Mernagh, T, Ryan, C., van Achterbergh, E., Adshead, D., 2004. The role of unmixing in magnetite–copper deposition in the Fe oxide–Cu–Au systems. *In:* Predictive mineral discovery *CRC* Conference, Barossa Valley.

Nelson, E.P. Hitzman, M.W., Monteiro, L.V.S. 2007. Hydrothermal metamorphism and transient depth fluctuations of the brittle-ductile transition during shear-zone hosted IOCG mineralization. *Geological Society of America Abstracts with Programs*, 39(6), 535.

Neves, M.P., 2006. Estudos isotópicos (Pb-Pb, Sm-Nd, C e O) do depósito Cu-Au do Sossego, Província Mineral de Carajás. M.Sc. Thesis, *Universidade Federal do Pará*, Brazil. 116 pp.

Nogueira, A.C.R., Truckenbrod, W., Costa, J.B.S., Pinheiro, R.V.L., 1994. Análise faciológica e estrutural da Formação Águas Claras, Pré-Cambriano da Serra dos Carajás. IV Simpósio de Geologia da Amazônia, 363–364.

Nogueira, A.C.R., Truckenbrod, W., Pinheiro, R.V.L., 2000. Storm and tide-dominated siliciclastic deposits of the Archean Águas Claras Formation, Serra dos Carajás, Brazil. 31st International Geological Congress, Rio de Janeiro. Soc. Brasil. Geol. Abstract volume CD-ROM.

Oliveira, M.A., Dall'Agnol, R., Althoff, F.J., Leite, A.A.S., 2009. Mesoarchean sanukitoid rocks of the Rio Mari Granite-Greenstone Terrane, Amazonian craton, Brazil. *J. South Am. Earth Sci.* 27, 146–160.

Pelleter, E., Cheilletz, A., Gasquet, D., Mouttaqi, A., Annich, M., El Hakourd, A., Deloule, E., Féraude, G., 2007. Hydrothermal zircons: a tool for ion microprobe U–Pb dating of gold mineralization (Tamlalt-Menhouhou gold deposit—Morocco). *Chem. Geol*. 245, 135–161.

Perring, C.S., Pollard, P.J., Dong, G., Nunn, A.J., Blake, K.L., 2000. The Lightning Creek sill complex, Cloncurry district, northwest Queensland: a source of fluid for Fe oxide–Cu–Au mineralization and sodic–calcic alteration. *Econ Geol* 95, 1067–1069.

Pidgeon, R.T., Nemchin, A.A., Hitchen, G.J., 1998. Internal structures of zircons from Archean granites from the Darling Range batholith: Implications for zircon stability and the interpretation of zircon U-Pb ages. *Contrib. Mineral. Petrol.* 132, 288–299.

Pidgeon, R.T., 1992. Recrystallization of oscillatory zoned zircon: some geochronological and petrological implications. *Contrib. Mineral. Petrol.* 110, 463–472.

Pidgeon, R.T., Macambira, M.J.B., Lafon, J.M., 2000. Th–U–Pb isotopic systems and internal structures of complex zircons from an enderbite from the Pium Complex, Carajás Province, Brazil: evidence for the ages of granulite facies metamorphism and the protolith of the enderbite. *Chem. Geol.* 166, 159–171.

Pidgeon, R.T., O'Neil, J., Silver, L.T., 1966. Uranium and lead isotopic stability in a metamict zircon under experimental hydrothermal conditions. *Science* 154, 1538–1540.

Pidgeon, R.T., Wilde, S.A., Comston, W., Shield, M.W., 1990. Archean Evolution of the Wongan Hills Greenstone Belt, Yilgarn Craton, Western Australia. *Aust. J. Earth Sci.* 37, 279–292.

Pimentel, M.M., Lindenmayer, Z.G., Laux, J.H., Armstrong, R., Araújo, J.C., 2003. Geochronology and Nd geochemistry of the Gameleira Cu-Au deposit, Serra dos Carajás, Brazil: 1.8–1.7 Ga hydrothermal alteration and mineralization. *J. South Am. Earth Sci.* 15, 803–813.

Pimentel, M.M., Machado, N., 1994. Geocronologia U−Pb dos terrenos granito-greenstone de Rio Maria, Pará. In: Cong. Bras. Geol., Anais, Sociedade Brasileira de Geologia, vol. 2, pp. 390−391.

Pollard, P.J., 2001. Sodic–(calcic) alteration in Fe-oxide–Cu–Au districts: an origin via unmixing of magmatic H_2O–CO_2–NaCl + $CaCl_2$-KCl fluids. *Miner. Depos.* 36, 93−100.

Pollard, P.J., 2006. An intrusion-related origin for Cu–Au mineralization in iron oxide–copper–gold (IOCG) provinces. *Miner. Depos.*, 41, 179–187.

Rasmussen, B., 2005. Zircon growth in very low grade metassedimentary rocks: evidence for zirconium mobility at ~250 °C. *Contrib. Mineral. Petrol.* 150, 146–155

Réquia K., Stein H., Fontboté L., Chiaradia M. 2003. Re–Os and Pb–Pb geochronology of the Archean Salobo iron oxide copper–gold deposit, Carajá Mineral Province, northern Brazil. *Miner. Depos.* 38, 727–738.

Rigon, J.C., Munaro, P., Santos, L.A., Nascimento, J.A.S., Barreira, C.F., 2000. Alvo 118 copper–gold deposit: geology and mineralization, Serra dos Carajás, Pará, Brazil. *31st International Geological Congress*, Rio de Janeiro. SBG, Abstract Volume, [CD-ROM].

Rodrigues, E.S., Lafon, J.M., Scheller, T., 1992. Geocronologia Pb-Pb da Província Mineral de Carajás: primeiros resultados. In: Cong. Bras. Geol., 37, *Bol. Res. Exp*., SBG, São Paulo, vol. 2, pp. 183–184.

Rolando, A.P., Macambira, M.J.B., 2003. Archean crust formation in Inajá Range area, SSE of Amazonian Craton, Brazil, based on zircon ages and Nd isotopes. IV South American Symposium on Isotope Geology, Short papers [CD-ROM]/

Rubin, J. N., Henry, C. D., Price, J. G., 1989. Hydrothermal zircons and zircon overgrowths, Sierra Blanca Peaks, Texas. *Am. Mineral* 74, 865–869.

Sardinha, A.S., Barros, C.E. de M., Krymsky, M., 2006. Geology, geochemistry and U–Pb geochronology of the Archean (2.74 Ga) Serra do Rabo granite stocks, Carajás Metalogenetic Province, northern Brazil. *J. South Am. Earth Sci.* 20, 327–339.

Sardinha, A.S., Dall'Agnol, R., Gomes, A.C.B., Macambira, M.J.B., Galarza, M.A., 2004. Geocronologia Pb-Pb e U-Pb em zircões de granitóides arqueanos da região de Canaã dos Carajás, Província Mineral de Carajás. In: SBG, Congresso Brasileiro de Geologia, 42 (CD-ROM).

Sato K., Tassinari C.C.G. 1997. Principais eventos de acreção continental no Cráton Amazônico baseados em idademodelo Sm-Nd, calculada em evoluções de estágio único e estágio duplo. In: Costa M.L.C. & Angélica R.S. (coords.) Contribuição à Geologia da Amazônia. SBG-NO, p. 91–142.

Schaltegger, U., Fanning, C.M., Gunther, D., Maurin, J.C., Schulmann, K., Gebauer, D., 1999. Growth, annealing and recrystallization of zircon and preservation of monazite in high-grade metamorphism: Conventional and *in situ* U-Pb isotope, cathodoluminescence and microchemical evidence. *Contrib. Mineral. Petrol.* 134, 186–201.

Silva, M.G., Teixeira, J.B.G., Pimentel, M.M., Vasconcelos, P.M., Arielo, A., Rocha, W.J.S.F., 2005. Geologia e mineralizações de Fe-Cu-Au do Alvo GT46 (Igarapé Cinzento, Carajás). In: Marini, O.J., Queiroz, E.T., Ramos, B.W. (eds.), *Caracterização de Depósitos Minerais em Distritos Mineiros da Amazônia*, 94–151.

Soares, A.D.V., Macambira, M.J.B., Santos, M.G.S., Vieira, E.A.P., Massoti, F.S., Souza, C.I.J., Padilha, J.L., Magni, M.C.V., 2001. Depósito Cu(Au) Cristalino, Serra dos Carajás, PA: Idade da mineralização com base em análises Pb–Pb em sulfetos (dados preliminares). SBG, Simpósio de Geologia da Amazônia, 7, Res. Expandidos [CD-ROM].

Souza, L.H., Vieira, E.A.P., 2000. Salobo 3 Alpha Deposit: Geology and Mineralisation. In: T.M. Porter (ed.), *Hydrothermal iron Oxide Copper-gold & related Deposits: A global perspective*, Austral. Miner. Found., Adelaide, 213−224.

Souza, S.R.B., Macambira, M.J.B., Sheller, T., 1996. Novos dados geocronológicos para os granitos deformados do Rio Itacaiúnas (Serra dos Carajás, PA); implicações estratigráficas. *V Simpósio de Geologia da Amazônia*, Belém, Proceedings, 380–383.

Souza, Z.S., Medeiros, H., Althoff, F.J., Dall'Agnol, R., 1990. Geologia do terreno ''granitogreenstone'' da região de Rio Maria, sudeste do Pará. Congresso Brasileiro de Geologia, Natal 6, 2913–2928.

Souza, Z.S., Potrel, H., Lafon, J.M., Althoff, F.J., Pimentel, M.M., Dall'Agnol, R., Oliveira, C.G., 2001. Nd, Pb and Sr isotopes of the identidade belt, an archaean greenstone belt of the Rio Maria region (Carajás Province, Brazil): implications for the archaean geodynamic evolution of the Amazonian craton. *Precamb. Res.* 109, 293–315.

Stacey, J.S., Kramers, J.D., 1975. Approximation of terrestrial lead isotope evolution by a two-stage model. *Earth Planet. Sci. Lett*. 26, 207–221.

Stein, H.J., Cathles, L.M. 1997. The Timing and Duration of Hydrothermal Events. *Econ. Geol.* 92, 763-765.

Tallarico F.H.B., McNaughton N.J., Groves D.I., Fletcher I.R., Figueiredo B.R., Carvalho J.B., Rego J.L., Nunes A.R., 2004. Geological and SHRIMP II U-Pb constraints on the age and origin of the Breves Cu-Au-(W-Bi-Sn) deposit, Carajás, Brazil. *Miner. Depos.* 39, 68–86.

Tallarico, F.H.B., 2003. O cinturão cupro-aurífero de Carajás, Brasil. Ph.D. Thesis. Universidade Estadual de Campinas, Brazil. 229p.

Tallarico, F.H.B., Figueiredo, B.R., Groves, D.I., Kositcin, N., McNaughton, N.J., Fletcher, I.R., Rego, J.L. 2005. Geology and SHRIMP U–Pb geochronology of the Igarapé Bahia deposit, Carajás copper–gold belt, Brazil: an Archean (2.57 Ga) example of iron–oxideCu–Au–(U– REE) mineralization. *Econ. Geol.* 100, 7–28.

Tassinari C.C.G., Macambira M.J.B. 1999. Geochronological provinces of the Amazonian Craton. *Episodes* 22(3),174−182.

Tassinari, C.C.G., Mellito, M.K., Babinski, M., 2003. Age and origin of the Cu (Au–Mo–Ag) Salobo 3A ore deposit, Carajás Mineral Province, Amazonian Craton, northern Brazil. *Episodes* 26, 2–9.

Tavaza, E., Oliveira, C.G., 2000. The Igarapé Bahia Au−Cu−(REE−U) Deposit, Carajás Mineral Province, Northern Brazil In: TM Porter (ed), Hydrothermal iron Oxide Copper-gold & related Deposits: A global perspective, Australia Mineral Foundation, Adelaide, 203−212.

Teixeira, N.P., Bettencourt, Moura C.A.V., Dall'Agnol, R., Macambira. E.M.B. 2002. Archean crustal sources for Paleoproterozoic tin-mineralized granites in the Caraja´s Province, SSE Para´, Brazil: Pb/Pb geochronology and Nd isotope geochemistry. *Precamb Res* 119, 257−275

Tomaschek, F., Kennedy, A. K., Villa, I. M., Lagos, M., Ballhaus, C., 2003. Zircons from Syros, Cyclades, Greece–-recrystallization and mobilization of zircon during high-pressure metamorphism. *J Petrol.* 44, 1977–2002.

Torresi, I., 2009. Evolução química e isotópica dos fluidos associados à mineralização de Cu-Au do depósito Alvo 118, Província Mineral de Carajás (PA.) MSc. Thesis. Universidade Estadual de Campinas. 80pp.

Torresi, I., Bortholoto, D.F.A., Xavier, R.P., Monteiro, L.V.S., Submitted. Hydrothermal alteration, fluid inclusions and stable isotope systematics of the Alvo 118 Iron Oxide-Copper-Gold Deposit, Carajás Mineral Province (Brazil): Implications For Ore Genesis. *Miner. Depos*.

Trendall, A.F., Basei, M.A.S., De Laeter, J.R., Nelson, D.R., 1998. SHRIMP U-Pb constraints on the age of the Carajás formation, Grão Pará Group, Amazon Craton. *J. South Am. Earth Sci.* 11, 265–277.

Valley, P.M., Hanchar, J.M., Whitehouse, M.J. 2009. Direct dating of Fe oxide-(Cu-Au) mineralization by U/Pb zircon geochronology. *Geology* 37, 223–226.

Vanko, D.A., Bishop, F.C., 1982 Occurrence and origin of marialitic scapolite in the Humboldtt Lopolith, N.W. Nevada. *Contrib. Mineral. Petrol*. 81, 277–289.

Vavra, G., 1990. On the kinematics of zircon growth and its petrogenetic significance: A cathodoluminescence study. *Contrib. Mineral. Petrol.* 106, 90–99.

Vavra, G., Gebauer, D., Schmid, R., Compston, W., 1996. Multiple zircon growth and recrystallization during polyphase Late Carboniferous to Triassic metamorphism in granulites of the Ivrea zone (Southern Alps): An ion microprobe (SHRIMP) study. *Contrib. Mineral. Petrol*. 122, 337–358.

Villas, R.N., Neves, M.P., Moura, C.V., Toro, M.A.G., Aires, B., Maurity, C., 2006. Estudos isotópicos (Pb, C e O) no depósito Cu-Au do Sossego, Província Mineral de Carajás. *IX Simpósio de Geologia da Amazônia*, SBG/Núcleo Norte, [CD-ROM].

Williams, I.S., Claesson, S., 1987. Isotopic evidence for the Precambrian provenance and Caledonian metamorphism of high grade paragneisses from the Seve Nappes, Scandinavian Caledonides. *Contrib. Mineral. Petrol*. 97, 205–217.

Wirth, K.R., Gibbs, A.K., Olszewski, W.J.Jr., 1986. U–Pb ages of zircons from the Grão Pará Group and Serra dos Carajás granite, Pará, Brasil. *Rev. Brasil.Geoci.* 16, 195–200.

Xavier, R..P., Wiedenbeck, M., Trumbull, R.B., Dreher, A.M., Monteiro, L.V.S., Rhede, D., Araújo, C.E.G., Torresi, I., 2008. Tourmaline B-isotopes fingerprint marine evaporites as the source of high-salinity ore fluids in iron oxide-copper-gold deposits, Carajás Mineral Province (Brazil). *Geology* 36(9), 743–746.

Xavier, R.P., Monteiro, L.V.S., Souza Filho, C.R., Torresi, I., Carvalho, E.R., Dreher, A.M., Pestilho, A.L.S., Moreto, C.P.N. In press. The iron oxide copper-gold deposits of the Carajás Mineral Province, Brazil: an updated and critical review. In: Porter, T.M. (Ed), 2010 - Hydrothermal Iron Oxide Copper-Gold & Related Deposits: A Global Perspective, vol. 3, Advances in the Understanding of IOCG Deposits, PGC Publishing, Adelaide.

Appendix

Table 4. Summary of LA–ICP–MS data of zircon from the Serra Dourada Granite (sample BACD15/237,40)

	Isotopic ratios								Ages							
Grain area	Th/U	$^{206}Pb/^{204}Pb$	$^{207}Pb/^{206}Pb$	1σ	$^{207}Pb/^{235}U$	1σ	$^{206}Pb/^{238}U$	1σ	$^{207}Pb/^{206}Pb$	1σ	$^{207}Pb/^{235}U$	1σ	$^{206}Pb/^{238}U$	1σ	Rho	Conc (%)
1	0.56	35639	0.14265	2.1	2.8900	1.8	0.14693	1.1	2259.6	36.1	1379.3	13.4	883.8	9.3	0.54	39.11
2	0.37	41554	0.16077	2.0	4.1302	1.7	0.18632	1.2	2463.8	33.6	1660.3	13.4	1101.4	11.6	0.64	44.70
3 (c)	0.34	35615	0.13473	1.9	2.4300	1.5	0.13081	1.1	2160.5	32.0	1251.5	10.9	792.5	7.9	0.63	36.68
3 (r)	0.27	16623	0.11910	4.2	1.5563	3.3	0.09477	2.6	1942.8	73.3	953.0	20.1	583.7	14.6	0.73	30.04
4	0.49	25877	0.14241	2.0	3.0601	1.6	0.15584	1.2	2256.8	34.6	1422.8	12.5	933.6	10.4	0.61	41.37
5	0.27	37336	0.15104	2.2	3.4728	1.8	0.16676	1.3	2357.7	37.0	1521.1	13.8	994.2	12.0	0.68	42.17
6	0.41	34121	0.14269	1.8	2.5607	1.4	0.13015	1.0	2260.1	30.0	1289.5	10.4	788.7	7.5	0.60	34.90
7	0.58	50188	0.12448	1.7	2.1713	1.4	0.12651	1.0	2021.5	30.5	1171.9	9.8	767.9	7.3	0.63	37.99
8 (c)	0.59	41184	0.18148	1.7	7.0773	1.4	0.28284	1.1	2666.4	28.4	2121.2	12.2	1605.7	14.9	0.71	60.22
8 (r)	0.47	39056	0.15111	1.9	3.2812	1.5	0.15748	1.1	2358.5	32.1	1476.6	12.0	942.8	9.7	0.66	39.97
9	0.50	85475	0.12319	2.0	2.1549	1.6	0.12687	1.2	2002.9	35.2	1166.6	11.3	770.0	8.4	0.65	38.44
10 (c)	0.48	43804	0.14650	2.1	3.4599	1.8	0.17129	1.2	2305.4	36.3	1518.1	13.9	1019.2	11.3	0.63	44.21
10 (r)	0.44	23452	0.15076	2.6	3.4565	2.0	0.16628	1.7	2354.6	44.5	1517.4	15.9	991.6	15.6	0.69	42.11
11	0.44	30787	0.13330	1.9	2.1598	1.5	0.11751	1.1	2141.9	33.1	1168.2	10.6	716.2	7.7	0.70	33.44
12	0.33	36724	0.16734	1.9	5.0309	1.5	0.21804	1.1	2531.2	30.8	1824.5	12.4	1271.5	13.0	0.71	50.23
13	0.40	60875	0.12754	3.1	2.4800	2.4	0.14103	1.9	2064.4	53.9	1266.2	17.5	850.5	15.4	0.66	41.20
14 (c)	0.40	17613	0.13657	2.3	2.3571	1.8	0.12517	1.3	2184.2	39.1	1229.7	13.0	760.3	9.6	0.66	34.81
14 (r)	0.51	40323	0.10463	2.3	1.3444	1.9	0.09319	1.3	1707.9	41.3	865.1	10.7	574.3	7.2	0.66	33.63
15	0.50	37079	0.12520	2.0	2.1823	1.6	0.12642	1.2	2031.6	35.6	1175.4	11.3	767.4	8.8	0.69	37.77
16 (c)	0.48	50286	0.15514	2.9	3.3231	2.2	0.15535	1.9	2403.4	49.2	1486.5	17.4	930.9	16.5	0.72	38.73
16 (r)	0.59	24274	0.13697	1.8	2.4889	1.5	0.13179	1.0	2189.2	31.4	1268.8	10.8	798.1	7.8	0.65	36.45
17	0.45	63966	0.14205	2.0	2.8944	1.6	0.14778	1.2	2252.3	34.3	1380.5	12.0	888.5	10.0	0.73	39.45
18 (c)	0.35	45660	0.11224	2.0	1.6909	1.6	0.10926	1.1	1836.1	35.1	1005.1	10.3	668.5	6.9	0.62	36.41
18 (r)	0.36	20186	0.13401	3.5	2.2757	2.8	0.12316	2.1	2151.2	59.9	1204.8	19.3	748.7	15.1	0.69	34.81
19 (c)	0.41	54792	0.19497	2.1	8.8903	1.6	0.33070	1.2	2784.6	33.3	2326.8	14.9	1841.8	19.7	0.71	66.14
19 (r)	0.38	199688	0.12958	2.0	2.2027	1.6	0.12328	1.1	2092.3	34.5	1181.9	11.3	749.4	8.0	0.66	35.82
20	0.48	26129	0.14881	1.8	3.0940	1.5	0.15080	1.0	2332.3	30.4	1431.2	11.3	905.4	8.6	0.64	38.82
21	0.52	42577	0.17051	2.8	5.4755	2.2	0.23291	1.7	2562.6	45.5	1896.8	18.8	1349.7	20.3	0.65	52.67
22	0.52	39243	0.14381	2.0	2.6870	1.6	0.13551	1.2	2273.6	33.4	1324.9	11.5	819.2	9.1	0.73	36.03
23 (c)	0.51	36800	0.19802	2.0	10.7728	1.7	0.39456	1.1	2810.0	32.3	2503.7	15.2	2143.9	20.4	0.64	76.30
23 (r)	0.36	12101	0.13717	2.1	2.6132	1.7	0.13817	1.2	2191.8	36.0	1304.4	12.4	834.3	9.7	0.70	38.07
24	0.50	45412	0.10038	2.3	1.3464	1.9	0.09728	1.3	1631.1	41.6	866.0	10.9	598.5	7.2	0.61	36.69
25	0.59	79912	0.14323	1.9	2.8780	1.6	0.14573	1.1	2266.7	32.3	1376.2	11.8	877.0	8.6	0.59	38.69
26	0.38	35726	0.13263	2.0	2.1746	1.6	0.11892	1.2	2133.0	34.7	1172.9	11.1	724.3	8.3	0.72	33.96
27	0.38	28910	0.13801	3.2	2.5458	2.5	0.13378	2.0	2202.4	54.2	1285.2	18.1	809.4	14.8	0.67	36.75
28	0.37	45019	0.13574	1.9	2.2974	1.5	0.12275	1.1	2173.6	32.7	1211.5	10.8	746.4	7.9	0.69	34.34
29	0.57	32151	0.12447	2.0	2.4632	1.6	0.14353	1.1	2021.2	34.3	1261.3	11.4	864.6	9.2	0.67	42.78
30	0.55	39016	0.13929	3.3	2.8370	2.7	0.14772	2.0	2218.3	56.7	1365.4	19.8	888.2	16.7	0.66	40.04
31	0.15	43553	0.17516	1.9	6.1890	1.6	0.25626	1.1	2607.6	31.3	2002.9	13.6	1470.7	14.0	0.58	56.40
32	0.65	34479	0.13178	1.9	2.3744	1.6	0.13068	1.0	2121.9	32.5	1234.9	11.4	791.7	7.2	0.50	37.31
33	0.51	29441	0.16758	2.0	4.6830	1.6	0.20267	1.2	2533.6	33.1	1764.2	13.3	1189.7	12.9	0.70	46.95
34	0.32	27437	0.16573	2.9	4.6836	2.3	0.20496	1.8	2515.0	47.6	1764.3	18.7	1201.9	19.6	0.69	47.79
35	0.50	28409	0.13862	2.0	2.4602	1.7	0.12872	1.1	2210.1	34.6	1260.4	12.0	780.5	8.4	0.65	35.32
36	0.58	25989	0.16890	1.7	5.6116	1.4	0.24097	1.0	2546.8	29.0	1917.9	12.1	1391.7	13.0	0.71	54.65
37	0.49	40810	0.13271	2.0	2.5037	1.7	0.13683	1.1	2134.1	34.7	1273.1	12.1	826.7	8.5	0.61	38.74
38	0.44	35785	0.16220	3.1	4.4145	2.4	0.19739	2.0	2478.7	52.0	1715.1	19.5	1161.3	21.7	0.73	46.85
39 (r)	0.57	36130	0.16325	1.8	4.0797	1.5	0.18125	1.1	2489.6	30.5	1650.2	12.1	1073.8	10.4	0.65	43.13
39 (c)	0.46	52244	0.15270	1.9	3.8084	1.6	0.18089	1.1	2376.3	32.5	1594.5	12.7	1071.8	10.9	0.66	45.10
40	0.53	175678	0.13065	2.0	2.4650	1.7	0.13684	1.1	2106.7	34.5	1261.8	11.9	826.8	8.5	0.63	39.24
41 (c)	0.57	39809	0.13343	2.8	2.7704	2.5	0.15059	1.4	2143.6	48.8	1347.6	18.1	904.2	12.1	0.52	42.18
41 (r)	0.42	50963	0.12711	1.8	1.8605	1.5	0.10615	1.1	2058.4	32.2	1067.2	9.9	650.4	6.6	0.69	31.60
42	0.53	17259	0.12556	1.9	2.1057	1.5	0.12163	1.1	2036.7	33.3	1150.7	10.4	739.9	8.0	0.74	36.33
43	0.58	37155	0.12938	1.8	2.4245	1.5	0.13590	1.0	2089.6	31.3	1249.9	10.5	821.5	8.1	0.69	39.31
44	0.44	51037	0.11902	2.3	2.0795	2.0	0.12672	1.2	1941.5	40.7	1142.1	13.6	769.1	8.4	0.47	39.61
45	0.45	49128	0.13181	2.0	2.6962	1.6	0.14836	1.1	2122.2	34.5	1327.4	12.0	891.8	9.5	0.66	42.02
46 (r)	0.35	127598	0.15409	1.9	3.5227	1.5	0.16580	1.0	2391.8	31.3	1532.3	12.1	988.9	9.6	0.64	41.35
46 (c)	0.42	71636	0.13038	1.7	2.2784	1.4	0.12674	1.0	2103.1	30.2	1205.6	9.9	769.2	7.3	0.67	36.58
47	0.47	34375	0.12985	3.2	2.1696	2.6	0.12119	1.9	2095.9	55.2	1171.4	17.7	737.4	13.3	0.66	35.18
48	0.43	68166	0.15422	1.8	3.9583	1.5	0.18614	1.0	2393.3	30.9	1625.7	12.2	1100.5	10.4	0.64	45.98

Abbreviations: (c) = zircon core; (r) = zircon rim

Table 5. Summary of LA–ICP–MS data of zircon from the Bacaba Tonalite (sample BACD17/73,30)

	Isotopic ratios								Ages							
Grain area	Th/U	$^{206}Pb/^{204}Pb$	$^{207}Pb/^{206}Pb$	1σ	$^{207}Pb/^{235}U$	1σ	$^{206}Pb/^{238}U$	1σ	$^{207}Pb/^{206}Pb$	1σ	$^{207}Pb/^{235}U$	1σ	$^{206}Pb/^{238}U$	1σ	Rho	Conc (%)
1	0.19	146520	0.22408	1.2	20.0537	1.7	0.64907	1.2	3010.2	18.9	3093.9	16.1	3224.6	29.7	0.67	107.12
2	0.28	258450	0.22165	1.8	17.5451	1.4	0.57410	1.0	2992.7	28.1	2965.1	13.8	2924.6	23.6	0.66	97.73
3 (c)	0.29	82419	0.22197	1.4	16.8387	1.2	0.55018	0.8	2995.1	22.7	2925.7	11.2	2825.9	18.3	0.63	94.35
3 (r)	0.25	60468	0.22153	2.5	17.0211	1.9	0.55726	1.7	2991.8	39.5	2936.0	17.7	2855.3	38.0	0.76	95.44
4	0.37	51184	0.22226	0.7	18.7068	1.0	0.61044	0.7	2997.1	11.8	3026.8	9.9	3071.8	17.7	0.64	102.49
5	0.07	63299	0.22449	0.7	19.0599	1.1	0.61576	0.8	3013.2	11.5	3044.9	10.4	3093.0	19.8	0.72	102.65
6	0.28	24163	0.22112	1.8	17.5062	1.5	0.57419	1.1	2988.9	28.9	2963.0	13.9	2925.0	25.5	0.74	97.86
7	0.16	24706	0.22341	3.0	18.2798	2.2	0.59344	2.0	3005.4	47.1	3004.6	21.2	3003.3	47.5	0.82	99.93
8 (c)	0.27	33894	0.21735	1.8	17.4497	1.5	0.58228	1.1	2961.1	29.4	2959.9	14.4	2958.1	25.1	0.67	99.90
8 (r)	0.30	6227	0.22261	1.0	18.4631	1.4	0.60153	1.0	2999.7	16.2	3014.2	13.8	3036.0	24.6	0.68	101.21
9	0.27	19251	0.22387	3.0	17.3262	2.3	0.56132	2.0	3008.7	47.9	2953.1	22.0	2872.1	45.5	0.79	95.46
10	0.28	17479	0.22321	1.6	17.8468	1.3	0.57988	1.0	3004.0	26.0	2981.5	12.1	2948.3	24.4	0.82	98.14
11	0.29	48433	0.22551	1.3	17.4431	1.0	0.56100	0.8	3020.4	20.6	2959.5	10.0	2870.8	17.5	0.67	95.04
12	0.20	41136	0.22330	1.5	17.4694	1.1	0.56740	0.9	3004.6	23.2	2961.0	11.0	2897.1	20.8	0.76	96.42
13 (c)	0.33	37011	0.22402	2.5	17.8941	1.9	0.57931	1.6	3009.8	38.9	2984.1	17.7	2946.0	37.9	0.76	97.88
13 (r)	0.31	48316	0.22291	1.6	17.6038	1.3	0.57275	1.0	3001.9	25.2	2968.3	12.0	2919.1	22.4	0.72	97.24
14	0.31	28690	0.22366	1.3	18.7706	1.0	0.60867	0.7	3007.3	20.0	3030.1	9.8	3064.7	17.5	0.61	101.91
15	0.20	65121	0.22261	1.3	17.8048	1.1	0.58010	0.8	2999.6	21.3	2979.2	10.2	2949.1	18.8	0.70	98.32
16 (c)	0.29	35761	0.22306	1.8	17.8693	1.4	0.58101	1.1	3002.9	28.0	2982.7	13.0	2952.9	26.4	0.68	98.33
16 (r)	0.28	47242	0.22271	1.2	17.8314	1.0	0.58068	0.7	3000.4	19.8	2980.7	9.8	2951.5	16.8	0.63	98.37
17	0.17	75558	0.22558	0.8	19.7505	1.3	0.63501	1.0	3020.9	12.6	3079.2	12.4	3169.4	25.5	0.78	104.91
18	0.16	297887	0.21740	2.8	16.4820	2.1	0.54986	1.9	2961.5	44.9	2905.2	19.7	2824.6	43.8	0.93	95.38
19	0.33	41408	0.21732	1.1	17.9437	2.4	0.59884	2.2	2960.9	17.3	2986.7	23.4	3025.1	52.6	0.81	102.17
20 (c)	0.11	42317	0.22430	1.8	18.2850	1.4	0.59125	1.1	3011.8	28.7	3004.9	13.8	2994.5	26.2	0.74	99.42
20 (r)	0.27	10967	0.21924	1.7	16.3504	1.4	0.54088	1.0	2975.1	26.5	2897.5	12.9	2787.1	21.8	0.68	93.68
21	0.32	46426	0.22279	1.6	17.3411	1.3	0.56451	1.0	3001.0	25.9	2953.9	12.2	2885.2	23.3	0.77	96.14
22	0.15	59038	0.22455	1.6	17.1689	1.2	0.55453	1.0	3013.6	25.0	2944.3	11.9	2844.0	21.9	0.74	94.37
23	0.35	5330	0.21619	1.3	16.1071	1.8	0.54036	1.3	2952.5	20.5	2883.2	17.0	2785.0	28.3	0.67	94.33
24	0.31	9485	0.22260	3.3	17.3727	2.6	0.56603	2.0	2999.6	51.8	2955.6	25.0	2891.5	45.4	0.68	96.40
25	0.33	30309	0.22320	1.9	18.2576	1.5	0.59325	1.2	3003.9	30.0	3003.4	14.2	3002.6	27.9	0.74	99.96
26	0.35	192603	0.22601	1.5	18.1820	1.2	0.58347	0.9	3024.0	23.7	2999.4	11.5	2962.9	20.9	0.65	97.98
27	0.20	53823	0.22284	1.8	17.9936	1.4	0.58563	1.2	3001.3	29.1	2989.4	13.5	2971.7	27.6	0.81	99.01
28	0.25	74267	0.22497	0.8	18.5527	2.0	0.59811	1.8	3016.6	13.3	3018.8	19.0	3022.2	43.2	0.80	100.19
29	0.32	38874	0.22155	0.8	18.2799	1.2	0.59842	0.9	2992.0	12.9	3004.6	11.7	3023.5	21.9	0.72	101.05
30	0.32	35610	0.22175	0.9	18.6792	1.1	0.61093	0.8	2993.4	13.7	3025.4	10.9	3073.7	18.4	0.59	102.68
31	0.26	58159	0.21950	2.7	17.4874	2.2	0.57782	1.6	2977.0	42.8	2962.0	20.6	2939.8	37.9	0.64	98.75
32	0.32	22419	0.21996	1.7	17.5920	1.4	0.58007	0.9	2980.4	26.7	2967.7	13.3	2949.0	21.9	0.62	98.95
33	0.28	22525	0.22147	1.5	17.9801	1.2	0.58882	0.8	2991.4	23.4	2988.7	11.7	2984.6	19.2	0.60	99.77
34	0.24	4100	0.21914	0.9	18.2899	1.5	0.60533	1.2	2974.4	14.1	3005.1	14.0	3051.3	28.1	0.79	102.59
35	0.31	4491	0.21792	3.4	16.9578	2.6	0.56438	2.2	2965.4	53.5	2932.5	24.6	2884.7	50.3	0.77	97.28
36	0.31	3563	0.21680	1.0	17.5006	1.7	0.58546	1.3	2957.0	16.8	2962.7	15.9	2971.0	30.6	0.77	100.47
37 (c)	0.32	9324	0.21698	2.0	17.2840	1.6	0.57771	1.2	2958.5	31.9	2950.7	15.2	2939.4	28.3	0.73	99.36
37 (r)	0.13	18278	0.22367	1.2	18.4443	2.1	0.59808	1.8	3007.3	18.8	3013.2	20.3	3022.1	42.3	0.73	100.49
38	0.25	23986	0.22238	1.7	16.7774	1.4	0.54717	1.1	2998.0	27.8	2922.2	13.2	2813.4	24.1	0.72	93.84
39	0.20	14792	0.22083	1.8	16.2283	1.4	0.53297	1.1	2986.8	29.0	2890.3	13.6	2754.0	25.2	0.76	92.21
40	0.09	59745	0.22188	0.8	18.3232	1.2	0.59894	0.9	2994.4	12.7	3006.9	11.3	3025.5	21.1	0.69	101.04
41	0.31	15007	0.22167	1.5	18.2529	2.5	0.59721	2.0	2992.8	23.8	3003.2	23.8	3018.6	47.8	0.74	100.86
42	0.20	63885	0.22412	0.7	19.7311	1.0	0.63853	0.7	3010.5	11.9	3078.3	9.8	3183.2	17.5	0.59	105.74
43	0.31	27265	0.21947	0.9	18.6583	1.2	0.61660	0.8	2976.8	14.5	3024.3	11.5	3096.4	19.3	0.58	104.02
44	0.09	45661	0.22201	1.0	18.1544	2.5	0.59308	2.3	2995.3	16.4	2998.0	24.0	3001.9	54.5	0.80	100.22
45	0.27	23835	0.22020	1.1	18.2940	1.6	0.60255	1.2	2982.1	17.0	3005.3	15.1	3040.1	28.0	0.71	101.94
46	0.26	214592	0.21800	1.7	16.2131	1.4	0.53939	1.0	2966.0	27.4	2889.4	13.3	2780.9	22.4	0.67	93.76
47	0.16	4838	0.21743	2.9	17.1220	2.2	0.57112	1.9	2961.8	46.7	2941.7	21.0	2912.4	45.2	0.88	98.33
48	0.23	10991	0.21660	3.2	15.5427	2.5	0.52044	2.0	2955.6	50.6	2849.1	23.5	2701.1	44.0	0.73	91.39
49	0.26	4709	0.21686	1.1	17.3366	2.1	0.57979	1.8	2957.6	18.1	2953.6	20.5	2947.9	42.8	0.85	99.67
50	0.29	139520	0.22098	1.7	17.3369	1.4	0.56900	1.1	2987.9	27.9	2953.7	13.2	2903.7	25.1	0.77	97.18
51	0.17	33150	0.22333	1.7	17.6711	1.4	0.57387	1.0	3004.8	27.0	2972.0	12.9	2923.7	23.9	0.73	97.30
52	0.30	29852	0.22261	1.0	18.3452	1.8	0.59769	1.5	2999.7	16.1	3008.0	17.5	3020.5	36.7	0.69	100.70

Abbreviations: (c) = zircon core; (r) = zircon rim

Table 6. Summary of LA–ICP–MS data of zircon from the Bacaba Tonalite (sample BACD29/225,29)

	Isotopic ratios								Ages							
Grain area	Th/U	$^{206}Pb/^{204}Pb$	$^{207}Pb/^{206}Pb$	1σ	$^{207}Pb/^{235}U$	1σ	$^{206}Pb/^{238}U$	1σ	$^{207}Pb/^{206}Pb$	1σ	$^{207}Pb/^{235}U$	1σ	$^{206}Pb/^{238}U$	1σ	Rho	Conc (%)
1	0.47	34513	0.21539	2.0	15.5081	1.6	0.52220	1.3	2946.5	32.3	2847.0	14.9	2708.5	28.0	0.80	91.92
2	0.21	11889	0.22162	1.8	17.6913	1.4	0.57896	1.1	2992.5	28.2	2973.1	13.5	2944.5	25.0	0.71	98.40
3	0.36	23349	0.22287	1.4	19.4186	2.3	0.63193	1.7	3001.5	23.2	3062.8	21.9	3157.2	43.5	0.65	105.19
4	0.27	7778	0.22392	1.2	18.4580	1.8	0.59786	1.4	3009.1	18.7	3013.9	17.3	3021.2	32.9	0.71	100.40
5	0.18	6550	0.21658	2.1	16.3948	1.7	0.54903	1.2	2955.4	33.8	2900.1	16.4	2821.1	28.1	0.66	95.46
6	0.23	18271	0.21655	1.2	17.4905	2.8	0.58579	2.6	2955.2	20.0	2962.1	27.3	2972.3	60.8	0.81	100.58
7	0.25	5623	0.22319	1.0	18.6376	1.6	0.60564	1.3	3003.8	15.4	3023.2	15.3	3052.5	30.7	0.77	101.62
8	0.26	14722	0.22048	2.2	17.7951	1.8	0.58538	1.3	2984.2	35.6	2978.7	17.2	2970.7	31.7	0.71	99.55
9	0.30	10582	0.22479	2.1	18.4188	1.6	0.59426	1.3	3015.3	33.4	3011.9	15.5	3006.7	32.2	0.81	99.71
10	0.24	5355	0.21523	3.5	15.5768	2.7	0.52491	2.2	2945.3	55.2	2851.2	25.4	2720.0	49.0	0.76	92.35
11	0.16	7900	0.21873	1.0	17.7018	1.5	0.58696	1.1	2971.4	15.9	2973.7	14.5	2977.1	27.4	0.69	100.19
12	0.19	6287	0.21720	2.0	17.1496	1.6	0.57265	1.3	2960.1	31.9	2943.2	14.8	2918.7	29.3	0.77	98.60
13	0.29	6241	0.22216	2.2	16.6308	1.7	0.54294	1.4	2996.4	34.9	2913.8	16.1	2795.8	31.5	0.80	93.30
14	0.24	12184	0.22117	1.3	17.9085	2.8	0.58725	2.4	2989.3	21.2	2984.8	26.8	2978.3	58.4	0.83	99.63
15	0.19	14596	0.21006	2.0	14.1014	1.6	0.48688	1.3	2906.0	32.5	2756.5	14.7	2557.2	27.1	0.81	88.00
16	0.28	6191	0.21782	0.8	17.6306	1.5	0.58703	1.2	2964.7	13.5	2969.8	14.2	2977.4	29.1	0.81	100.43
17	0.20	16537	0.21149	1.9	15.0346	1.5	0.51558	1.2	2917.0	30.5	2817.4	14.2	2680.4	25.6	0.76	91.89
18	0.27	55922	0.21954	3.5	17.7034	2.6	0.58484	2.3	2977.3	54.7	2973.8	24.5	2968.5	54.6	0.81	99.70
19 (r)	0.17	9681	0.22606	1.1	20.3152	1.6	0.65177	1.2	3024.4	17.8	3106.5	15.5	3235.1	29.4	0.68	106.97
19 (c)	0.22	8035	0.22028	2.6	17.3244	2.0	0.57040	1.7	2982.8	42.0	2953.0	19.2	2909.4	39.8	0.84	97.54
20 (r)	0.17	28242	0.22767	1.0	19.8868	1.5	0.63351	1.1	3035.8	15.4	3085.9	14.1	3163.5	27.4	0.73	104.21
20 (c)	0.39	18509	0.21951	2.8	17.0266	2.2	0.56257	1.7	2977.1	43.7	2936.3	20.5	2877.3	39.4	0.69	96.65
21	0.25	18877	0.22259	0.9	19.4226	1.2	0.63285	0.9	2999.5	13.8	3063.0	12.0	3160.8	22.5	0.69	105.38
22	0.18	10329	0.22155	1.7	18.2565	1.4	0.59764	1.0	2992.0	27.7	3003.3	13.6	3020.3	24.1	0.68	100.95
23	0.26	21837	0.21653	2.4	16.8810	1.9	0.56542	1.4	2955.1	37.9	2928.1	18.5	2889.0	31.7	0.69	97.76
24	0.47	17964	0.21977	2.2	17.7798	1.8	0.58675	1.3	2979.0	35.4	2977.9	16.9	2976.2	32.0	0.75	99.91
25	0.26	53260	0.21899	2.1	16.9406	1.7	0.56104	1.2	2973.3	33.0	2931.5	15.8	2870.9	28.6	0.73	96.56
26	0.24	16079	0.22208	1.2	18.1245	1.7	0.59190	1.2	2995.9	19.3	2996.4	16.6	2997.1	29.7	0.70	100.04
27	0.27	6072	0.21650	2.6	17.3262	2.0	0.58041	1.6	2954.9	41.1	2953.1	19.3	2950.4	37.9	0.79	99.85
28	0.32	6260	0.21935	1.2	18.1878	2.2	0.60136	1.8	2975.9	20.1	2999.7	21.1	3035.3	43.6	0.81	102.00
29	0.29	8475	0.21933	2.4	17.6590	1.9	0.58395	1.5	2975.7	37.9	2971.3	17.6	2964.8	35.6	0.79	99.63
30	0.28	7795	0.21712	3.6	17.4546	2.8	0.58306	2.3	2959.4	57.6	2960.2	26.5	2961.2	55.3	0.72	100.06
31	0.17	6019	0.21784	3.2	17.1198	2.5	0.56997	2.1	2964.8	51.1	2941.6	23.5	2907.7	48.2	0.82	98.07
32	0.21	7753	0.21793	2.5	16.8461	2.0	0.56063	1.5	2965.5	39.7	2926.1	18.7	2869.2	35.5	0.76	96.75
33	0.22	3690	0.21428	2.9	16.0291	2.3	0.54253	1.8	2938.2	46.0	2878.5	21.5	2794.0	40.5	0.78	95.09
34	0.31	11735	0.22118	2.0	18.0412	2.9	0.59157	2.1	2989.3	32.1	2991.9	27.9	2995.8	50.6	0.65	100.22
35	0.31	17338	0.21889	1.8	15.7709	1.4	0.52256	1.1	2972.5	28.2	2863.0	13.4	2710.0	23.4	0.71	91.17
36 (c)	0.29	15431	0.22284	1.7	16.8039	1.4	0.54691	1.0	3001.3	27.0	2923.7	13.0	2812.3	22.9	0.70	93.70
36 (r)	0.20	27532	0.22476	1.8	18.3881	1.4	0.59336	1.0	3015.1	28.1	3010.3	13.7	3003.0	25.0	0.69	99.60
37 (r)	0.22	8268	0.21708	3.3	17.0659	2.5	0.57019	2.2	2959.1	52.8	2938.5	23.5	2908.6	52.0	0.78	98.29
37 (c)	0.21	8220	0.22477	2.0	17.4856	1.6	0.56422	1.1	3015.1	31.0	2961.9	15.1	2884.1	26.5	0.68	95.65
38	0.27	8602	0.22034	2.1	17.5303	1.7	0.57702	1.3	2983.2	33.0	2964.3	15.8	2936.6	29.5	0.74	98.44
39	0.23	19524	0.22048	1.8	17.7029	1.5	0.58234	1.1	2984.2	29.1	2973.7	14.1	2958.3	25.6	0.70	99.13
40 (c)	0.15	7313	0.21756	3.2	17.4208	2.4	0.58073	2.1	2962.8	50.3	2958.3	22.9	2951.7	48.8	0.75	99.63
40 (r)	0.18	7104	0.22014	2.4	17.8515	1.9	0.58813	1.5	2981.7	38.4	2981.8	17.9	2981.8	36.2	0.80	100.00
41	0.23	4696	0.22620	2.3	17.6607	1.8	0.56625	1.4	3025.4	35.8	2971.4	16.9	2892.4	32.5	0.78	95.60
42	0.22	10480	0.22055	3.7	17.8282	2.9	0.58628	2.2	2984.7	57.7	2980.5	27.8	2974.3	51.9	0.65	99.65
43	0.30	9474	0.22395	2.1	18.2547	1.7	0.59118	1.2	3009.3	33.8	3003.3	16.6	2994.2	29.3	0.65	99.50
44	0.15	4548	0.22695	1.2	19.2502	1.5	0.61518	1.0	3030.7	18.5	3054.4	14.8	3090.7	24.7	0.57	101.98
45	0.25	8705	0.22404	1.2	18.5145	1.6	0.59934	1.1	3010.0	19.0	3016.9	15.6	3027.2	26.6	0.63	100.57
46	0.27	6188	0.22636	1.7	18.6639	2.6	0.59801	2.0	3026.5	26.9	3024.6	25.2	3021.8	48.3	0.67	99.85
47	0.31	7048	0.21770	2.5	16.9396	1.9	0.56435	1.5	2963.7	39.4	2931.4	18.4	2884.6	35.7	0.78	97.33

Abbreviations: (c) = zircon core; (r) = zircon rim

Table 7. Summary of LA–ICP–MS data of zircon from the Bacaba Tonalite (sample BACD9/257,45)

	Isotopic ratios								Ages							
Grain area	Th/U	$^{206}Pb/^{204}Pb$	$^{207}Pb/^{206}Pb$	1σ	$^{207}Pb/^{235}U$	1σ	$^{206}Pb/^{238}U$	1σ	$^{207}Pb/^{206}Pb$	1σ	$^{207}Pb/^{235}U$	1σ	$^{206}Pb/^{238}U$	1σ	Rho	Conc (%)
1	0.42	22163	0.18579	2.9	5.4945	2.1	0.21449	1.9	2705.2	46.4	1899.7	18.3	1252.7	21.4	0.87	46.31
2	0.56	210612	0.22627	2.1	17.9861	1.6	0.57650	1.3	3025.9	32.7	2989.0	15.3	2934.5	30.4	0.76	96.98
3	0.38	40222	0.19056	2.4	4.9236	1.8	0.18739	1.6	2747.0	38.8	1806.3	15.1	1107.2	15.9	0.86	40.31
4	0.36	7498	0.21085	5.0	10.7517	3.6	0.36983	3.4	2912.1	78.2	2501.9	32.9	2028.6	59.3	0.90	69.66
5	0.45	20266	0.18718	2.8	5.9483	2.2	0.23048	1.7	2717.5	45.7	1968.3	19.1	1337.0	21.0	0.75	49.20
6	0.31	14811	0.22132	2.4	14.6641	1.8	0.48054	1.5	2990.3	38.0	2793.7	17.2	2529.6	32.2	0.82	84.59
7 (r)	0.22	20372	0.20480	2.2	8.5055	1.7	0.30121	1.4	2864.8	35.8	2286.5	15.4	1697.3	21.3	0.82	59.25
7 (c)	0.20	20529	0.19611	3.1	6.4168	2.4	0.23731	2.0	2794.1	50.6	2034.6	21.2	1372.7	24.6	0.73	49.13
8	0.14	99219	0.22474	6.8	17.4284	4.9	0.56244	4.7	3015.0	104.4	2958.7	45.6	2876.7	107.9	0.97	95.41
9	0.27	8328	0.21766	3.2	17.4684	2.4	0.58207	2.0	2963.5	50.3	2960.9	23.2	2957.2	47.9	0.82	99.79
10	0.10	25988	0.16453	3.8	3.4321	3.1	0.15129	2.2	2502.8	61.8	1511.8	23.8	908.2	18.3	0.63	36.29
11	1.10	25989	0.21288	3.0	13.6883	2.3	0.46636	1.9	2927.6	47.7	2728.4	21.6	2467.6	39.2	0.82	84.29
12	0.16	7733	0.22508	1.6	18.5674	2.2	0.59830	1.4	3017.4	25.8	3019.6	20.8	3023.0	34.7	0.63	100.19
13	0.23	13261	0.22456	3.0	17.8715	2.4	0.57721	1.9	3013.7	48.0	2982.8	22.6	2937.4	44.4	0.79	97.47
14	0.26	26049	0.20896	1.9	8.9446	1.6	0.31045	1.1	2897.5	31.1	2332.4	14.5	1742.9	16.6	0.64	60.15
15	0.16	16790	0.21763	2.3	14.5999	1.9	0.48656	1.3	2963.2	36.9	2789.5	18.2	2555.8	26.9	0.63	86.25
16	0.20	465733	0.21897	3.7	16.0082	2.8	0.53023	2.4	2973.1	57.9	2877.3	26.3	2742.4	53.0	0.71	92.24
17	0.19	14797	0.21298	2.4	11.9672	2.0	0.40752	1.4	2928.4	38.8	2601.8	18.2	2203.6	26.8	0.71	75.25
18	0.29	7175	0.16291	2.4	3.7701	2.0	0.16784	1.3	2486.1	40.2	1586.4	16.1	1000.2	12.3	0.63	40.23
19	0.24	30157	0.22141	2.0	15.5335	1.7	0.50884	1.1	2990.9	32.0	2848.5	15.9	2651.7	24.0	0.62	88.66
20	0.20	31862	0.22496	1.1	19.6310	1.6	0.63291	1.2	3016.5	17.0	3073.4	15.1	3161.1	28.9	0.71	104.79
21	0.04	26526	0.21935	1.9	17.3150	1.6	0.57252	1.1	2975.9	30.6	2952.5	14.9	2918.2	26.1	0.67	98.06
22	0.33	20219	0.21653	2.4	15.3467	1.9	0.51403	1.5	2955.1	38.6	2837.0	18.1	2673.8	32.4	0.75	90.48
23	0.20	64179	0.22736	1.2	20.8031	1.8	0.66361	1.3	3033.6	19.6	3129.5	17.2	3281.2	33.0	0.69	108.16
24	0.18	8489	0.22822	1.1	20.0178	1.9	0.63614	1.5	3039.6	18.2	3092.2	18.5	3173.8	38.4	0.79	104.41
25	0.29	3342	0.22259	2.0	17.3374	1.7	0.56491	1.1	2999.5	31.7	2953.7	15.8	2886.9	25.7	0.62	96.24
26	0.17	22138	0.22163	1.4	18.1231	1.9	0.59306	1.3	2992.6	22.1	2996.3	18.1	3001.8	30.6	0.63	100.31
27	0.15	5326	0.18265	3.9	4.4922	3.2	0.17837	2.3	2677.1	63.2	1729.5	26.0	1058.1	22.1	0.58	39.52
28	0.38	10066	0.18668	2.8	6.6750	2.3	0.25933	1.6	2713.1	45.9	2069.3	20.4	1486.4	21.3	0.65	54.79
29	0.08	13179	0.21389	2.5	13.4998	2.0	0.45776	1.4	2935.3	39.2	2715.3	18.9	2429.6	28.5	0.66	82.77
30	0.10	20948	0.17865	4.1	4.0812	3.2	0.16568	2.6	2640.4	67.1	1650.5	26.2	988.3	23.5	0.68	37.43
31	0.21	28920	0.21613	3.2	15.4522	2.5	0.51853	2.1	2952.1	51.3	2843.5	23.1	2692.9	46.4	0.86	91.22
32	0.25	10582	0.22407	1.2	18.9841	1.8	0.61449	1.4	3010.1	19.9	3041.0	17.7	3087.9	33.4	0.71	102.58
33	0.19	23213	0.22579	2.3	17.5390	1.9	0.56339	1.4	3022.4	36.5	2964.8	17.7	2880.6	31.3	0.69	95.31
34	0.18	24504	0.22354	2.3	18.1336	1.9	0.58834	1.3	3006.4	36.4	2996.8	17.9	2982.7	31.7	0.65	99.21
35	0.20	161971	0.19547	2.2	6.7631	1.8	0.25094	1.3	2788.7	35.0	2080.9	15.4	1443.3	16.2	0.66	51.76
36	0.26	40960	0.21989	3.9	14.9755	2.9	0.49395	2.6	2979.9	60.8	2813.7	27.1	2587.7	54.5	0.75	86.84
37	0.18	12856	0.21683	2.5	15.8806	2.0	0.53119	1.5	2957.3	40.0	2869.6	18.9	2746.5	34.2	0.75	92.87
38	0.19	7993	0.21902	2.3	17.6555	1.9	0.58465	1.4	2973.5	37.0	2971.2	17.9	2967.7	32.5	0.69	99.80
39	0.31	32489	0.21070	2.6	9.7859	2.1	0.33685	1.5	2910.9	41.2	2414.8	19.1	1871.5	24.5	0.68	64.29
40	0.07	13627	0.19234	3.5	6.8229	2.8	0.25728	2.1	2762.3	56.0	2088.7	24.1	1475.9	28.1	0.59	53.43
41	0.25	21908	0.20336	3.0	9.0367	2.4	0.32230	1.8	2853.3	48.4	2341.7	22.1	1800.9	28.1	0.69	63.12
42 (r)	0.13	5860	0.19792	2.9	7.6023	2.4	0.27858	1.6	2809.1	46.4	2185.1	21.5	1584.2	21.9	0.60	56.40
42 (c)	0.14	6422	0.20590	2.8	10.6074	2.2	0.37363	1.7	2873.6	44.6	2489.4	20.6	2046.5	29.1	0.71	71.22
43	0.30	3961	0.22276	1.4	18.5416	2.2	0.60369	1.7	3000.7	22.1	3018.3	20.9	3044.7	40.8	0.75	101.47
44	0.11	61831	0.20751	2.4	8.9258	2.0	0.31197	1.4	2886.2	38.2	2330.4	17.7	1750.4	20.9	0.65	60.65
45	0.17	13203	0.21981	2.5	15.4628	2.1	0.51019	1.4	2979.3	39.7	2844.2	19.7	2657.4	30.0	0.61	89.20
46	0.26	16677	0.22989	1.3	20.6361	2.1	0.65104	1.7	3051.3	20.5	3121.7	20.3	3232.3	42.0	0.77	105.93

Abbreviations: (c) = zircon core; (r) = zircon rim

8. CONCLUSÕES

As idades de ca. 3,0 Ga e 2,86 Ga obtidas para as rochas graníticas hospedeiras do depósito Bacaba fornecem novas perspectivas a respeito da Província Mineral de Carajás, assim listadas:

• Ao menos um processo de distúrbio afetou os zircões do Tonalito Bacaba e do Granito Serra Dourada, evidenciado por processos de recristalização do zircão, que apresenta áreas com zonamento oscilatório magmático ofuscado, domínios sem textura e morfologias ovais e arredondadas.

• A perda de Pb radiogênico foi associada tanto com os processos de recristalização (provavelmente na amostra mineralizada BACD9/257,45, Tonalito Bacaba), quanto com estrago causado pela radiação provocando metamitização parcial a total dos zircões (possivelmente na amostra albitizada BACD15/237,40, Granito Serra Dourada).

• O Granito Serra Dourada de 2,86 Ga e o Tonalito Bacaba de ca. 3,0 Ga são as rochas graníticas mais antigas reconhecidas no Cinturão de Cisalhamento Itacaiúnas. Essas idades não somente implicam na existência de um magmatismo significativo, porém pouco compreendido, antes da instalação da Bacia de Carajás; mas também indicam uma história evolutiva mais complexa para a área em questão.

• As rochas do embasamento sob a Bacia de Carajás incluem, além dos complexos Xingu e Pium, o Granito Serra Dourada e o Tonalito Bacaba, por serem mais antigos que o Supergrupo Itacaiúnas de 2,76 Ga.

• Pelo fato do Granito Serra Dourada e do Tonalito Bacaba apresentarem idades similares às de leucogranitos cálcio-alcalinos (Granito Xinguara e Granito Mata Surrão) e de rochas tonalíticas (Tonalito Arco Verde e Tonalito Caracol), respectivamente, presentes no Terreno Granito-*Greenstone* Rio Maria, essas rochas podem ser cogenéticas. Este fato implica tanto num magmatismo de ca. 3,0 e 2,86 Ga mais amplo e extenso em Carajás, quanto numa história evolutiva similar entre o Cinturão de Cisalhamento Itacaiúnas e o Terreno Granito-*Greenstone* Rio Maria, previamente à instalação da Bacia de Carajás.

• O evento hidrotermal associado com a gênese do minério não pôde ser datado devido à ausência total de abertura do sistema isotópico U-Pb pelos fluidos hidrotermais, ou pelo fato de que as possíveis coberturas hidrotermais não puderam ser analisadas pela técnica LA–ICP–MS.

• O Granito Serra Dourada e o Tonalito Bacaba provavelmente não foram responsáveis pelo estabelecimento de um sistema magmático-hidrotermal associado com a gênese do depósito Bacaba. Outros depósitos IOCG com características similares são hospedados pelo Supergrupo Itacaiúnas (2,76 Ga), mais novo que as hospedeiras do depósito Bacaba.

• Os depósitos IOCG da porção sul do Cinturão de Cisalhamento Itacaiúnas são geneticamente relacionados com a circulação em escala regional de fluidos ao longo de discontinuidades crustais importantes, como a zona de cisalhamento regional com direção WNW–ESSE. Neste caso, os depósitos IOCG de Carajás seriam condicionados à existência de trapas estruturais.

• Extensa interação fluido-rocha ao longo das zonas de cisalhamento promoveu lixiviação de metais das rochas mesoarqueanas ou de outras unidades provenientes das fontes de 3,0 Ga. Fontes externas de calor seriam necessárias, assim como um longo tempo de circulação dos fluidos envolvendo salmouras derivadas de magmas e de fontes externas com contribuição de evaporito residual.

• Esses resultados indicam que o potencial de ocorrência dos depósitos IOCG não é limitado à Bacia de Carajás. A exploração mineral deve ser extendida às áreas do embasamento mesoarqueano cortadas por zonas de cisalhamento regionais neoarquenanas.

REFERÊNCIAS BIBLIOGRÁFICAS

Augusto, R.A., Monteiro, L.V.S., Xavier, R.P., Souza Filho, C.R., 2008. Zonas de alteração hidrotermal e paragênese do minério de cobre do Alvo Bacaba, Província Mineral de Carajás (PA). *Rev. Brasil. Geoci.* 38(2), 263–277.

Avelar, V.G., Lafon, J.M., Correia, F.C.Jr., Macambira, B.E.M., 1999. O magmatismo arqueano da região de Tucumã, Província Mineral de Carajás, Amazônia Oriental, Brasil: novos dados geocronológicos. *Rev. Brasil. Geoci.* 29, 453–460.

Barbosa, A.A., Lafon, J.-M., 1996. Geocronologia Pb–Pb e Rb–Sr de granitóides arqueanos da região de Redenção, sul do Pará. *Rev. Brasil. Geoci*. 26, 255–264.

Barros, C.E.M., Macambira, M.J.B., Barbey, P., Scheller, T., 2004. Dados isotópicos Pb–Pb em zircão (evaporação) e Sm–Nd do Complexo Granítico Estrela, Província Mineral de Carajás, Brasil: implicações petrológicas e tectônicas. *Rev. Brasil. Geoci.* 34, 531–538.

Barton, M.D., Johnson, D.A., 1996. Evaporitic source model for igneous-related Fe oxide–(REE–Cu–Au–U) mineralization. *Geology* 24, 259–262.

Barton, M.D., Johnson, D.A., 2000. Alternative brine sources for Fe-oxide(–Cu–Au) systems: implications for hydrothermal alteration and metals. In: Porter TM (ed) *Hydrothermal iron oxide copper-gold and related deposits: A global perspective*. Austral Miner Fund, Adelaide, pp. 43–60.

Dall'Agnol, R., Lafon, J.M., Macambira, M.J.B., 1994. Proterozoic Anaorogenic Magmatism In The Central Amazonian Province, Amazonian Craton: Geochronological, Petrological And Geochemical Aspects. *Mineral. Petrol*. 50, 113–118.

Dall'Agnol, R., Oliveira, M.A., Almeida, J.A.C., Althoff, F.J., Leite, A.A.S., Oliveira, D.C., Barros, C.E.M., 2006. Archean and paleoproterozoic granitoids of the Carajás Metallogenic Province, eastern Amazonian craton. *In*: Symposium on magmatism, crustal evolution and metallogenesis of the Amazoniam Craton, Belém, *Excursion Guide*, 99–150.

Dardenne, M.A., Schobbenhaus, C.S., 2001. Metalogênese do Brasil. Editora Universidade de Brasília/CNPq, Brasília, 392 p.

DOCEGEO, 1988. Revisão litoestratigráfica da Província Mineral de Carajás – Litoestratigrafia e principais depósitos minerais. *35º Congr. Brasil. Geol.*, Belém, SBG, Proceedings, 11−54.

Dreher, A.M., 2004. O depósito primário de Cu−Au de Igarapé Bahia, Carajás: Rochas fragmentárias, fluidos mineralizantes e modelo metalogenético. Tese de Doutorado, Universidade Estadual de Campinas, 221p.

Dreher, A.M., Xavier, R.P., 2005. The Igarapé Bahia deposit, Carajás: A Fe oxide (Cu–Au) hydrothermal system evolved in a submarine Archean setting. In: Simp. Brasil. Metalogenia, 1, [CD-ROM].

Galarza, M.A., 2002. Geocronologia e Geoquímica Isotópica dos Depósitos de Cu-Au Igarapé Bahia e Gameleira, Província Mineral de Carajás (PA), Brasil. Tese de Doutorado, Universidade Federal do Pará.

Galarza, M.A., Macambira, M.J.B., 2002. Geocronologia e Evolução Crustal da Área do Depósito de Cu−Au Gameleira, Província Mineral de Carajás (Pará), Brasil. *Geol. USP Série Científica* 2, 143–159.

Galarza, M.A., Macambira, M.J.B., Villas, R.N., 2008. Dating and isotopic characteristics (Pb and S) of the Fe oxide–Cu–Au–U–REE Igarapé Bahia ore deposit, Carajás mineral province, Pará state, Brazil. *J South Am Earth Sci* 25, 377–397.

Grainger, C.J., Groves, D.I., Tallarico, F.H.B, Fletcher, I.R., 2008. Metallogenesis of the Carajás Mineral Province, Southern Amazon Craton, Brazil: Varying styles of Archean through Paleoproterozoic to Neoproterozoic base- and precious-metal mineralisation. *Ore Geol. Rev*, 33, 451–489.

Hirata, W.K., Rigon, J.C., Kadekaru, K., Cordeiro, A.A.C., Meireles, E.A., 1982. Geologia Regional da Província Mineral de Carajás. *I Simp. Geol. Amazônia*, Belém, SBG/NO, 1: 100–110.

Hitzman, M.W., Oreskes, N, Einaudi, M.T. 1992. Geological characteristics and tectonic setting of Proterozoic iron oxide (Cu-U-Au-REE) deposits. *Precamb Res* 58, 241–287.

Hitzman, M.W., 2000. Iron oxide–Cu–au deposits: what, where, when, and why. In: Porter TM (ed) Hydrothermal iron oxide cooper-gold and related deposits: a global perspective. *Australian Miner. Fund*, Adelaide, 9–25.

Huhn, S.R.B., Souza, C.I.J., Albuquerque, M.C., Leal, E.D., Brustolin, V., 1999. Descoberta do depósito Cu–(Au) Cristalino: Geologia e mineralização associada região da Serra do Rabo, Carajás – PA. *VI Simpósio de Geologia da Amazônia*, SBG/NO, 140−143.

Huhn, S.R.B., Souza, C.I.J., Albuquerque, M.C., Leal, E.D., Brustolin, V., 1999. Descoberta do depósito Cu(Au) Cristalino: Geologia e mineralização associada região da Serra do Rabo, Carajás – PA. *VI Simpósio de Geologia da Amazônia*, SBG/NO, 140−143.

Lafon, J.-M., Rodrigues, E., Duarte, K.D., 1994. Le granite Mata Surrão: un magmatisme monzogranitique contemporain des associations tonalitiques-trondhjé-mitiques-granodioritiques archeénnes de la région de Rio Maria (Amazonie orientale, Brésil). C. R. *Acad. Sci. Paris* 318, 643–649.

Leite, A.A.S., Dall'Agnol, R., Macambira, M.J.B., Althoff, F.J., 2004. Geologia e geocronologia dos granitóides arqueanos da região de Xinguara (PA) e suas implicações na evolução do Terreno Granito-Greenstone de Rio Maria. *Rev. Brasil. Geoci*. 34, 447–458.

Lindenmayer, Z.G., 1990. Salobo sequence, Carajás, Brasil: Geology, Geochemistry and Metamorphism. Tese doutorado, *University of Ontario, Canada*, 407p.

Lindenmayer, Z.G., 2003. Depósito de Cu–Au do Salobo, Serra dos Carajás: Uma revisão. In: L.H. Ronchi and F.J. Althoff (Eds.), Caracterização e modelamento de depósitos minerais. Editora Unisinos, São Leopoldo, 69–98.

Lindenmayer, Z.G., Teixeira, J.B.G., 1999. Ore genesis at the Salobo Copper deposit, Serra dos Carajás. In: Silva, M.G. and Misi, A. (eds), *Base Metal Deposits of Brazil*. MME/CPRM/DNPM, 33–43.

Lindenmayer, Z.G., Teixeira, J.B.G., 1999. Ore genesis at the Salobo Copper deposit, Serra dos Carajás. In: Silva, M.G. and Misi, A. (eds), *Base Metal Deposits of Brazil*. MME/CPRM/DNPM, 33–43.

Macambira, M.J.B., Costa, J.B.S., Althoff, F.J., Lafon, J.-M., Melo, J.C.V., Santos, A., 2000. New geochronological data for the Rio Maria TTG terrane; implications for the time constraints of the Carajás Province, Brazil. In: 31st Intern. Geol. Congr., Rio de Janeiro, CD-ROM.

Macambira, M.J.B., Lafon, J.-M., Pidgeon, R.T., 1998. Crescimento crustal arqueano registrado em zircões de sedimentos da região de Rio Maria, Província Carajás, Pará. In: 40th Congr. Bras. Geol., SBG, Belo Horizonte. Proceedings, p. 55.

Macambira, M.J.B., Lancelot J., 1996. Time constraints of Archean Rio Maria crust, Southeastern Amazonian Craton, Brazil. Intern. *Geol. Rev*. 38 (12), 1134–1142.

Macambira, M.J.B., Lancelot, J., 1992. Idade U–Pb em zircocões de metavulcânica do greenstone do Supergrupo Andorinhas; delimitante da estratigrafia arqueana de Carajás, Estado do Pará. Congr. Bras. Geol., São Paulo 2, 188– 189.

Machado, N., Lindenmayer, D.H., Krough, T.E., Lindenmayer, Z.G. 1991. U-Pb geochronology of Archean magmatism and basement reactivation in the Carajás area, Amazon Shield, Brazil. *Precamb. Res.* 49, 329-354.

Marschik, R., Mathur, R., Ruiz, J., Leveille, R., Almeida, A.J., 2005. Late Archean Cu-Au-Mo mineralization at Gameleira and Serra Verde, Carajás Mineral Province, Brazil: constraints from Re-Os molybdenite ages. *Miner. Depos.* 39, 983–991.

Monteiro, L.V.S., Xavier, R.P., Carvalho, E.R., Hitzman, M.W., Johnson, C.A., Souza Filho, C.R., Torresi, I., 2008a. Spatial and temporal zoning of hydrothermal alteration and mineralization in the Sossego iron oxide–copper–gold deposit, Carajás Mineral Province, Brazil: paragenesis and stable isotope constraints. *Miner. Depos.* 43, 129–159.

Monteiro, L.V.S., Xavier, R.P., Hitzman, M.W., Juliani, C., Souza Filho, C.R., Carvalho, E.R., 2008b. Mineral chemistry of ore and hydrothermal alteration at the Sossego iron oxide–copper–gold deposit, Carajás Mineral Province, Brazil. *Ore Geol. Rer.* 34, 317–336.

Morais, R.P.S. and Alkmim, F.F., 2005. O controle litoestrutural da mineralização de cobre do Depósito Sequeirinho, Canaã dos Carajás, PA. In: *I Simpósio Brasileiro de Metalogenia*, Gramado, [CD-ROM].

Neves, M.P., 2006. Estudos isotópicos (Pb-Pb, Sm-Nd, C e O) do depósito Cu-Au do Sossego, Província Mineral de Carajás. Dissertação de Mestrado, *Universidade Federal do Pará*. 116pp.

Nogueira, A.C.R., Truckenbrod, W., Costa, J.B.S., Pinheiro, R.V.L., 1994. Análise faciológica e estrutural da Formação Águas Claras, Pré-Cambriano da Serra dos Carajás. IV Simpósio de Geologia da Amazônia, 363–364.

Nogueira, A.C.R., Truckenbrod, W., Pinheiro, R.V.L., 2000. Storm and tide-dominated siliciclastic deposits of the Archean Águas Claras Formation, Serra dos Carajás, Brazil. 31st International Geological Congress, Rio de Janeiro. Sociedade Brasileira de Geologia. Abstract volume CD-ROM.

Oliveira, M.A., Dall'Agnol, R., Althoff, F.J., Leite, A.A.S., 2009. Mesoarchean sanukitoid rocks of the Rio Mari Granite-Greenstone Terrane, Amazonian craton, Brazil. *J. South Am. Earth Sci.* 27, 146–160.

Pidgeon, R.T., Macambira, M.J.B., Lafon, J.M., 2000. Th–U–Pb isotopic systems and internal structures of complex zircons from an enderbite from the Pium Complex, Carajás Province, Brazil: evidence for the ages of granulite facies metamorphism and the protolith of the enderbite. *Chem. Geol.* 166, 159–171.

Pimentel, M.M., Lindenmayer, Z.G., Laux, J.H., Armstrong, R., Araújo, J.C., 2003. Geochronology and Nd geochemistry of the Gameleira Cu-Au deposit, Serra dos Carajás, Brazil: 1.8–1.7 Ga hydrothermal alteration and mineralization. *J. South Am. Earth Sci.* 15, 803–813.

Pimentel, M.M., Machado, N., 1994. Geocronologia U−Pb dos terrenos granito-greenstone de Rio Maria, Pará. In: Cong. Bras. Geol., Anais, Sociedade Brasileira de Geologia, vol. 2, pp. 390−391.

Pollard, P.J., 2001. Sodic–(calcic) alteration in Fe-oxide–Cu–Au districts: an origin via unmixing of magmatic H_2O–CO_2–NaCl + $CaCl_2$-KCl fluids. *Miner. Depos.* 36, 93−100.

Pollard, P.J., 2006. An intrusion-related origin for Cu–Au mineralization in iron oxide–copper–gold (IOCG) provinces. *Miner. Depos.* 41, 179–187.

Réquia K., Stein H., Fontboté L., Chiaradia M. 2003. Re–Os and Pb–Pb geochronology of the Archean Salobo iron oxide copper–gold deposit, Carajá Mineral Province, northern Brazil. *Miner. Depos.* 38, 727–738.

Rigon, J.C., Munaro, P., Santos, L.A., Nascimento, J.A.S., Barreira, C.F., 2000. Alvo 118 copper–gold deposit: geology and mineralization, Serra dos Carajás, Pará, Brazil. *31st International Geological Congress*, Rio de Janeiro. SBG, Abstract Volume, [CD-ROM].

Roberts, D.E., Hudson, G.R.T., 1983. The Olympic Dam copper-uranium-gold-silver deposit, Roxby Downs, South Australia. *Econ. Geol.* 78, 799–822.

Rodrigues, E.S., Lafon, J.M., Scheller, T., 1992. Geocronologia Pb-Pb da Província Mineral de Carajás: primeiros resultados. In: Cong. Bras. Geol., 37, Bol. Res. Exp., SBG, São Paulo, vol. 2, pp. 183–184.

Silva, M.G., Teixeira, J.B.G., Pimentel, M.M., Vasconcelos, P.M., Arielo, A., Rocha, W.J.S.F., 2005. Geologia e mineralizações de Fe-Cu-Au do Alvo GT46 (Igarapé Cinzento, Carajás). In: Marini, O.J., Queiroz, E.T., Ramos, B.W. (eds.), *Caracterização de Depósitos Minerais em Distritos Mineiros da Amazônia*, 94–151.

Soares, A.D.V., Macambira, M.J.B., Santos, M.G.S., Vieira, E.A.P., Massoti, F.S., Souza, C.I.J., Padilha, J.L., Magni, M.C.V., 2001. Depósito Cu(Au) Cristalino, Serra dos Carajás, PA: Idade da mineralização com base em análises Pb–Pb em sulfetos (dados preliminares). SBG, Simpósio de Geologia da Amazônia, 7, Res. Expandidos [CD-ROM].

Souza, L.H., Vieira, E.A.P., 2000. Salobo 3 Alpha Deposit: Geology and Mineralisation. In: T.M. Porter (ed.), *Hydrothermal iron Oxide Copper-gold & related Deposits: A global perspective*, Austral. Miner. Found., Adelaide, 213−224.

Souza, S.R.B., Macambira, M.J.B., Sheller, T., 1996. Novos dados geocronológicos para os granitos deformados do Rio Itacaiúnas (Serra dos Carajás, PA); implicações estratigráficas. *V Simpósio de Geologia da Amazônia*, Belém, Proceedings, 380–383.

Souza, Z.S., Potrel, H., Lafon, J.M., Althoff, F.J., Pimentel, M.M., Dall'Agnol, R., Oliveira, C.G., 2001. Nd, Pb and Sr isotopes of the Identidade Belt, an Archaean greenstone belt of the Rio Maria region (Carajás Province, Brazil): implications for the Archaean geodynamic evolution of the Amazonian craton. *Precamb. Res.* 109, 293–315.

Tallarico, F.H.B., 2003. O cinturão cupro-aurífero de Carajás, Brasil. Tese de Doutorado, Universidade Estadual de Campinas, 229p.

Tallarico, F.H.B., Figueiredo, B.R., Groves, D.I., Kositcin, N., McNaughton, N.J., Fletcher, I.R., Rego, J.L. 2005. Geology and SHRIMP U–Pb geochronology of the Igarapé Bahia deposit, Carajás copper–gold belt, Brazil: an Archean (2.57 Ga) example of iron–oxideCu–Au–(U– REE) mineralization. *Econ. Geol.* 100, 7–28.

Tassinari, C.C.G., Mellito, M.K., Babinski, M., 2003. Age and origin of the Cu (Au–Mo–Ag) Salobo 3A ore deposit, Carajás Mineral Province, Amazonian Craton, northern Brazil. *Episodes* 26, 2–9.

Tavaza, E., Oliveira, C.G., 2000. The Igarapé Bahia Au−Cu−(REE−U) Deposit, Carajás Mineral Province, Northern Brazil In: TM Porter (ed), Hydrothermal iron Oxide Copper-gold & related Deposits: A global perspective, Australia Mineral Foundation, Adelaide, 203−212.

Trendall, A.F., Basei, M.A.S., De Laeter, J.R., Nelson, D.R., 1998. SHRIMP U-Pb constraints on the age of the Carajás formation, Grão Pará Group, Amazon Craton. *J. South Am. Earth Sci.* 11, 265–277.

Villas, R.N. and Santos, M.D., 2001. Gold deposits of the Carajás Mineral Province: deposit types and metallogenesis. *Miner. Depos.* 36, 300–331.

Villas, R.N., Neves, M.P., Moura, C.V., Toro, M.A.G., Aires, B., Maurity, C., 2006. Estudos isotópicos (Pb, C e O) no depósito Cu-Au do Sossego, Província Mineral de Carajás. *IX Simpósio de Geologia da Amazônia*, SBG/Núcleo Norte, [CD-ROM].

Williams, P.J., Barton, M.B., Johnson, D.A., Fontboté, L., Haller, A., Mark, G., Oliver, N.H., Marschik, R., 2005. Iron oxide copper-gold deposits: geology, space-time distribution, and possible modes of origin. *Econ. Geol. 100 th Anniversary* Volume, 371-405.

Wirth, K.R., Gibbs, A.K., Olszewski, W.J.Jr., 1986. U−Pb ages of zircons from the Grão Pará Group and Serra dos Carajás granite, Pará, Brasil. *Rev. Brasil.Geoci.* 16, 195−200.

Xavier, R.P., Monteiro, L.V.S., Souza Filho, C.R., Torresi, I., Carvalho, E.R., Dreher, A.M., Pestilho, A.L.S., Moreto, C.P.N. No prelo. The iron oxide copper-gold deposits of the Carajás Mineral Province, Brazil: an updated and critical review. In: Porter, T.M. (Ed), 2010 - Hydrothermal Iron Oxide Copper-Gold & Related Deposits: A Global Perspective, vol. 3, Advances in the Understanding of IOCG Deposits, PGC Publishing, Adelaide.